ELECTRODE POLARIZATION AND ITS INFLUENCE

ON THE ELECTRICAL PROPERTIES OF MINERALIZED ROCKS

by

THEODORE R. MADDEN

S.B., Massachusetts Institute of Technology
(1949)

SUBMITTE IN PARTIAL FULFILLMENT OF THE

REQUIREMENTS FOR THE DEGREE OF

DOCTOR OF PHILOSOPHY

at the

MASSACHUSETTS INSTITUTE OF TECHNOLOGY

February, 1961

Signature of Author_____
        Department of Geology and Geophysics, February, 1961

Certified by_____   , _____
                                              Thesis Supervisor

Accepted by_____
        Chairman, Departmental Committee on Graduate Students

ABSTRACT

Title: Electrode Polarization and Its Influence on the
Electrical Properties of Mineralized Rocks

Author: Theodore R. Madden

The electrical properties of mineralized rocks known as the
"induced polarization" effects, are mostly due to electrode
effects associated with the metal solution interfaces within
the rocks. To understand these effects one must understand
the electrode polarization phenomenon and the electrical
environment within the rocks.

A kinetic model is used to study the factors that should
affect the electrical behavior of electrode-solution inter-
faces. This model incorporates the usual flow equations
for ion motions in a viscous medium, and assumes a linear
dependance of the reaction rates on the changes in the
concentrations and voltages occurring at the electrode.
The "fixed layer" concept used to describe the properties
of ideal polarized electrodes is also included. The solu-
tion of the equations derived from this model leads to the
representation of the electrode impedance by an equivalent
circuit. The parameters of this circuit are simply related
to the concentrations and diffusivities of the reacting
species, and the standard free energy change associated with
the reaction barriers. The magnitude of these parameters
is determined experimentally for a number of metal and semi-
conducting electrodes. A general behavior for these electrodes
is established, but several puzzling factors emerge from
examining the magnitudes of the parameters deduced. There
is strong evidence that the reactions occurring at the elec-
trodes are different from those that are often assumed.

The data from the electrode studies is applied to the rock
polarization problem. The results are confusing unless the
importance of surface conduction is appreciated. A model
is developed that agrees well with the measured rock pro-
perties. The parameter values of this model emphasize the
role of minor constituents within the pore structure. Be-
cause of this, and because the principle polarization mecha-
nism is a diffusion phenomenon, there is reason to expect simi-
larities between the polarization due to metallic minerals,
and that due to membrane effects. The empirical data on induced
polarization in rocks is reviewed, and the most troublesome
samples are examined in detail. Rule of thumb guides are set
up to help distinguish the two polarization effects, but some
samples must be considered anomalous.

Thesis Supervisor: Stephen M. Simpson
Assistant Professor of Geophysics

PREFACE

During the academic year 1952-53, Prof. Hurley of the M.I.T. Department of Geology and Geophysics encouraged a group of graduate students to start investigations on the induced polarization method of geophysical exploration. Funds were advanced by the department to carry out a program of experimentation in Nova Scotia during the summer of 1953. This was the beginning of a program concerned with many aspects of induced polarization that has been carried on in M.I.T. Department of Geology and Geophysics. Some of this work has been sponsored by the Raw Materials Division of the Atomic Energy Commission. Important contributions were also made by the Bear Creek Mining Company, which supported some of the field work, and provided equipment for field and laboratory studies.

The problems that faced this program were concerned with the measurement and interpretation of induced polarization effects in earth materials. These problems break down into two distinct categories. One category involves an understanding of the physical-chemical effects that give rise to the induced polarization properties, and the iden-tification of these effects in geologic materials. The other category is involved with the interpretation of field measurements. This latter one is a difficult problem in mathematical physics very closely allied to the problem of resistivity interpretations. Dr. Phillip Hallof and Dr. Norman Ness made contributions to this problem in their Ph.D. theses. The work done on the first category of

induced polarization problems at M.I.T. was largely supported by A.E.C. contract AT(05-1)-718. Dr. Donald Marshall and the author were the chief investigators working on this project. Much of the material for this thesis is to be found in the reports of this project:

RME-3150 Background effects in the I.P. method
of geophysical prospecting, 1957

RME-3156 A laboratory investigation of I.P., 1958

RME-3157 Electrode and membrane polarization, 1959

RME-3160 I.P., a study of its causes and magnitudes
in geologic materials, 1959

It is generally realized that induced polarization effects are caused by metallic or semiconducting minerals within a rock. The awareness that other causes can also lead to induced polarization effects, motivated a closer study of the polarizing effects of metallic minerals, in the hope that the various causes could be differentiated in the electrical measurements. This is the study the author undertook and which is presented here. The parallel work undertaken by Dr. Donald Marshall to investigate all other possible causes of induced polarization in geologic materials is a necessary companion to this work, and his results will be referred to constantly throughout this thesis.

TABLE OF CONTENTS

LIST OF FIGURES

LIST OF TABLES

LIST OF SYMBOLS

a_i	activity of ith ion species
ac	alternating current
c	total salt concentration
c_i	concentration of ith ion species
C_{ch}	chemical capacitance
C_D	diffuse layer capacitance
C_e	electrode capacitance
C_F	fixed layer capacitance
cps	cycles per second
DC	direct current
D_p	positive ion diffusivity
D_n	negative ion diffusivity
E	electric field
F	Faraday constant
f	frequency in cps.
freq.	frequency in cps.
$\Delta G_o^{\ddagger}$	standard free energy difference of activated complex
h	Planck's constant
I	electric current
i_∞	total current
i_{α_i}	current associated with electrode reaction of ith ion species
i_o	exchange current of electrode reaction
j	imaginary unit
K	diffuse layer parameter
k	Boltzman constant
L	sample length
mf.	metal factor
mv.	milivolts
M	active ion concentration term
N	active ion concentration term
n	negative ion concentration
p	positive ion concentration
Q_D	diffuse layer charge

R	gas constant
$R(f)$	resistance at frequency f
R_o	rock impedance parameter
R_1	rock impedance parameter
R_S	solution resistance
r_1	inverse diffusion layer thickness
r_2	inverse diffusion zone thickness
s	path length variable
T	absolute temperature
t	time
t^+	transference number for positive ions
V	electric potential
V_P	diffuse layer voltage drop
V_F	fixed layer voltage drop
W	Warburg inpedance
X	reaction product concentration
$X^{\ddagger}$	activated complex concentration
x	distance variable
Y	reaction product concentration
Z	impedance
Z_e	electrode impedance
Z_F	fixed layer impedance
Z_M	rock impedance parameter
Z_R	rock impedance
Z_s	solution impedance
Z_α	reaction impedance
α	reaction rate theory parameter
α_i	complex fraction of total current carried by i^{th} ion reaction
β, γ	reaction rate coefficients
γ, Δ	diffusion zone parameters
Δ, δ	incremental quantity
δ	diffusion zone parameter
ϵ	dielectric constant
η, θ	reaction rate coefficients

μ_i	mobility of ith ion species
μf	microfarad
ν	stoichiometric number
ξ	reaction rate coefficient
ρ	electrical resistivity
σ	electrical conductivity
σ	ratio of negative and positive ion mobilities
ψ	electric potential
ψ_0	Zeta potential
Ω	ohm
ω	angular frequency
Υ	tortuosity

ACKNOWLEDGEMENTS

INTRODUCTION

There is little need to introduce the subject of induced polarization in great detail, since a good deal of literature is now available on the subject (Bleil, 1953; Madden et al, 1957; Vacquier et al, 1957, Marshall and Madden, 1959). A short review is presented here, however, for the sake of completeness.

During the past 10 years an increasing interest has developed around the application of electrical measurements, popularly known as "induced polarization measurements." These measurements have been predominantly applied to the problem of detecting metallic mineral zones, but an increasing awareness of the polarizing effects of non-metallic minerals has arisen with the development of these methods.

The predominant cause of induced electrical polarization in geologic materials is believed to be due to the polarizing of metallic minerals in the rock. When these minerals block the pore passages of a rock, and an electric current is passed through the rock, an electro-chemical barrier must be overcome by the current flowing through the interface between the metallic minerals and the solution in the pore passage. The forces which oppose the current flow are said to polarize the interface, and the added voltage necessary to drive the current across this barrier is sometimes known as the overvoltage. When the inducing current is turned off

1

the overvoltages that were set up decay in time. Observing these voltages represents one method of detecting the polarization effects within the rock. Since it also take a finite time to build up these overvoltages, one finds that the impedance of these zones decreases with increasing frequency so that measurements may also be made in the frequency domain. Qualitatively then, these effects behave somewhat as the ordinary dielectric properties of the materials. These effects, however, occur at audio and subaudio frequencies which are much too low for the ordinary displacement currents to be of any significance. Regardless of the origin of the phenomena, any time-dependent or frequency dependent behavior of the electrical impedance of rock materials at these low frequencies is referred to as the "induced polarization effect."

Several different techniques are used to measure these effects, and several different parameters are used to describe the results of these measurements. When the measurements are made in the time domain, it is a common procedure to turn the current source on for a period, and then turn it off for a period, before starting a new cycle with opposite polarity. The voltage remaining just at the beginning of the "off period" or at some fixed interval later, is often measured and compared with the "on period" voltage. The ratio of the two voltages is taken as a measure of the magnitude of the polarization effects, and is usually evaluated in terms of millivolts per volts (mv/v). Another practice consists of inte-

grating the "off period" voltage. The polarization effects
are then evaluated in terms of millivolt seconds per volt
(mv-sec/v).

When measurements are made in the frequency domain it is
usual to compare the impedance at some alternating frequency
with that at some very low frequency, which is often referred
to as the "D.C. impedance." The effect is then evaluated as
a certain percentage increase in the conductance at the A.C.
frequency. Sometimes phase-shift measurements are made.
These phase-shifts are usually very small, of the order of a
degree or less.

Because time and frequency domain data are related to each
other, when the phenomenon is linear, through the Fourier
transform we can expect to derive frequency information from
the transient measurements or vice-versa. There is not an
exact one-to-one correspondence between a point in a fre-
quency domain and a point in a time domain, but there is
often an approximate one. The percentage frequency effect
and the millivolts per volt parameters are found to be
closely related (Madden and Marshall, 1958). If the per-
centage decrease of the impedance is used instead of the
percentage increase in conductivity the relationship is
given as:

$\%$ effect at frequency $f_1 = 0.1 \times$ mv/volt value

at $t_1 = 1/2 \pi f_1$

Throughout this work we will keep the convention of refer-
ring everything to the frequency domain.

As was discussed in report RME-3150, it is sometimes ad-
vantageous to weight these parameters so that they are more
diagnostic. Since the magnitude of the previously mentioned
parameters can be diluted when new conduction paths are
opened up in a rock, it is sometimes appropriate to weigh
these parameters in a way which better reflects the total
amount of polarizing material within the rock. One such
weighting is given by taking the total increase in the con-
ductance of the rock rather than by taking the percentage
increase in conductance. This is the parameter which we
have used throughout these reports, and which is called the
"metal factor." When using units of ohm-feet, the metal
factor can be expressed in terms of the DC and AC resis-
tivity as:

$$\text{m.f.} = 2\pi \, [R(DC) - R(AC)] \times 10^5 / R(DC) \, R(AC)$$

The metal factor is very useful in evaluating the amount
of polarizable material within igneous rocks, but because
the parameter depends on the conductivity of the pore
fluids, it is not as useful in evaluating the sedimentary
rocks. Some typical values of the metal factor encountered
in igneous rocks are given in Table I.1.

Table I.1

Common Metal Factor Values (10 cps.)

rock type and mineralization	metal factors
unmineralized granites	1
unmineralized basic rocks	1-10
finely disseminated sulphides	10-100
disseminated sulphides (1-3)	100-1000
fracture filling sulphides (3-10)	1000-10,000
massive sulphides	> 10,000

The metal factor is also a useful parameter for evaluating core samples in the laboratory. Core samples represent a biased sample of the rocks cored, since the badly sheared and altered rocks often do not core. For this reason the resistivity of the core samples is often higher than the resistivity of the rock aggregate from which the samples came. The metal factor parameter however is unaffected by the development of purely ionic conduction paths acting in parallel with the other conduction paths through the rock. Thus one can expect the metal factor values obtained from core samples to represent more faithfully the average properties of the rock in situ. An interesting test of these ideas was discussed in RME-3150, which involved an extensive comparison of field measurements and laboratory measurements. The resistivities obtained by the two methods differed by a factor of six, but the metal factor values were essentially equal.

When massive metallic mineralization is present in a rock, the sampling problem for rock cores is greatly increased. Unless the core samples are much larger than the metallic

minerals present, the electrical properties measured in the laboratory can be very misleading. Fortunately, however, such rocks usually represent such good electrical targets, there is little need to study their properties in the laboratory.

Although the metal factor values are dependent on the geometry of the metallic mineral emplacement, it is seen from Table I.1 that the values are quite sensitive to the amount of metallic minerals present. This makes the parameter quite useful in distinguishing between well mineralized zones and slightly mineralized backgrounds. Some field examples showing the increased resolving power of measuring this parameter to detect sulphide zones were given in Report RME-3150.

The application of these measurements to detecting sulphide mineralization is not always as straightforward as those field examples cited would indicate. One complication arises from the fact that other electronic conducting minerals such as graphite, magnetite and pyrolusite also give induced polarization effects. It also appears however, that polarization effects can arise without any metallic minerals being present. Schlumberger, in perhaps the first reference to these measurements, stated that background-induced polarization effects tended to drown out the effects of metallic mineral zones (Schlumberger, 1920). This view is somewhat exaggerated, but several groups have been studying the influence of clay minerals on induced polarization measurements, (Vacquier et al, 1957; Henkel and Van Nostrand, 1957; and A.A. Brant –

personal communication).

Because of the presence of these complicating factors, the present study was undertaken. It was hoped that through an increased understanding of the causes of induced polarization in geologic materials, one could better interpret the electrical measurements. A very general approach to the problem of electrical polarization in unmineralized rocks can be set up in terms of the coupling between various flows and electric current flow. The efficiency of these coupling effects in causing an electrical polarization can be estimated by examining the magnitude of the conductance terms in the matrix used to describe the flow properties of a material. This approach was used by D.J. Marshall in his aforementioned thesis. The data that he collected on the flow properties of rock samples demonstrated that although some very prominent cross coupling phenomena occur, only the diffusion potentials associated with electrical current flow across a membrane system can lead to the finite polarization effects that are measured. A simple mathematical model of this effect was set up and evaluated in order to obtain a quantitative picture of the electrical properties of such a system. Laboratory measurements were also used to check these results. These studies showed that there was an upper limit to the magnitude of the polarizing effect of such systems, and that the frequency spectrum was limited to very low frequencies unless extremely fine-grained materials such as individual

clay particles were involved.

In order to be able to make diagnostic evaluations of the causes of electrical polarization in natural rocks, a similar comprehensive study of the polarizing effect of metallic or semiconducting-solution interfaces must be undertaken. Such a study is made in Chapter I. A mathematical model is set up for the behavior of an electrode which involves the ion motion in the solution, and the reaction rates associated with the sequence of reactions involved in the charge transfer between the solution and the electrode. It is shown that the ion motion in the solution affects the magnitude of the electrode impedance, but that the greatest control is exhibited by the electrode capacitance and the reaction rate parameters. The form of the impedance can be very varied, but is represented by easily assembled equivalent circuits. Each element of the equivalent circuit represents some step in the charge transfer reaction chain. The limitations of such a linear representation are also examined, and it is shown that at reasonably low current densities the approximations involved are justified.

In Chapter II experimental data on electrode impedances is presented and compared with the mathematical models. The experimental data included a variety of metal and semiconducting electrodes under different conditions of temperature and solution concentrations. Some of this data was obtained from the literature. The comparison

8

of the experimental data with the mathematical models was generally good. A rather remarkable uniformity of results with different electrodes under varying conditions was found. The explanation of this result remains an open question. There is little evidence that the reactions actually taking place at the electrodes are the ones usually postulated.

In Chapter III the electrical environment in natural rocks is examined in order to try and understand the role that electrode interface impedances will play in the polarization properties of such rocks. It is shown that the conduction is largely due to ion motion through the pore fluids, but that in tight rocks most of these ions are excess ions associated with the mineral surfaces. This conduction mechanism is known as surface conduction, and when it is taken into account, the typical polarization properties of natural rock samples appear quite reasonable.

Unfortunately, it was found in studying electrode impedances that the dominant factor controlling the impedance in the frequency range of interest for exploration measurements was a diffusion flow phenomenon. This was the same mechanism causing polarization effects in membrane systems, and thus the likelihood of finding dignostic variations in the electrical properties of rocks depending on whether their polarization effects are due to electrode or membrane polarization is reduced. The most promising difference is that associated with the finite limits set up for the polarizing effects of membrane systems. An

examination of this problem of identifying anomalous

samples is made in Chapter IV, and rule of thumb guides

are set up that can be used to distinguish the effects of

significant metallic mineralization in the majority of

cases. Examples are shown that do not conform to these

rules, but the great usefulness of induced polarization

measurements in mining exploration is not eliminated by

the existence of such anomalous examples.

CHAPTER I

THEORY OF ELECTRODE IMPEDANCES

Many aspects of the problems of electrode impedances are
thoroughly treated in the electrochemical literature. The
experimental studies are more limited that the theoretical
studies, especially in the low frequency ranges of interest
in geophysical measurements. The theoretical treatments,
however, also appear in many instances to inadequately
demonstrate the validity of the assumptions used. In many
references, for instance, the Nernst equation is used to
derive the electric potentials, even though the electrode
phenomenon are, to a great extent, irreversible. The usual
treatments also specialize their conditions by assuming an
excess of inert electrolyte, and simple reaction boundary
conditions. There are reasons to expect these conditions
will not always show up in actual practice. Therefore,
it seems worthwhile to undertake a critical review of the
factors involved in controlling the impedance of an electrode
solution interface. In developing this review we lean
heavily on combining two approaches that are discussed in
the literature. One approach develops the details of the
ion motion by setting up their equations of motion (Mac-
Donald, 1953). The other approach concerns the electrode
reaction boundary conditions for complicated reactions at
the electrode (Grahame, 1952).

D.C. Grahame gives an excellent review of the concepts

used in describing the electrical properties of ideal polarized electrodes (Grahame, 1947). The electrode solution interface is divided into two zones. One zone, called the "fixed layer", is pictured as a compact layer of ions and molecules rather rigidly held in place on the electrode by chemical and adsorption forces. This zone often contains a net charge. The other zone is adjacent to the fixed layer on the solution side. It is considered to be similar to the rest of the solution, except that any net charge in the fixed layer creates an electric field that unbalances the positive and negative ion concentrations in the zone. This zone is called the "diffuse layer."

The fixed layer is a thin enough zone to have an appreciable electrical capacitance coupling the diffuse zone to the electrode. This capacitance is known as the "fixed layer capacitance." When the electrode is not an ideal polarized electrode, some charge transfer can take place across it by means of a chemical reaction at the electrode.

The diffuse layer has an electric field because of a net imbalance of charge in the fixed layer, and the ion density in the diffuse layer is derived by assuming a Boltzmann distribution . The total electric potential drop across the diffuse layer is called the "zeta potential." It is not subject to direct measurement, but many experimental electro-kinetic parameters such as the

streaming potential are related to it theoretically. The diffuse layer, by expanding and contracting under the influence of an applied field, has an effective electrical capacitance acting in series with the fixed layer capacitance. The value of this capacitance is given in the theory as $C_d = \epsilon K \cosh (\psi_0 F / 2 RT)$. ψ_0 here   1.1 stands for the zeta potential.

The theory demands that the dielectric properties of the solution in the diffuse layer zone remain the same as further out in the solution. This is probably not very exact, but the error does not seem to affect seriously the electrical properties of the diffuse layer. Grahame has extended the statistical mechanical predictions mentioned above, to include a saturation effect in the dielectric constant (Grahame, 1950). His calculations indicate that the diffuse layer capacitance is negligibly altered by this effect unless very high zeta potentials exist.

Diffuse Layer Kinetics

The success of this model in describing many different electro-kinetic effects makes it seem an adequate starting point for developing the theory of electrode impedances. The equilibrium assumptions involved in assuming an ideal polarized electrode and static conditions must be relaxed to study non-ideal polarized electrodes at audio and subaudio frequencies. Grahame states that the static

13

capacitance of ideally polarized electrodes is equal to the capacitance determined using high frequencies (Grahame, 1946). This would seem to indicate that the equilibrium state is reached very rapidly. When dealing with non-ideal polarized electrodes, however, the application of an impressed voltage causes irreversible flows to take place so that one cannot speak of thermodynamic equilibrium even at very low frequencies.

The treatment of such distinctly non equilibrium situations will require a more specific model, so that equations of motion can be set up to describe the behavior of the system. The simplest such model treats the ions of the diffuse layer as point charges moving through a viscous media due to the influence of any existing electric field and ion concentration gradients (MacDonald, 1953).

If p represents the ion concentration of the positive ions, and n represents the concentration of the negative ions, both assumed to be univalent, the equations of motion of this model would be given as:

$$\frac{\partial p}{\partial t} = D_p \frac{\partial^2 p}{\partial x^2} - \mu_p \frac{\partial(pE)}{\partial x} \qquad 1.2$$

$$\frac{\partial n}{\partial t} = D_n \frac{\partial^2 n}{\partial x^2} + \mu_n \frac{\partial(nE)}{\partial x} \qquad 1.3$$

There is also the condition on E from Poisson's equation:

$$\frac{\partial E}{\partial x} = \frac{F}{\epsilon}(p-n)$$

1.4

μ is the mobility, and D the diffusivity of the ion species in question, and ϵ is the dielectric constant of the solution. It is usually assumed that Einstein's relationship $\mu/D = F/RT$ holds, and that D is a constant independent of the concentrations. These assumptions appear fairly safe in our problem when we are interested in relatively dilute solutions. We shall also assume the dielectric permitivity is constant, which is a less correct assumption, but would probably not affect the basic behavior of the solution to any large extent, as mentioned before.

This model is not concerned with thermodynamic equilibrium or disequilibrium, but the solutions of its equations of motion lead, as we shall see, to results which reduce to our previous results in the case of ideal polarized electrodes at low frequencies. It would seem therefore to be an adequate model to use to extend the behavior of the diffuse layer beyond the simple equilibrium conditions. Inertial terms have been left out of the equations, but it is well known that the inertial effects of ions in aqueous solutions are unimportant until the frequencies reach the radar frequency range.

The appearance of product terms, pE and nE, makes the system

of differential equations, 1.2, 1.3, and 1.4, non linear. In practice we will restrict our current flows to very low densities, so that a linear set of equations can be developed for the changes in concentration. The only remaining complication is the solution for the static case and the presence of non-constant coefficients due to the static E,p,n being functions of position.

These difficulties also disappear when we treat the special case of no zeta potential and no applied DC bias, for then the static $E = 0$ and $p_0 = n_0 = C$ the salt concentration in the bulk of the solution.

Let

$$P = P_0 + P_1(x,\tau) \quad ; \quad P_1 \ll P_0$$

$$n = n_0 + n_1(x,\tau) \quad ; \quad n_1 \ll n_0$$

$$D_n = \sigma D_p = \sigma D$$

$$\mu_n = \sigma \mu_p = \sigma \mu$$

Ignoring products of small terms p_1, n_1, E, 1.2, 1.3, and 1.4 can be combined into:

$$\frac{\partial P_1}{\partial \tau} = D \frac{\partial^2 P_1}{\partial x^2} - \frac{\mu c F}{\epsilon}(P_1 - n_1) \qquad 1.5$$

$$\frac{\partial n_1}{\partial \tau} = \sigma D \frac{\partial^2 n_1}{\partial x^2} + \frac{\sigma \mu c F}{\epsilon}(P_1 - n_1) \qquad 1.6$$

Defining

$$K^2 = \frac{2c F^2}{\epsilon RT} \qquad\qquad \gamma = \frac{j\omega}{D}$$

We have on assuming sinusoidal time dependence:

$$\gamma P_1 = \frac{d^2 P_1}{dx^2} - \frac{K^2}{2} P_1 + \frac{K^2}{2} n_1 \qquad 1.7$$

$$\frac{\gamma n_1}{\sigma} = \frac{d^2 n_1}{dx^2} + \frac{K^2}{2} P_1 - \frac{K^2}{2} n_1 \qquad 1.8$$

Assuming solutions of the form

$$P_1 = A_\ell e^{-r_\ell x}$$

$$n_1 = B_\ell e^{-r_\ell x}$$

which is valid if the solution zone is much thicker than $\frac{1}{r_\ell}$, leads to the conditions on r_ℓ given by the determinant

$$\begin{vmatrix} \gamma - r_\ell^2 + \frac{K^2}{2} & -\frac{K^2}{2} \\ \\ -\frac{K^2}{2} & \frac{\gamma}{\sigma} - r_\ell^2 + \frac{K^2}{2} \end{vmatrix} = 0$$

For concentrations greater than 10^{-5} moles/liter, and for frequencies less than 1000 cps.:

$$K^2 \gg \gamma \qquad \text{(see Table 1.1)}$$

This approximation simplifies the results to

$$r_1^2 \hat{=} K^2 + \gamma \frac{1+\sigma}{2\sigma} = K^2 (1+\delta) \qquad 1.9$$

$$r_2^2 \hat{=} \gamma \frac{1+\sigma}{2\sigma} = K^2 \delta \qquad 1.10$$

17

Substituting 1.9 and 1.10 into 1.7 and 1.8 gives one the
ratio between A_1 and B_1 and between A_2 and B_2

$$B_1 = -A_1 (1-\Delta) \qquad\qquad 1.11$$

$$B_2 = A_2 (1+\Delta) \qquad\qquad 1.12$$

$$\Delta = \gamma(\sigma-1)/K^2\sigma$$

The solutions of our original linearized equations 1.7
and 1.8 are now given completely within two arbitrary
constants A_1 and A_2 as follows:

$$P_1 \cong A_1 e^{-\Gamma_1 X} + A_2 e^{-\Gamma_2 X} \qquad\qquad 1.13$$

$$n_1 \cong -A_1 [1-\Delta] e^{-\Gamma_1 X} + A_2 [1+\Delta] e^{-\Gamma_2 X} \qquad\qquad 1.14$$

$$E \cong -\frac{F}{\epsilon \Gamma_1}(2-\Delta)A_1 e^{-\Gamma_1 X} + \frac{F}{\epsilon \Gamma_2}\Delta A_2 e^{-\Gamma_2 X} + E_\infty \qquad 1.15$$

The $e^{-\Gamma_1 X}$ terms represent a charge separations in the diffuse
layer. Actually we assumed that there was no diffuse layer
to begin with, but the voltage associated with the current
flow sets up a weak diffuse layer. The $e^{-\Gamma_2 X}$ terms re-
present a typical diffusion equation solution:

$$j\omega P = D' \frac{d^2 P}{dX^2}$$

where D' is a mean diffusion coefficient $= \dfrac{2D_p D_n}{D_p + D_n}$

There is only an incipient charge separation associated with
this diffusion solution when $\sigma \neq 1$

The boundary conditions that must be coupled with the reactions at the electrode can be stated as:

$$\frac{\mu p_o E}{D} - \frac{dp_1}{dx} = \frac{\alpha_p i_\infty}{DF} \qquad 1.16$$

$$\frac{\mu n_o E}{D} + \frac{dn_1}{dx} = \frac{\alpha_n i_\infty}{\sigma DF} \qquad 1.17$$

$\alpha_p i_\infty/F$ represents the flow of p into the solution and $\alpha_n i_\infty/F$ represents the flow of n out of the solution as a result of the chemical reactions. i_∞ stands for the total current which is equal to the ion current in the bulk of the solution. At the fixed layer some displacement current will occur across the fixed layer capacitance, so that in general

$$\alpha_p + \alpha_n < 1$$

The amplitude coefficients are determined, when α_p and α_n are known, from 1.16 and 1.17.

$$A_1 \cong \frac{i_\infty}{DF} \left[\alpha_p + \alpha_n - 1 \right] \frac{r_1}{2\gamma} \qquad 1.18$$

$$A_2 \cong \frac{i_\infty}{DF} \left[\alpha_p - \alpha_n + \frac{\sigma-1}{\sigma+1} \right] \frac{r_2}{2\gamma} \qquad 1.19$$

The approximation sign refers to the assumption of low frequencies as well as the linearization procedure.

TABLE 1.1

Kinetic Model Parameters cgs.

C	K^2		freq	γ	δ for $C=10^{-3}$	δ for $C=10^{-1}$
10	10^{16}		1	3×10^5	3×10^{-7}	3×10^{-9}
10^{-1}	10^{14}		10	3×10^6	3×10^{-6}	3×10^{-8}
10^{-3}	10^{12}		100	3×10^7	3×10^{-5}	3×10^{-7}
10^{-5}	10^{10}		1000	3×10^8	3×10^{-4}	3×10^{-6}

C in moles /liter

frequency in c.p.s.

$D = 2\times10^{-5}$, $\epsilon/\epsilon_o = 80$, $T = 25^{\circ}C$

When α_p and α_n are both $= 0$, no chemical reactions take place at the electrode, and the electrode is described as an ideal polarized electrode. Mercury electrodes in inert electrolytes approximate this behavior. If $\sigma = 1$ we have in this case:

$$A_1 = - \frac{i_\infty \Gamma_1}{2DF\gamma} \quad ; \quad A_2 = 0 \qquad 1.20$$

$$V = - \int_0^L E\,dx = \frac{i_\infty}{DF\Gamma_1\gamma} + E_\infty L \qquad 1.21$$

The diffuse layer impedance is

$$Z_D = \frac{V_D}{i_\infty} = \frac{1}{j\omega\epsilon K} + \text{solution resistance} \qquad 1.22$$

This result means that the diffuse layer can be represented as a capacity, $C_D = \epsilon K$, in series with the solution resistance. The fixed layer capacity, C_F, is in series with

the diffuse layer so that the ideal polarized electrode can
be represented as in Figure 1.1.

$$C_F \quad C_D \qquad R \text{ solution}$$
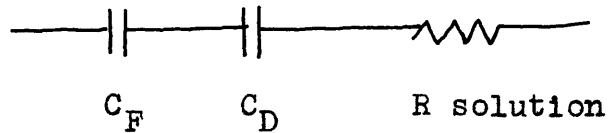
Figure 1.1   Equivalent Circuit of Ideal Polarized Electrode.

This capacitance derived from our kinetic model is the same
as that derived from statistical mechanical considera-
tions for the static case for low zeta potentials as given
in 1.1.   This suggests that the properties of ideal polar-
ized electrodes are virtually the same from DC to high audio
frequencies.   This result has been experimentally verified
by Grahame (1946).   He measured the capacity of the system
Hg/inert electrolyte (KNO_3, NaCl, HCl) at 240, 1000, and
5000 cps., and he also applied a DC bias varying from .5
to - 1.2 volts.   The deviation of the capacitance was always
less than 1 %.

When chemical reactions do take place at an electrode they
usually involve ions such as H^+ which do not represent the
most common ion species in the solution.   The usual treat-
ments of electrode kinetics assume that in the presence
of a high concentration of supporting inert electrolyte,
the electrochemically active ion abeys the simple diffusion
equation in the solution.   It is actually not very diffi-
cult to obtain a more correct answer than is possible using
the above-mentioned assumptions.

To simplify the algebra we make the further assumption
that all the ions have the same mobility. This assump-
tion should not materially alter the behavior of the results.
What we are principally concerned with is the magnitude of the
charge separation effect of the changes of the active ion
concentration at the electrode.

Let p_1, n_1, be the supporting electrolyte concentration.
Let p_2, n_2, be the active ion species concentration.

$$D_{p_1} = D_{p_2} = D_{n_1} \cdots\cdots = D$$

$$\mu_{p_1} = \mu_{p_2} = \mu_{n_1} \cdots\cdots = \mu$$

We define

$$\Delta p_1 + \Delta p_2 = p_3 \quad ; \quad P = P_0 + \Delta P \text{ etc.}$$
$$\Delta n_1 + \Delta n_2 = n_3$$

The equations for p_3 and n_3 are the sum of the flow equa-
tions for Δp_1 and Δp_2, and Δn_1 and Δn_2 respectively,
giving us:

$$\frac{\partial p_3}{\partial t} = D \frac{\partial^2 p_3}{\partial x^2} - \mu \frac{\partial (p_3 E)}{\partial x} \qquad 1.23$$

$$\frac{\partial n_3}{\partial t} = D \frac{\partial^2 n_3}{\partial x^2} + \mu \frac{\partial (n_3 E)}{\partial x} \qquad 1.24$$

$$\frac{\partial E}{\partial x} = \frac{F}{\epsilon} (p_3 - n_3) \qquad 1.25$$

This system of equations has already been solved (1.13, 1.14,
1.15) so that the results can be written immediately as:

$$p_3 = A_1 e^{-r_1 x} + A_2 e^{-r_2 x} \qquad 1.26$$

$$n_3 = -A_1 e^{-r_1 x} + A_2 e^{-r_2 x} \qquad 1.27$$

$$E = -\frac{2F}{\epsilon r_1} A_1 e^{-r_1 x} + E_\infty \qquad 1.28$$

$$r_1^2 = K^2 \quad ; \quad r_2^2 = \gamma$$

The solution for E can now be used in the flow equation for the active ion species, $\rho_4 = \Delta \rho_2$

$$\frac{\partial \rho_4}{\partial \tau} = D \frac{\partial^2 \rho_4}{\partial x^2} - \mu \frac{\partial (\rho_2 E)}{\partial x} \qquad 1.29$$

The linearized approximation then becomes for sinusoidal time dependence:

$$j \omega \rho_4 = D \frac{d^2 \rho_4}{dx^2} - \mu C_2 \frac{2F}{\epsilon} A_1 e^{-\Gamma_1 x} \qquad 1.30$$

$$C_2 \equiv \rho_{o2}$$

Assuming a solution $\rho_4 = M e^{-\Gamma_2' x} + N e^{-\Gamma_1 x}$ we have:

$$j \omega M = M D \Gamma_2'^2$$

$$\therefore \Gamma_2'^2 = \frac{j \omega}{D} = \gamma = \Gamma_2^2 \qquad 1.31$$

$$j \omega N = N D \Gamma_1^2 - \mu C_2 \frac{2F}{\epsilon} A_1$$

$$\therefore N \cong \frac{2 \mu C_2 F}{D \epsilon K^2} A_1 \qquad 1.32$$

At low frequencies when $\Gamma_1^2 \gg \Gamma_2^2$, 1.32 reduces to:

$$N \cong \frac{C_2}{C} A_1 \qquad 1.33$$

C = total salt concentration = $p_1 + p_2$

These results can be summarized as follows:

$$E = - \frac{2F}{\epsilon \Gamma_1} A_1 e^{-\Gamma_1 x} + E_\infty \qquad 1.34$$

$$n_3 = - A_1 e^{-\Gamma_1 x} + A_2 e^{-\Gamma_2 x} \qquad 1.35$$

$$\Delta \rho_1 = A_1 \left(1 - \frac{C_2}{C} \right) e^{-\Gamma_1 x} + (A_2 - M) e^{-\Gamma_2 x} \qquad 1.36$$

$$\rho_4 = \frac{C_2}{C} A_1 e^{-\Gamma_1 x} + M e^{-\Gamma_2 x} \qquad 1.37$$

23

This procedure could be used to also establish solutions for any number of separate ion species. The matter of having different mobilities for each species takes further looking into, however.

We see from equation 1.37 that the presence of an inert electrolyte does suppress the space charge separation term in the solution for Δp_2 , but we cannot yet say it may be neglected, since the space charge term, A_1, is usually $\gg A_2$.

If we suppose that only the p_2 species reacts at the electrode we can determine the various amplitudes in terms of α , where α will stand for the complex fraction of the total current carried across the boundary by the reaction involving p_2.

The boundary conditions will be therefore:

at x = 0, flow of p_2 = $\alpha\, i_\infty / F$

flow of p_1 = 0

flow of n_3 = 0

From 1.34, 1.35, 1.36 and 1.37 these become:

$$-\mu \frac{c_2\, 2F}{D\epsilon\, r_1} A_1 + r_2 M + r_1 \frac{c_2}{c} A_1 = \frac{i_\infty}{DF}\left(\alpha - \frac{c_2}{2c}\right) \qquad 1.38$$

$$-\mu \frac{(c-c_2)2F}{D\epsilon\, r_1} A_1 + r_1\left(1-\frac{c_2}{c}\right)A_1 + r_2\left(A_2 - M\right) = -\frac{i_\infty (c-c_2)}{2DFc} \qquad 1.39$$

$$-\mu \frac{2FC}{D\epsilon\, r_1} A_1 + r_1 A_1 - r_2 A_2 = -\frac{i_\infty}{2DF} \qquad 1.40$$

Solving these equations in terms of α we have:

$$
\begin{array}{ccc}
A_1 & A_2 & M
\end{array}
$$

$$
\begin{bmatrix}
\frac{c_2}{c}r_1\delta & 0 & r_2 \\[2mm]
\frac{c-c_2}{c}r_1\delta & r_2 & -r_2 \\[2mm]
r_1\delta & -r_2 & 0
\end{bmatrix}
=
\begin{bmatrix}
\frac{i\omega}{DF}\left(\alpha - \frac{c_2}{c}\right) \\[2mm]
-\frac{i\omega\,(c-c_2)}{2DFc} \\[2mm]
-\frac{i\omega}{2DF}
\end{bmatrix}
\qquad 1.41
$$

giving

$$
A_1 = \frac{i\omega}{2DFr_1\delta}\left[\alpha - 1\right] \qquad 1.42
$$

$$
A_2 = \frac{\alpha\,i\omega}{2DFr_2} \qquad 1.43
$$

$$
M = \frac{\alpha\,i\omega\left(2 - \frac{c_2}{c}\right)}{2DFr_2} \qquad 1.44
$$

It is interesting to note that the diffuse zone term for p_2 can compare with the diffusion zone term for low enough frequencies even though $c \gg c_2$, since

$$
\frac{c_2}{c}A_1/M = \frac{\alpha-1}{\alpha}\,\frac{c_2}{c}\,\frac{1}{2\sqrt{\delta}}
$$

and $\delta \to 0$ at low frequencies (Table 1.1)

The voltage drop across the solution is given by

$$V = -\int_0^L E \, dx = i_\infty \left\{ \frac{\alpha - 1}{D \epsilon \Gamma_i \gamma} \right\} + E_\alpha L \qquad 1.45$$

$$\frac{1}{D \epsilon \Gamma_i \gamma} = \frac{1}{j \omega C_D} \qquad 1.46$$

Boundary Conditions and Fixed Layer Reactions

From our previous kinetic model calculations a voltage drop across the solution due to an impressed current was computed (1.45). This result contains an undetermined parameter, α, so that we still do not know the impedance of the diffuse layer and the diffusion zone. This parameter represents the balance between the faradaic current, which must involve a charge transfer reaction at the electrode, and the non-faradaic current, which represents the contribution from the fixed and diffuse layer capacitance. At the frequencies of interest, no significant contribution to the total current results from the volume displacement currents of the solution.

An even larger contribution to the total impedance will come from the voltage drop that takes place across the fixed layer where it is assumed the charge transfer reactions are taking place. Some space charge effects also occur in the electrode, but unless the electrode is a weak semiconductor, the impedance level is too low to contribute to the overall impedance. Even in this latter

case, the time scale for the usual semiconductor space charge phenomenon is so short, that the electrode can be considered a simple resistance at the frequencies of interest.

To complete the solution for the electrode-electrolyte system impedance, we must investigate the problem of the reaction rates of the electrode reactions. We can develop a phenomenological approach by assuming a linear law for the reaction rates. Later we can investigate the values of these parameters according to the transition-state reaction rate theory.

When making actual impedance measurements on these electrode systems, it appears that the impedance is linear for small current densities. This would imply that the functional relationship between the faradaic current and the variables that are affected by the current flow can be expressed in a Taylor expansion. If the concentrations of the species involved in the reactions are given by c_1, and the driving voltage which is assumed to act across the fixed layer is denoted by V_F, the faradaic current relationship

$$i_\alpha = f(c_i, V_F) \qquad 1.47$$

can be expressed as

$$i_\alpha = i_{\alpha o} + \sum \frac{\partial f}{\partial c_i} \Delta c_i + \frac{\partial f}{\partial V_F} V_F + \text{higher order Terms} \qquad 1.48$$

In the electrode systems we are concerned with, the electrode is considered at equilibrium with the solution so that

$$\dot{i}_{\alpha 0} = 0 \qquad 1.49$$

For very small current densities we can consider the linear approximation that neglects the higher order terms. Equation 1.48 must be coupled with our diffuse layer solutions, 1.41 and 1.45. If other species besides p_2 are involved in the reaction, equations describing their behavior must also be set up. For complicated reaction chains, the simultaneous solution of all these relationships can lead to a rich diversity of impedances. We shall see, however, that these can be broken down quite easily into a finite set of circuit elements, each element having a simple physical significance. To demonstrate this, several different reaction chains will be considered and their equivalent circuits will be developed below.

Case A $\qquad p_2 \rightleftharpoons \overline{X}$

In this case we consider that the product of the p_2 reaction is a phase of unit activity, so that the accumulation of this phase does not influence the reaction. A direct reaction between a metal and its ions would be an example of this. Therefore we have:

$$\alpha \, \dot{i}_{\infty} = V_F / \theta - \beta \, p_4 \qquad 1.50$$

From 1.37, 1.41, and 1.43 we have:

$$\frac{P_4}{i_\omega} = \frac{C_2(\alpha-1)}{2cDFr_i\delta} + \frac{\alpha\left(2-\frac{C_2}{c}\right)}{2DFr_i\sqrt{\delta}} \qquad 1.51$$

The third relationship needed can be obtained from our assumption that V_F acts across the fixed layer. In this case the displacement current will be given as:

$$(1-\alpha)\,i_\omega = j\omega C_F V_F \qquad 1.52$$

The reaction impedance is defined as:

$$Z_\alpha = \frac{V_F}{\alpha\,i_\omega} \qquad 1.53$$

From the solution of 1.50, 1.51, and 1.52 this can be expressed as:

$$Z_\alpha = R + \frac{\beta\left(2-\frac{C_2}{c}\right)R}{2F\sqrt{j\omega D}} \qquad 1.54$$

$$R = \frac{1}{1/\theta + \frac{C_2\beta KC_F}{2c}} \qquad 1.55$$

The first term represents a resistance. The second term re presents an impedance proportional to $\omega^{-\frac{1}{2}}\cdot e^{-i\pi/4}$. Such an impedance has been called a Warburg impedance, and is given a representation as a circuit element (Grahame, 1952). This idea of representing such a Warburg impedance as a circuit element (symbol -W-) is a very useful one and greatly simplifies the equivalent circuit representation of our electrode impedances, (Fig. 1.2). It is always associated with a diffusion phenomenon.

Both the resistive term and the Warburg term represent
two elements in parallel. The two resistances are given
by:

$$\theta \quad and \quad \frac{2cF}{C_2 \beta K C_F}$$

The first resistance is associated with the energy barrier
of the reaction, while the second term represents a modi-
fication that results from the space charge term in the so-
lution for p_4. The modification of the Warburg term is in
exactly the same proportion.

This reaction impedance acts in parallel with the fixed
layer capacitance, so that the combined fixed layer im-
pedance is given by:

$$Z_F = \frac{1-\alpha}{j\omega C_F} \qquad \qquad 1.56$$

From 1.45 and 1.46 we have for the solution impedance:

$$Z_S = \frac{1-\alpha}{j\omega C_D} + R_S \qquad \qquad 1.57$$

Thus we see that the impedance contribution of the diffuse
zone mirrors that of the fixed layer, so that we can write
for the electrode-electrolyte impedance:

$$Z_e = Z_F \left(1 + \frac{C_F}{C_D} \right) + R_S \qquad \qquad 1.58$$

This result is quite general and does not depend on the form
of Z_F.

Figure 1.2: Equivalent Circuit for Fixed Layer Impedance

Case A $P_2 \rightleftharpoons \overline{X}$

Case B

$$P_2 \rightleftharpoons X \xrightarrow{\text{slow}}$$
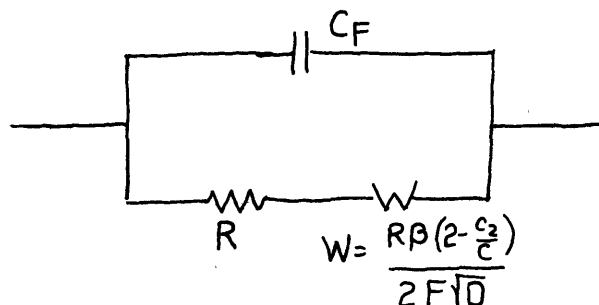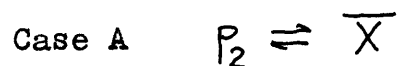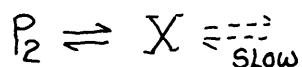
In this case we can consider X to change its activity as the reaction goes on, but X just keeps on accumulating because the reaction taking its excess away is so slow. We also consider X to be neutral. Accordingly, we have:

$$\alpha \, i_\infty = \frac{V_F}{\theta} - \beta P_4 + \gamma \Delta \overline{X} \qquad 1.59$$

$$j \omega \Delta \underline{X} = - \frac{\alpha \, i_\infty}{F} \qquad 1.60$$

together with 1.51 and 1.52.

1.59 and 1.60 can be combined into an equation of the same form as 1.50:

$$i_\alpha = \frac{V_F}{\theta'} - \beta' P_4 \qquad 1.61$$

$$\theta' = \theta \left(1 + \frac{\gamma}{j \omega F} \right) \qquad 1.62$$

$$\beta' = \beta \Big/ \left(1 + \frac{\gamma}{j \omega F} \right) \qquad 1.63$$

31

Thus we can immediately write:

$$Z_\alpha = R \left(1 + \frac{\gamma}{j\omega F} \right) + \frac{\beta \left(2 - \frac{C_2}{C} \right) R}{2F \sqrt{j\omega D}} \qquad 1.64$$

This is identical with our previous result, except that the accumulation of $\triangle x$ acts like an additional series capacitance, which is a sort of chemical capacitance:

$$C_{CH} = \frac{F R^{-1}}{\gamma} \qquad 1.65$$

Figure 1.3: Equivalent Circuit for Fixed Layer Impedance

Case B $\qquad P_2 \rightleftharpoons X \rightleftharpoons$
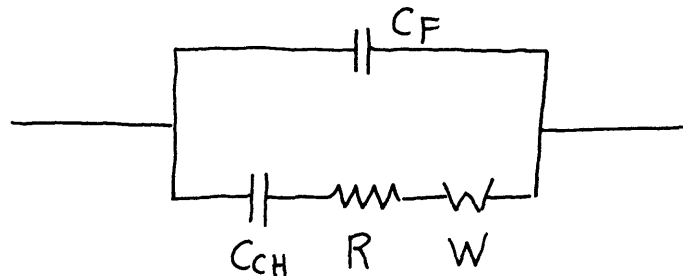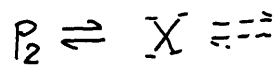
Case C $\qquad P_2 \rightleftharpoons X \xrightarrow{\text{diffusion}}$

In this case we consider $\triangle x$ itself diffusing off as a neutral molecule with diffusion constant D'.

$$\triangle \bar{X} = B e^{-\beta_2' X} \qquad 1.66$$

The diffusion flow of $\triangle x$ away from the fixed layer will be given by:

$$- \beta_2' D' \triangle \bar{X} \Big|_{\text{boundary}}$$

We therefore have:

$$j \omega \Delta X = - \frac{\alpha i_\infty}{F} - \Gamma_2' D' \Delta X \qquad 1.67$$

This modifies our previous results when combined with 1.59
to give:

$$\alpha i_\infty = \frac{V_F}{\Theta''} - \beta'' P_4 \qquad 1.68$$

$$\Theta'' = \Theta \left(1 + \frac{\gamma}{F(j\omega + \Gamma_2' D')} \right) \qquad 1.69$$

$$\beta'' = \beta \Big/ \left(1 + \frac{\gamma}{F(j\omega + \Gamma_2' D')} \right) \qquad 1.70$$

This result is identical with Case B, except that the
chemical capacitance is now in parallel with another War-
burg element:

$$W' = R\gamma / F \sqrt{D'} \qquad 1.71$$

Figure 1.4:Equivalent Circuit for Fixed Layer Impedance

Case C $\quad P_2 \rightleftharpoons X \xrightarrow{\frac{diffusion}{coef = D'}}$

33

Case D

$$P_2 \underset{\alpha i_\infty/F}{\rightleftharpoons} \bar{X} \rightleftharpoons Y \xrightarrow[coef = D'']{diffusion}$$
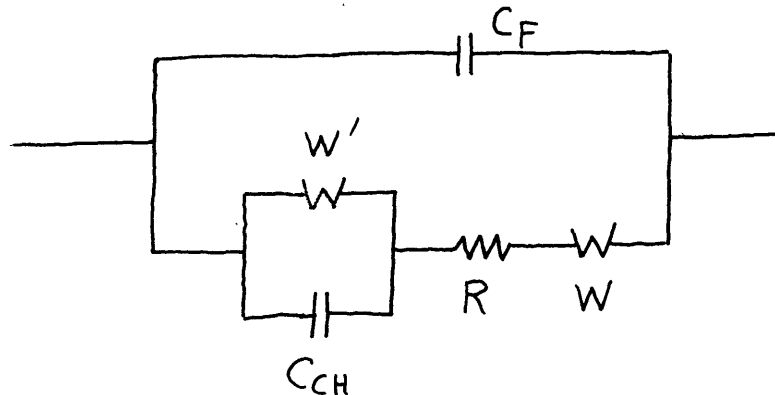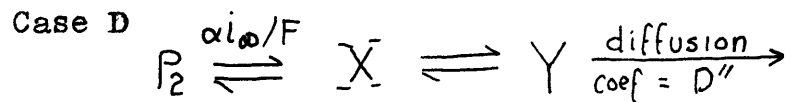
In this case we consider a model often proposed for the hydrogen reaction. p_2 is supposed to react to form a neutral atom, which in turn reacts to form a neutral molecule which can diffuse away. The additional equations needed to describe the boundary conditions are:

$$i_x = -\xi \Delta \bar{X} + \eta \Delta Y \qquad\qquad 1.72$$

$$\Delta Y = \alpha e^{-\Gamma_2'' x} \quad ; \quad \Gamma_2'' = \sqrt{j\omega/D''} \qquad 1.73$$

These equations can again be reduced until we develop an equation similar to 1.61 or 1.68. The results are shown as an equivalent circuit in Fig. 1.5.

Figure 1.5: Equivalent Circuit for Fixed Layer Impedance

Case D $\qquad P_2 \rightleftharpoons X \rightleftharpoons Y \xrightarrow{diffusion}$
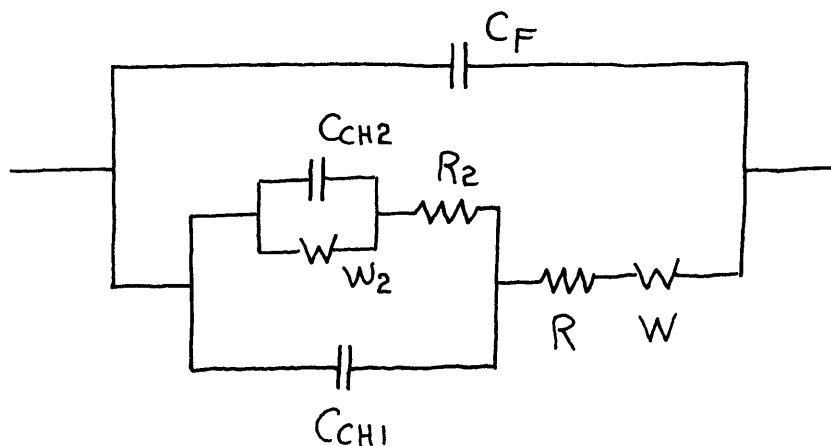
$$R_2 = \frac{\gamma}{\varsigma} R \qquad 1.74$$

$$C_{CH2} = \frac{\varsigma}{\gamma} C_{CH1} \qquad 1.75$$

$$W_2 = R\gamma\eta/F\varsigma\sqrt{D''} = R_2\eta/F\sqrt{D''} \qquad 1.76$$

Although there is no great difficulty in working out these cases, it is interesting to note that all these equivalent circuits follow a simple pattern, and they could be written down at a glance. At each point of the reaction chain the accumulation of the reaction product represents a capacitance to the electrode. The escape of the product is achieved either by diffusion, represented by a warburg impedance, or by a reaction, represented by a resistor. The product of this reaction in turn follows a similar circuit behavior. The inclusion of the diffuse layer effects does not change the equivalent circuit, but it does increase the impedance level by the fraction of the fixed layer capacitance to the diffuse zone capacitance. Typical values of the fixed layer capacitance run about 10 μf/cm^2. The diffuse zone capacitance depends on the zeta-potential and the solution concentrations. At low concentrations the voltage drop across the diffuse layer predominates over that across the fixed layer, unless very high zeta-potentials exist.

Table 1.2
(Grahame 1947)

Diffuse Zone Capacitance for Inivalent Electrolyte at 25°

zeta potential in volts

conc.	.00	.02	.04	.08	.12	.16	.20	.24
10^{-1}	72	78	96	180	378	560	1790	3900
10^{-3}	7	8	9.6	18	38	56	179	390
10^{-5}	.7	.8	1.0	1.8	3.8	5.6	17.9	39

concentrations in moles/liter, C_D in $\mu f/cm^2$

The solution resistance is of course always in series with the interface impedance.

Relaxation of Constraints

The treatment followed up to now was restricted to a rather specialized case. It was assumed that only one ion species was reacting at the electrode, that no zeta-potential existed, and that all the ions had equal mobilities. Most of these restrictions can be removed now without too much difficulty.

We shall first consider relaxing the conditions concerning the reacting ions. The system of equations describing the ion motions, 1.38, 1.39, and 1.40 are still applicable, only the boundary conditions are changed. If α_{p_i} and α_{n_i} represent the fraction of the total current carried by the p_1 and n_1 ions respectively, and if p_2 is generalized to p_i and c is generalized to $\sum p_i$, our boundary conditions become:

$$\text{flow } P_i = \alpha_i\, i_\infty / F \qquad\qquad 1.77$$

$$\text{flow} \sum_{j \neq i} P_j = \sum_{j \neq i} \alpha_{P_j}\, i_\infty / F \qquad\qquad 1.78$$

$$-\text{flow} \sum_j n_j = \sum_j \alpha_{n_j}\, i_\infty / F \qquad\qquad 1.79$$

In place of 1.42, 1.43, and 1.44 we now obtain:

$$A_1 = \frac{i_\infty}{2DF r_1 \delta} \left[\sum_j \alpha_{P_j} + \sum_j \alpha_{n_j} - 1 \right] \qquad\qquad 1.80$$

$$A_2 = \frac{i_\infty}{2DF r_2} \left[\sum_j \alpha_{P_j} - \sum_j \alpha_{n_j} \right] \qquad\qquad 1.81$$

$$M_i = \frac{\alpha_i\, i_\infty}{2DF r_2} \left[2 - \frac{c_i}{c} \right] \qquad\qquad 1.82$$

To develop the reaction impedance we now use in place of 1.50, 1.51 and 1.52:

$$\alpha_{P_i}\, i_\infty = V_F / \theta - \beta_i\, \Delta P_i \qquad\qquad 1.83$$

$$\frac{\Delta P_i}{i_\infty} = \frac{c_i \left(\sum_j \alpha_{P_j} + \sum_j \alpha_{n_j} - 1 \right)}{2cD r_1 \delta} + \frac{\alpha_i \left(2 - \frac{c_i}{c} \right)}{2DF r_1 \sqrt{\delta}} \qquad\qquad 1.84$$

$$\left(1 - \sum_j \alpha_{P_j} - \sum_j \alpha_{n_j} \right) i_\infty = j\omega C_F V_F \qquad\qquad 1.85$$

The solution of this set of equations gives us:

$$Z_{\alpha P_i} = R_{P_i} + \frac{\beta_{P_i} \left(2 - \frac{c_i}{c} \right) R_{P_i}}{2F \sqrt{j\omega D}} \qquad\qquad 1.86$$

$$R_{P_i} = \frac{1}{\dfrac{1}{\theta_{P_i}} + \dfrac{c_i \beta_{P_i} K C_F}{2cF}} \qquad\qquad 1.87$$

This solution is identical with our previous one (1.54, 1.55) and shows that each reaction impedance can be computed independently of the other reactions. This is in part due to our assumption that the concentration of the other ions did not directly affect the reaction rate of a particular ion.

If we assume all the reactions take place across the fixed layer, the reaction impedances can be considered in parallel with each other and with the fixed layer capacitance. We therefore have:

$$Z_F = 1 \bigg/ \left(j\omega C_F + \frac{\left[\Sigma \alpha_{P_i} + \Sigma \alpha_{n_j} \right] i\omega}{V_F} \right) \qquad 1.88$$

and using 1.85 this becomes:

$$Z_F = \left(1 - \Sigma \alpha_{P_j} - \Sigma \alpha_{n_j} \right) \bigg/ j\omega C_F \qquad 1.89$$

When 1.80 is incorporated into 1.45 we obtain for the solution impedance:

$$Z_S = \frac{1 - \Sigma \alpha_{P_j} - \Sigma \alpha_{n_j}}{j\omega C_D} + R_{Solution} \qquad 1.90$$

This means that our relation 1.58 is unchanged by the inclusion of many reacting species and we still have:

$$Z_e = Z_F \left(1 + \frac{C_F}{C_D} \right) + R_{Solution}$$

The relaxation of the condition limiting the zeta-potential is a much more complicated algebraic problem. Our previous solutions, however, justify an approximation that can easily handle this situation. This approximation is simply that the diffuse layer space charge effects represent an equilibrium with the instantaneous zeta-potential. The justification of this assumption comes from noting that the space charge term in 1.13, $A_1 e^{-\Gamma_1 X}$ is in phase with V_D, and independent of frequency as long as $\delta \ll 1$. Thus for the low frequencies of interest to our study, the space charge effects are virtually the same as those for the DC case. The charge separation that this term brings amounts to a net charge in the diffuse layer = Q_D. The diffuse layer capacitance is defined as the slope of this charge: zeta-potential relationship:

$$C_D = \frac{\partial Q_D}{\partial (zeta\ potential)} \qquad 1.91$$

The charge in the diffuse layer can only change if a non faradaic current flows, thus:

$$\frac{dQ_D}{dT} = \left(1 - \sum \alpha_{p_j} - \sum \alpha_{n_j}\right) i_\infty \qquad 1.92$$

$$C_D = \frac{dQ_D}{dT} \frac{dT}{dV_D} \qquad 1.93$$

This result leads directly to 1.90, except that it is no longer limited to a zero zeta-potential situation. One has merely to use for C_D the exact expression based

on the DC assumptions given previously in 1.1. (see Table 1.2).

A similar modification can be made in the fixed layer impedance on the term involving the charge separation concentration change. This is the term

$$\frac{C_i \left(\mathcal{E} \alpha_{p_j} + \mathcal{E} \alpha_{n_j} - 1 \right)}{2c \, D F r_i \, \delta}$$

in 1.84. This reduces to

$$\Delta \rho_i = - C_i \, V_D \, F / RT \qquad\qquad 1.94$$

at the boundary. This space charge contribution is equal to the static term in the case of zero zeta-potential, since for the static case

$$\rho_i = C_i \, e^{- \psi_0 \, F / RT} \qquad\qquad 1.95$$

As long as the space charge term is following the diffuse layer voltage we can handle its contribution to the impedance by using the static solution. Thus we free ourselves from the zero zeta-potential limitation for low frequencies, $\delta \ll 1$, by redefining R in 1.87

$$R_{p_i} = 1 \Big/ \left(\frac{1}{\Theta_{p_i}} + \frac{C_i \, e^{- \psi_0 F / RT} \, K \, C_F \beta_{p_i}}{2cF} \right) \qquad 1.96$$

$$R_{n_i} = 1 \Big/ \left(\frac{1}{\Theta_{n_i}} + \frac{C_i \, e^{\psi_0 F / RT} \, K \, C_F \beta_{n_i}}{2cF} \right) \qquad 1.97$$

Relaxing the third restriction so that the ion mobili-
ties are constant does not involve any new mathematical
techniques, but it does add a great deal to the algebraic
complexity of the solution. It is probable that the re-
sults will not differ very much from our previous results.
A Warburg term would be added to the solution resistance
because of the diffusion potentials set up in the solu-
tion, but the magnitude of this term would be less than
the solution resistance of a path length equal to the
diffusion length, and is certainly small compared to the
actual electrode impedance. A similar situation is
treated fully by Marshall (Marshall, 1959).

Another constraint that was used to simplify the alge-
bra was the assumption that all the ions were univalent.
The simplicity of our results is essentially due to the
fact that at low frequencies the diffusion effects are
uncoupled from the space-charge effects, and this fact
is not altered by the modifications we are treating in
this section. The inclusion of higher valency ions does
influence the space charge distribution, but again we
should expect no change in the general form of the solu-
tion. As an example, if we assumed the positive ions
to be divalent, 1.2 and 1.4 would become:

$$\frac{\partial p}{\partial t} = D_p \frac{\partial^2 p}{\partial x^2} - \mu_p \frac{\partial (2pE)}{\partial x}$$ 1.98

$$\frac{\partial E}{\partial x} = \frac{F}{\epsilon} (2p-n)$$ 1.99

1.3 would remain unchanged. The solution of this system of equations for small perturbations gives us:

$$\Delta p = A_1 e^{-\Gamma_1 x} + A_2 e^{-\Gamma_2 x} \qquad 1.100$$

$$\Delta n = B_1 e^{-\Gamma_1 x} + B_2 e^{-\Gamma_2 x} \qquad 1.101$$

$$\Gamma_1^2 = K^2 \left(\tfrac{5}{2} + \delta \right) \qquad 1.102$$

$$\Gamma_2^2 = \gamma \qquad 1.103$$

$$B_1 = -\tfrac{1}{2} A_1 \qquad 1.104$$

$$B_2 = 2 A_2 \qquad 1.105$$

This solution indicates that the diffuse layer thickness is inversely proportional to the root mean squared valency, while the space charge concentrations are directly proportional to the valency. The diffusion terms are unaffected, except for the obvious correction for the greater number of negative ions resulting from a given salt concentration.

In most ground waters and in our experimental studies the preponderance of ions are univalent.

Limits on the Linear Behavior

The restriction that limits the current density to small values is of course fundamental to the entire linear treatment. It is observed in practice that the impedances are linear for current densities of 10^{-7} amps $/$ cm^2 or less at the low frequencies (.01 cps.). At higher frequencies more current can be passed without any appreciable non-linearity. We have not as yet discussed any theory for the reaction rates, but it seems reasonable that if the applied voltage is less than .025 volts, which represents the thermal energy at room temperature, it should either represent a small perturbation on the activation energy level, or the activation barrier is so low it does not represent any significant impedance to the current flow.

The space charge solution (1.94) behaves linearly for Δp_i if the diffuse layer voltage V_D is $\ll$ .025 volts. Since V_D is usually a fraction of the total applied voltage, this condition is automatically taken care of if the previous condition is upheld. At very low concentrations it may not be possible to approach .025 volts too closely.

The linearity condition of the diffusion term M_i cannot be discussed in terms of voltages until we know the values of the reaction rate parameters θ_i and β_i .

We can however, investigate the magnitude of M_1 in terms of the current flow, and make certain that $M_1 \ll c_1$. From 1.82 we can put this condition as:

$$i_\infty \ll DF\Gamma_2 C_i / \alpha_i \qquad\qquad 1.106$$

Assuming that $\alpha_i = 1$, and using a typical value of D, this condition reduces to:

$$i_\infty \ll f^{1/2} C_i \qquad\qquad C_i \text{ in moles/liter}$$

When the reacting ion has a concentration of 10^{-5} moles / liter, our linearity is threatened at .01 cps. even with a current density of only 10-7 amps $/ cm^2$.

Using the reaction rate predictions to be discussed later, this criteria can be reduced to a voltage criteria independent of frequency, concentration, and α. It again leads to the value of .025 volts as the voltage level one must keep well under to uphold the linearization criteria. At higher frequencies, however, the impedance is controlled by the solution resistance and the fixed layer capacitance which remain linear, so that one is not so aware of non-linearities in the other processes.

Reaction Rate Theory Predictions

Much of the literature in electrochemistry makes use of Eyring's transition state reaction rate theory

(Glasstone, Laidler, and Eyring, 1941), and much of the experimental work on electrodes is evaluated in terms of the parameters of this theory (Bockris, 1954). An excellent and short discussion of the basic premises and shortcomings of this theory is given by Denbigh (1955).

The theory is developed around the assumption that the reacting species at the saddlepoint of the reaction path form a phase, alled the activated complex, which is in equilibrium with the reactants. Conversely, the activated complex when considered as going from product to reactant, is in equilibrium with the product. It is further assumed that the velocity of the forward and backwards reactions are proportional to the population of the activated complexes, and to the vibration frequency of the translational motion involved in going through the reaction.

When it is assumed that one vibration is enough to send the activated complex over the hump, the theory leads to expressions for the forward and backwards rate of the reaction:

$$\nu_a A + \nu_b B + \cdots \underset{\overset{\leftarrow}{X^{\ddagger}}}{\overset{\overrightarrow{X}^{\ddagger}}{\rightleftharpoons}} \nu_c C + \nu_d D + \cdots \qquad 1.107$$
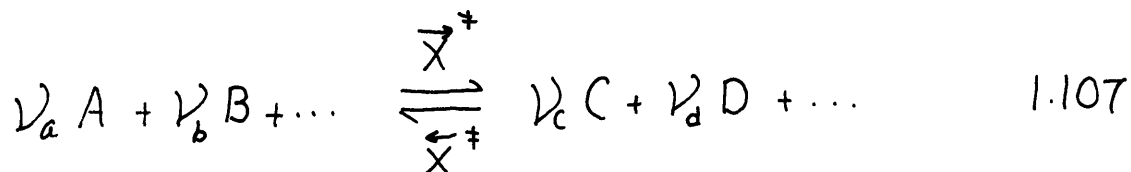
given by

$$\text{forward rate} = \frac{kT}{h} a_a^{\nu_a} a_b^{\nu_b} \cdots e^{-\overrightarrow{\Delta G_o}^{\ddagger}/RT} \qquad 1.108$$

$$\text{backward rate} = \frac{kT}{h} a_c^{\nu_c} a_d^{\nu_d} \cdots e^{-\overleftarrow{\Delta G_o}^{\ddagger}/RT} \qquad 1.109$$

a_i, stands for the activity of the i'th species. $\Delta G_0^{\ddagger}$ is not quite the standard free energy change between the activated complex and the regular phase, because the contribution from the translational vibration of the complex has been removed. It does, however, include an electric potential term.

If the reaction involves a single charge, the electric potential term for the forward rate would be $-aV_F/RT$, and for the backwards rate $(1-a)V_F/RT$. aV_F represents the fraction of the total driving potential V_F that changes the relative energy levels of the reactant and the activated complex, and $(1-a)V_F$ the fraction that changes the level between the activated complex and the product. See Fig. 1.6.

Figure 1.6: Effect of Applied Voltage on Energy Barriers of $A \rightleftharpoons C$ Reaction

Free energy

Distance
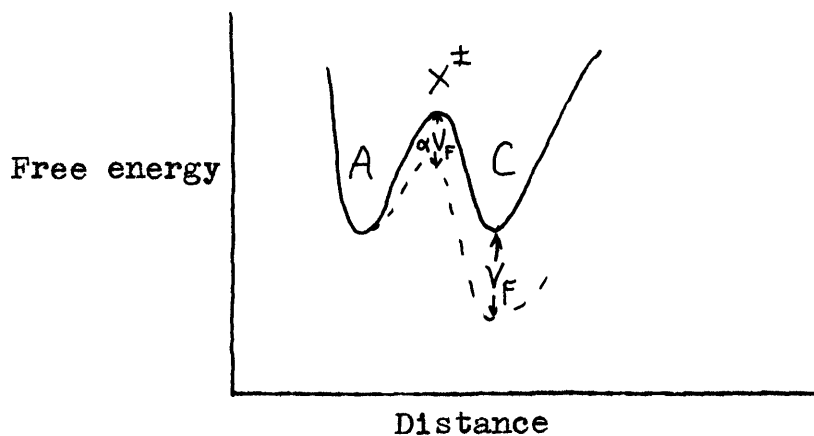
At equilibrium the forward rate equals the backward rate. In electrode processes it is common to call these equilibrium rates, the exchange current, i_o. It must be remembered that i_o is a function of the activities of the reactants or of the products.

When equation 1.108 and 1.109 are expanded about the equilibrium value we can write for a linear approximation:

Forward rate $= i_o + \dfrac{i_o}{a_a^{\nu_a}} \nu_a a_a^{\nu_a-1} \Delta a_a + \cdots \dfrac{\alpha F}{RT} i_o V_F$ 1.110

Backward rate $= i_o + \dfrac{i_o}{a_c^{\nu_c}} \nu_c a_c^{\nu_c-1} \Delta a_c + \cdots - \dfrac{(1-\alpha)F}{RT} i_o V_F$ 1.111

net flow $i_\alpha = i_o \left\{ \nu_a \dfrac{\Delta a_a}{a_a} + \cdots - \nu_c \dfrac{\Delta a_c}{a_c} - \cdots + \dfrac{F V_F}{RT} \right\}$ 1.112

When these factors are matched with the constants in the linear rate laws, such as in equation 1.59, the reaction rate theory gives us:

$$\theta = RT/F i_o \qquad\qquad 1.113$$

$$\beta = i_o \nu_{P_2} / P_2 \qquad\qquad 1.114$$

$$\gamma = i_o \nu_x / x \qquad\qquad 1.115$$

A similar set of relations would define ξ and η of equation 1.72 in terms of the concentrations X and Y, and another "exchange current."

Very often the experimental electrochemists are primarily interested in the non-linear behavior of electrode processes as a function of V_F, and use the reaction rate formulas to explain their observations. From such

observations they derive values for the parameters of the theory (i_o, α , $\Delta G_o^{\ddagger}$). An extensive listing of such determinations is given in Bockris (1954) for hydrogen evolution reactions, metal deposition reaction, oxygen evolution reactions, and certain redox reactions. i_o is the only parameter needed in the linear case at equilibrium, and the values listed range from 10^{-1} to 10^{-16} amps / cm^2. Most of the measurements were made in concentrated solutions, so that the reaction rate formulas would predict smaller i_o's in more dilute solutions. The dangers of too rigid an acceptance of the reaction rate theory predictions is pointed out by data on the hydrogen evolution reaction on Cu. Similar values of i_o are listed for the reaction in .1 N HCl and in .15 N NaOH, although the hydrogen ion concentrations differ by a factor of 10^{12}.[*]

[*] Glasstone, Laidler, and Eyring point this out as an indication that the reaction must simply involve water molecules. (Glasstone et al. 1941, p.588). This explanation ignores the fact that OH^- ions are involved in the reaction they assume, and that the theory predicts the backwards reaction is dependent on its concentration. This should mean then that in order to maintain equilibrium the potential acting across the fixed layer will have to adjust itself for different OH^- concentrations, until the energy levels for the activated complex and the reactants result in no net flow. Unless the activated complex is unaffected by the electric potentials, this should result in a new value of i_o.

It is possible, of course, that the surface conditions are greatly affected by the solution PH, and that the observed result was due to the changes in the activation energy. Other factors such as the smoothness or cleanliness of the surface might have been different for the two measurements mentioned, for in electrode measurements such extraneous fac-

tors often play a very important role.

Our phenomenological treatment, of course, did not depend
on any specific rate theory, but it appears useful to use
the rate theory and the listed rate theory parameters to
feel out the relative importance of the various equiva-
lent circuit elements derived in our previous treatment.
The equivalent circuits derived from a series of reaction,
such as that given in Fig. 1.5 can become quite complica-
ted, but it is very likely that certain elements of the
circuit are relatively unimportant in the frequency
ranges that one works with.

The reaction rate formulas 1.108 and 1.109 are written
for reactions taking place throughout the volume; when
the reactions are confined to a surface, one must redefine
the concentrations or activities as surface concentrations.
Inasmuch as the ratio

$$\frac{\Delta a \text{ surface}}{a \text{ surface}} = \frac{\Delta a \text{ volume}}{a \text{ volume}}$$

is valid, the equations 1.113 to 1.115 defining θ , β ,
and γ in terms of i_0 are unchanged. The definition of
i_0 however, must be given with surface concentrations.

Before examining the relative importance of the various
reaction steps of the total impedance, we can investigate
the importance of the diffuse layer on modifying R and the
Warburg impedance W. From 1.96 and 1.97 the relative

importance of the diffuse layer term is given by:

$$\frac{C_i}{C} e^{\pm \psi_0 F / RT} \quad \frac{KC_F}{2F} \beta_i \theta_i$$

From 1.113 and 1.114 this reduces to

$$\frac{\nu_i RTKC_F}{2CF^2} e^{\pm \psi_0 F / RT}$$

If we set $C_F = 10 \mu f / cm^2$ this ratio becomes 10^{-2} or $10^{-3} x e^{\pm} \psi_0 F / RT$ for concentrations of 10^{-5} or 10^{-3}

moles / liter respectively. Thus it would seem that except for situations involving large zeta-potentials of the proper sign, and very dilute solutions, the reaction resistance can be set equal to θ . Of course the diffuse zone has a role in contributing impedance, because of the diffuse zone capacitance, in inverse proportion to the value of the diffuse zone capacitance.

Looking at the individual impedance elements, we can compare the importance of R and W using 1.113 and 1.114.

$$\frac{R}{W} = \frac{F \sqrt{D\omega}}{\beta} \cong \frac{C_i (freq)^{1/2}}{i_0} \qquad C_i \text{ in } moles/liter \qquad 1.116$$

If we assume that the surface concentration is proportional to the mole fraction of a species, and if we use 10^{15} molecules per sq. cm. as the water molecule surface concentration, i_0 can be defined, using 1.108 as:

$$i_0 \cong F \frac{kT}{h} \left(\frac{C_a 10^{15}}{3.3 \, 10^{25}} \right)^{\nu_a} \cdots e^{-\Delta G_0^{\ddagger}/RT} \qquad 1.117$$

If we further assume a simple univalent ion reaction, 1.116 can be written as

$$\frac{R}{W} \cong (freq)^{1/2} \, 5.5 \, 10^{-8} \, e^{\Delta G_o^{\ddagger}/RT} \qquad 1.118$$

For an activation barrier of 10 K cal / mole the resistance and Warburg impedances should be about equal at one cycle per second. The heat of activation ΔH can be deduced from measurements at different temperatures, but because of the entropy term this does not determine $\Delta G_o^{\ddagger}$. From the listings of typical values of i_o one would expect R to be larger than W even at .01 cps.

The Warburg impedance W is independent of the activation energy, and assuming $c_i \ll c$, and $R \cong \Theta$ we have, using 1.54, 1.113 and 1.114:

$$W \cong \frac{2.5 \, 10^{-2}}{C_i \, (freq)^{1/2}} \qquad c_i \text{ in moles / liter} \qquad 1.119$$

The chemical capacitance resulting from the accumulation of the produce X can be compared to W again independently of i_o. Using 1.65 we have:

$$\frac{W}{1/\omega C_{CH}} \cong 6 \cdot 10^{5} \cdot (freq)^{1/2} \, \frac{X \, \nu_R}{C_i \, \nu_x} \qquad 1.120$$

Unless the concentration X is extremely low, the impedance of the chemical capacitance is much smaller than the Warburg term in the frequency range of interest.

When further reactions involve the product X, such as in Case D, the added circuit elements bear the same relationship to each other as the elements just discussed, provided the

appropriate concentrations and i_o's are used.

These results can be summarized by redrawing the equivalent circuits with only the most important impedance elements. These simplified circuits are shown in Fig. 1.7 in order of increasing complexity.

Figure 1.7: Simplified Equivalent Circuit for Fixed Layer
Impedance
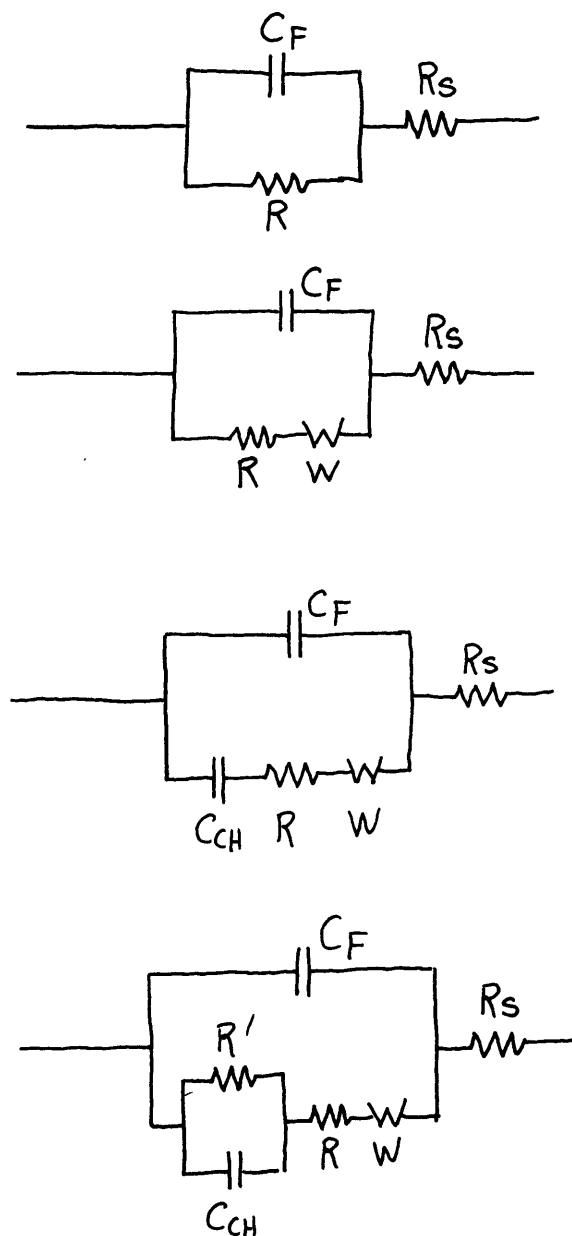
When other ions also react at the electrode, or when
the electrode is not homogeneous, the impedance representing
these reactions will also be parallel to C_F.

CHAPTER II

EXPERIMENTAL STUDY OF ELECTRODE IMPEDANCES

In Chapter I a model was developed to explain the electrical properties of electrode-solution interfaces. This model assumed a linear dependence of the reaction rates on the parameters involved, and predicted an impedance equal to that of relatively simple equivalent circuits with fixed elements. These results are identical to those discussed by Grahame (1952). By incorporating the transition state reaction rate theory, and taking account of the details of the ion motions in the solution, these equivalent circuit elements could be evaluated in terms of the equilibrium exchange current of the reaction, and the concentration of the ion species and reaction products in the solution. The derivation of the ion motion was dependent on an electrode model that has given good results with ideal polarized electrodes. The reaction rate theory is probably less certain.

To test these ideas, measurements on non-ideal polarized electrodes are needed under many different conditions. For this reason impedance measurements were undertaken over a wide range of frequencies on metal and semiconducting electrodes with different solutions and at several temperatures. This empirical data is of direct use in the geophysical applications of induced polarization that motivated this study, but electrochemists may balk at the crudeness of electrode preparation. No efforts were made to secure

ideal conditions of cleanliness and smoothness for the electrode surfaces. It was believed that our measurements would correspond more closely to the actual conditions encountered in the polarizing of the naturally occuring metallic minerals in rocks. The results of our measurements agree quite closely, we shall see, with those taken in other laboratories under much more careful experimental conditions.

The experimental data was also compared to the theoretical solutions developed in Chapter I. A program was written for the IBM 704 to analyze the measured impedances in terms of parameters of the theory. This program was made flexible enough to handle a wide variety of theoretical cases, and to use data given in several different forms. In this way it was hoped that data from other laboratories could also be analyzed. Some very interesting results were obtained from data published by Jaffe and Rider (1952). The significance of these results was not as apparent in their original article due to the form of their theoretical treatment.

In Fig. 1.7 the most likely equivalent circuits for electrode impedances are shown. These were based on reaction rate theory parameters that were obtained in most cases from measurements at high current densities. There is a good possibility that reactions that were unimportant in the high current density measurements, will contribute to

the measured impedance at low current densities. In almost all the impedance measurements reported in the literature (Randles, 1947; Hillson, 1954; Jones and Christian, 1935; Jaffe and Rider, 1952) the results could be explained by a simple equivalent circuit of a Warburg impedance in parallel with the electrode capacitance, both in series with the solution resistance. Hillson pointed out that these results indicated a highly catalyzed reaction was taking place at the electrode. This is in agreement with the theory given in Chapter I, for the reaction resistance must be very small to be unimportant compared to the Warburg impedance at audio frequencies.

Experimental Procedure

The experimental results just quoted were obtained using a rather limited frequency range, and were never extended to the subaudio frequencies that are of interest in induced polarization measurements. The results were also obtained using two similar electrodes. Any imbalance in the relative importance of the parameters in the two electrodes would require using two equivalent circuits in series to describe the impedance, and would greatly complicate the analysis. Such considerations were involved in the design of our impedance measurements. To obtain a wide enough frequency coverage, measurements were made using a KronHite Model 400-A oscillator. This provided a range of frequencies from

.01 to 1000 cps. To simplify the analysis, one electrode was a reversible electrode with a large surface area so as to have a low impedance. Silver-silver chloride electrodes were used for this purpose. To insure a simple geometry the polarized electrodes were imbedded in plastic, so that only their front faces were exposed to the solutions. The plastic holders were set at a fixed distance from the reversible electrode. This distance was chosen to insure no interaction between the diffusion zones of the electrodes at the low frequencies, and yet keep the solution resistance small so that the electrode impedance at the higher frequencies could be observed. The separation used was .3 cm. When measurements at elevated temperatures were made, the electrode apparatus was placed in a pressure chamber to prevent evaporation of the solution.

The electrodes used included copper, stainless steel, nickel, and graphite rods, pyrite, galena, and magnetite minerals. The magnetite and galena electrodes were not imbedded in plastic. The magnetite sample was actually a rock sample with a magnetite zone running through it, and both ends of the rock acted as electrode surfaces.

Because the electrodes were not identical, self-potential differences existed between them that had to be bucked out by an external voltage source to keep the system at equilibrium. A few measurements were made with a net DC

current flow taking place across the system.

The output from the oscillator was used to drive a current across a large resistor in series with the electrode system. The voltage across the electrode system was compared with the driving voltage by means of a Lissajou pattern on an oscilloscope, and from this measurement the electrode impedance was computed. The overall accuracy of the measuring system was about $\pm$ 5% .

No difficulties were encountered concerning the stability of the electrodes during the measurement period provided the electrodes were allowed to reach equilibrium before the measurements were started. Care had to be taken to allow enough cycles of current of a given frequency to establish the sinusoidal steady state of response of the electrode system. At the lowest frequency this took many minutes. The absence of distortion in the Lissajou pattern was used as a check on the linearity of the system. When proper shielding was used, there was little difficulty in working with voltages small enough to insure a linear behavior.

Equivalent Circuit Fitting

As was mentioned previously, the impedance data was compared to the theoretical solutions by attempting to find an equivalent circuit having the same impedance as the electrode. This fitting procedure was done on an I.B.M.

704 computer. The computer assumed a basic equivalent
circuit as shown in Fig. 2.1, and systematically altered
the values of the circuit parameters to improve the fit.
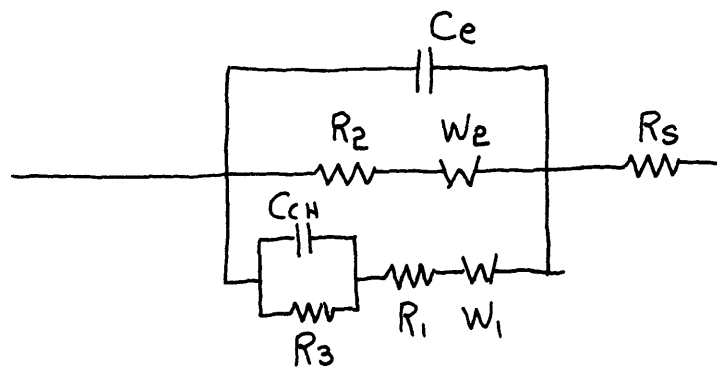
Figure 2.1 Basic Equivalent Circuit

The basic circuit could be simplified by merely assigning
open or short circuit values for certain parameters, and
not adjusting them further. The computer could also be
told to test the variation of a parameter over those fre-
quencies where it was felt the parameter contributed
significantly to the impedance. These steps helped speed
up the convergence of the adjustment, and the machine
could handle a case in about 30 seconds. The program
was written to accept data given in any of four different
forms. The four forms were: amplitude and phase values
of the impedance, Lissajou figure values together with
the value of the series resistor and scope impedance,
and bridge measurements with parallel or series RC circuits.

Since the circuit parameters are constrained to have only

positive values, the fitting procedure is essentially a non-linear problem, and a rigorous analysis of the iteration scheme would be very difficult. The techniques of the Simplex Method could probably be used on this problem, but the simple trial and error approach used worked well enough. Occasionally the scheme would get off to a bad start and adjust itself to a "meta-stable" minimum error, but in the great majority of runs the iterations worked smoothly.

The general picutre presented by the fitting results is that the equivalent circuits used have a real significance. The average root mean squared percentage error of the equivalent circuits was 6.5%. Since the impedances usually varied throughout the frequency range by a factor of more than 100:1, the errors in the magnitude of the impedance of the equivalent circuit are hardly noticeable. The errors in the phase of the equivalent circuit are easy to spot, and a qualitative judgement on the closeness of fit could be made from a comparison of the phase shifts. On this basis 7 cases were classified as close fits, 6 cases as fair fits, 1 case as a crude fit, and 2 cases as poor fits. Close fits were also achieved with the 7 cases reported by Jaffe and Rider.

A comparison of the impedance of the electrodes and the fitted equivalent circuits are shown in Fig. 2.2 through

IMPEDANCE STAINLESS STEEL ELECTRODE

.014 N KCL
T = 23°C

RMS ERROR
CIRCUIT FIT = 5.1%

.014 N KCL
T = 80°C

RMS ERROR
CIRCUIT FIT = 7.4%

FIG. 2.2

IMPEDANCE NICKEL ELECTRODE

.014 N KCL
T = 23°C

θ

Z

RMS ERROR
CIRCUIT FIT = 7.3%

FREQUENCY

CPS

.014 N KCL
T = 80°C

θ

Z

RMS ERROR
CIRCUIT FIT = 4.5%

FREQUENCY

CPS

FIG. 2.3

IMPEDANCE COPPER ELECTRODE

.014 N KCL
T = 23°C

RMS ERROR
CIRCUIT FIT = 10.1%

.014 N KCL
T = 80°C

RMS ERROR
CIRCUIT FIT = 4.1%

FIG. 2.4

63

GRAPHITE ELECTRODE A

.02 N KCL
T=23°C

RMS ERROR
CIRCUIT FIT = 7.1%

GRAPHITE ELECTRODE B

.02 N KCL
T=23°C

RMS ERROR
CIRCUIT FIT = 8.3%

FIG. 2.5

64

IMPEDANCE GRAPHITE ELECTRODE B

.011 N KCL
T = 25° C

RMS ERROR
CIRCUIT FIT = 9.9%

.011 N KCL
T = 80°C

RMS ERROR
CIRCUIT FIT = 6.4%

FIG. 2.6

65

IMPEDANCE GRAPHITE ELECTRODE B

.01 N KCL
T = 25°C
PH = 3.8

RMS ERROR
CIRCUIT FIT = 6.0%

.01 N KCL
T = 25°C
PH = 10

RMS ERROR
CIRCUIT FIT = 6.0%

FIG. 2.7

66

IMPEDANCE MAGNETITE ELECTRODES

SAT. NACL
T = 23°C

θ

Z

RMS ERROR
CIRCUIT FIT = 6.7 %

FREQUENCY

IMPEDANCE PYRITE ELECTRODE

.014 N KCL
T = 23°C

Z

θ

RMS ERROR
CIRCUIT FIT = 8.6 %

FREQUENCY

FIG. 2.8

IMPEDANCE Ag-Cl ELECTRODE

SAT NACL
T = 23°C

Z

θ

RMS ERROR
CIRCUIT FIT = 5.1%

IMPEDANCE GALENA ELECTRODE

SAT NACL
T = 23° C

θ

Z

RMS ERROR
CIRCUIT FIT = 9.0%

FIG. 2.9

68

IMPEDANCE Ni ELECTRODES
(Jaffe' and Rider)   .01 N KCL

RMS ERROR
CIRCUIT FIT = 6.8%

.005 N KCL

RMS ERROR = 6.0%
CIRCUIT FIT

FIG. 2.10

IMPEDANCE Ni ELECTRODES
(Jaffe' and Rider)

.002 N KCL

RMS ERROR
CIRCUIT FIT = 4.3 %

.001 N KCL

RMS ERROR
CIRCUIT FIT = 5.2 %

FIG. 2.11

IMPEDANCE Ni ELECTRODES
(Jaffe' and Rider)

.0005 N KCL

RMS ERROR
CIRCUIT FIT = 2.8 %

.0001 N KCL

RMS ERROR = 2.9%
CIRCUIT FIT

FIG. 2.12

Fig. 2.12. The equivalent circuit impedance is given by the solid curves, and the experimental points are given as circles and squares. Both the amplitude and phase are shown, and the rms. percentage error is also given.

Experimental Results

The existence of some sort of an equivalent circuit representation for the electrode is a natural consequence of the linear assumptions used. It seems very likely that if enough elements are introduced into the equivalent circuit a fit can always be obtained. [This is not strictly true. For instance, none of the boundary conditions considered could lead to an impedance increasing with frequency.] The real test of the theory is based more on predicting the magnitude of the circuit parameters and their dependence on other variables.

The most outstanding result of our measurements is the presence in every case, of a reaction involving essentially no reaction resistance. This reaction monopolizes the current flow over a large part of the observed frequency range, and leads to the Warburg impedance obtained by many observers in the audio frequency range. At the lower frequencies other parameters begin to influence the impedance.

From a crude analysis that had been made on electrode

impedances previously (Madden et al, 1957), it was
believed that the electrode capacitance could often
be masked, perhaps by a surface poisening. This
effect did not appear with the present measurements,
using a more accurate analysis, except in two cases.
These cases involved a pyrite electrode, and a copper
electrode at $100^{o}C$. In both cases the electrode had
undergone a good deal of oxidation, and such a result
was not unexpected. The occurence of a catalysed reaction
at the electrode was not inhibited, however.

At the low end of the frequency spectrum used, most of
the electrodes began to behave more purely resistive
again. This was the reason for including R_2 in the
equivalent circuit. Such a parallel resistive path is
very necessary to explain the data.

R_2 can represent a great many different reactions, each
with its own activation barrier, just as long as each
reaction impedance is monopolized by the resistive compo-
nent. When factors such as a Warburg impedance or a
capacitive effect become important, one would probably
need a circuit for each reaction. In the frequency
range in which the measurements were carried out, this
did not seem necesasary, with the aforementioned exception
of the pyrite sample.

The electrode impedances sometimes showed a new trend

Table 2.1

Summary of Electrode Impedances

Values are given for 1 cm^2 of surface at room temp.
Symbols are referred to Fig 2.1

Electrode	Reaction Resistance R_2	Electrode Capacitance C_e	Catalysed Reaction Resistance R_1	Warburg Impedance at 1 cps. W_1	Chemical Capacitance C_{CH}
Stainless steel	160,000	3.2	11	3960	247
Ni	8,500	112	3	670	830
Cu	3,080	3.8	19	1270	55,000
Graphite	49,500	80	26	2700	170
Pyrite	3,900	15	60	800	150,000
Galena*	3,800	8.5	6	760	43,000
Magnetite*	222,000	4.8	101	5,870	106

*area not known
  accurately

resistances given in ohms
capacities given in μf

beginning to appear at the lowest frequencies which tended to hold back the decay of the phase shift. C_{CH} and R_3 were included in the equivalent circuit as the most likely parameters modifying the catalysed reaction. Their influence on the overall impedance was usually minor, and thus less significance can be attached to the values obtained for these parameters. W_2 and R_3 were usually left out of the equivalent circuit completely.

In Table 2.1 typical equivalent circuit parameters are listed for the various electrodes. These represent room temperature measurements. The table emphasizes the low reaction resistance, and shows a rather narrow range of Warburg impedance values. The electrode capacities all appear a bit low, except for the nickel and graphite electrodes. It is well known that graphite tends to have a high effective area, and it is possible that the unpolished nickel rod did also. The impedance levels for these electrodes were not substantially lower than those for the other electrodes, so that the scale of any surface roughness must have been very small (compared to the diffusion length). A more likely explanation is that the other electrodes had small electrode capacities due to some surface poisening, but this surface poisening did not hinder the charge transfer reactions.

In Chapter I it was shown how the transition state reaction rate theory led to an evaluation of these circuit parameters in terms of the concentration of the reacting ion species and the activation energy barrier $\Delta G_o^{\ddagger}$. If we assume a value for the diffusion coeffeicient the concentration of ion species is derived from the magnitude of the Warburg impedance using equation 1.119. The reaction resistance depends both on the concentration and the activation energy, but the ratio of the reaction resistance and the Warburg impedance gives information concerning $\Delta G_o^{\ddagger}$. This relation is given in equation 1.118.

In Table 2.2 the results of such calculations are given for the catalysed reaction. There is also included in this table values derived from other experimentors. Randles analysed his electrode impedances at audio frequencies in terms of an R_2, W_2, and C_e, but he did not list his electrode areas. These were calculated, however, by running some of his computations backwards.

The Jones and Christian data is too limited to derive anything other than the approximate magnitude of a Warburg impedance, so that no attempt was made to compute $\Delta G_o^{\ddagger}$.

There is a surprising uniformity of these results, especially when one considers the usual difficulties in getting reproducible results from electrode measurements. If we can

Table 2.2

Effect of Electrodes on Electrode Parameters

Electrode	Solution	Concentration of reacting ion C_i in moles/liter	Standard free energy change of activated complex in Kcal/mole	Investigator
Stainless steel	.014 N KCL	$.63 \times 10^{-5}$	6.5	Madden
Ni	.014 N KCL	3.7×10^{-5}	6.8	"
Cu	.014 N KCL	2.0×10^{-5}	7.5	"
Graphite	.02 N KCL	$.93 \times 10^{-5}$	7.3	"
Pyrite*	.014 N KCL	3.1×10^{-5}	8.5	"
Galena*		3.0×10^{-5}	7.1	"
Magnetite*	saturated NaCL	4.3×10^{-5}	7.6	"
Hg	1 N $HClO_4$ 5×10^{-3}N V_{aq}^{2+}/V_{aq}^{3+}	17.3×10^{-5}	8.6	Randles
Hg	1 N KCN 1×10^{-3}N $Cr(CN)_6^{4-}/Cr(CN)_6^{3-}$	17.6×10^{-5}	7.0	"
Pt	1 N KCL 1×10^{-3}N $Fe(CN)_6^{4-}/Fe(CN)_6^{3-}$	5.4×10^{-5}	6.95	"
Ag	.1 N $AgNO_3$	12.5×10^{-5}	(approximate)	Jones and Christian
Ag	.01 N $AgNO_3$	10.7×10^{-5}		"
Ag	.02 N KNO_3	4.9×10^{-5}		"
Ag	.01 N KI	17.2×10^{-5}		"

*electrode area known only approximately

Table 2.2 (continued)

Effect of Electrodes on Electrode Reaction Parameters

Electrode	Solution	Concentration of reacting ion C_i in moles /liter	Standard free energy change of activated complex in Kcal /mole	Investigator
Ni	.01 N KNO_3	.67 x 10^{-5}		Jones and
Ni	.01 N $Ni(NO_3)_2$	.58 x 10^{-5}		Christian
Pt(smooth)	.015 N KCL	4.6 x 10^{-5}		"
Pt "	.01 N KCL	4.9 x 10^{-5}		"
Pt(Platinized)	.01 N KCL	192 x 10^{-5}		"
Ni	.01-.0001 N KCL	.55 x 10^{-5}	5-7.6	Jaffe and Rider
Cu	.01 N $CuSO_4$	.27 x 10^{-5}	6.9	Hillson
Cu	.025N "	.30 x 10^{-5}	7.3	"
Cu	.025N "	.34 x 10^{-5}	7.1	"
Cu	.025N "	.44 x 10^{-5}	6.6	"
Cu	.05 N "	.44 x 10^{-5}	7.6	"

It appears to the authors that a positive identification of the actual reaction at these very low current densities is a major problem in these electrode studies. One is tempted to postulate that water must be involved, but this would involve hydroxyl or hydrogen ions, and would imply a strong dependence on the solution PH. Such an effect was not found when measurements were made on the graphite electrodes.

The insensitivity of the electrode impedance to the major constituents of the solution is very well demonstrated by the data obtained by Jaffe and Rider (Jaffe and Rider 1952) with Ni electrodes. Their impedance data was quite extensive in the frequency range 18-18,000 cps, and was evaluated along with the authors' data by the 704 program. Because of the frequencies involved, only Ce, Rs, W_1 and R_1 were used in the equivalent circuit fit. The results of these calculations are given in Table 2.3.

<div align="center">

Table 2.3

Effect of solution concentration on
electrode impedance parameters

Ni electrodes, KCL solution   (Jaffe and Rider)

</div>

conc of KCL moles/liter	R_S $\Omega\text{-cm}^2$	C_F $\mu f/cm^2$	W_1 $\Omega\text{-cm}^2$	R_1 $\Omega\text{-cm}^2$	C_1 moles/liter	$\Delta G_o^{\ddagger}$ Kcal/mole
.01	16.6	6.0	4,170	1	$.6 \times 10^{-5}$	4.9
.005	32.4	5.84	4,210	1	$.595 \times 10^{-5}$	4.9
.002	76.2	5.95	4,770	6.5	$.525 \times 10^{-5}$	6.1
.001	152	5.4	4,720	8.3	$.53 \times 10^{-5}$	6.2
.0005	290	5.6	4,380	45	$.57 \times 10^{-5}$	7.3
.0001	1210	3.9	4,950	85	$.505 \times 10^{-5}$	7.6

In these results the electrode capacity and the Warburg impedance are essentially independent of the KCL concentration. The solution resistance depends linearly with the inverse of the salt concentration as is to be expected. The reaction resistance is not an important part of the electrode impedance, but it does show a definite trend with the KCL concentration.

The effect of changing the PH is shown in Table 2.4. Again those parameters that influence the impedance are essentially unaffected by drastic changes in the PH. In fact the results on different days showed greater variation than the results taken under different conditions but within a short time of each other. The first two rows in Table 2.4 represent runs made on different days, while the two runs at PH 10 and 3.8 were made within the same day.

The R_2 values are too small compared to the solution resistance to be known with any degree of certainty, and little significance can be attached to the $\Delta G_o^{\ddagger}$ values computed.

The vast changes in the H^+ and OH^- ion concentrations had such little effect on the Warburg impedance, it is difficult to visualize their having any connection with the electrode reaction.

The effect of temperature on the electrode impedances is summarized in Table 2.5. Again in computing C_1 a typical ion diffusivity for the temperature was used.

Table 2.4

Effect of PH on electrode impedance parameters

Graphite electrode B

solution	PH	reaction resistance R_2 $\Omega-cm^2$	electrode capacitance C_e $\mu f/cm^2$	catalysed reaction resistance R_1 $\Omega-cm^2$	Warburg impedance at 1 cps W_1 $\Omega-cm^2$	Reaction rate theory parameters C_1 moles/liter	$\Delta G_o^{\pm}$ Kcal/mole
.02 N KCL	7	460,000	41	31	3,980	.63 x 10^{-5}	7.1
.014 N KCL	7	456,000	33	(1)	1,610	1.55 x 10^{-5}	(5.5)
.01 N KCL	10	136,000	38	(1)	1,150	2.2 x 10^{-5}	(5.5)
.01 N KCL	3.8	98,000	41	(1)	1,210	2.1 x 10^{-5}	(5.5)

Table 2.5

Effect of temperature on electrode impedance parameters

electrode	T	reaction resistance R_2	electrode capacity C_e	catalyzed reaction resistance R_2	Warburg impedance at 1 cps W_2	Reaction rate theory parameters C_i	$\Delta G_o^{\ddagger}$
	C	$\Omega\text{-cm}^2$	$\mu f/\text{cm}^2$	$\Omega\text{-cm}^2$	$\Omega\text{-cm}^2$	moles /liter	Kcal /mole
st, steel	23	160,000	3.2	10.5	3,960	$.65 \times 10^{-5}$	6.5
	80	28,600	3.6	1	1,760	$.9 \times 10^{-5}$	---
Ni	23	8,500	112	3.1	670	3.7×10^{-5}	6.8
	80	1,700	74	.38	192	8.3×10^{-5}	8.4
Graphite	23	456,000	33	1	1,610	1.55×10^{-5}	---
	80	10^7	47	1	600	2.6×10^{-5}	---
Cu	23	3,080	3.8	19	1,270	2.0×10^{-5}	7.5
	100	1,670	0	9.2	510	2.9×10^{-5}	10.5
Pyrite	23	3,800	1.5	60	805	3.1×10^{-5}	8.5
	100	370	0.23	198	620	2.4×10^{-5}	12.9

Some of the electrodes showed so much oxidation at the
elevated temperatures, one would not expect to find much
correlation with the room temperature measurement. This was
especially true of the copper and pyrite electrodes.
The outstanding variation, however, was the disappearance of
the electrode capacitance for the copper electrode. A
similar result appeared with the pyrite electrode, but the
equivalent circuit fit was poor, and there was a poor electrical
contact to the pyrite mineral itself. There is no evidence
that the oxidation hindered the charge transfer reaction to
any extent.

Conclusions.

Our primary motivation in this study was to obtain a feeling
for the possible electrode polarization impedance magnitudes.
In this connection our results appear amazingly simple.
In all the measurements made or referred to from the literature,
the predominant factor at low audio frequencies was a Warburg
impedance, and this impedance was of the same order of magnitude
for every case. The behavior of the different electrodes
began to diverge more at lower frequencies when other parameters
began to be more important. The explanation of these results
is not such a simple matter, however. The transition state
reaction rate theory leads one to the conclusion that the reaction
involves ions with a concentration of about $1\text{-}10\text{x}10^{-5}$ moles/liter,
and a standard activation free energy level of about 7 Kcal/mole
above the ion energy level.

The theory also leads to the conclusion that the active ion concentration does not seem to be affected by the salinity, PH, or temperature of the solution, and the activation energy barrier is relatively similar on all surfaces. It appears to the authors that such conclusions are very difficult to accept. There appear to be two possible weaknesses to the theory we have been applying in these studies. One possible weakness is the use of a linear geometry for the diffusion processes in the solution.

When considering the possibilities of a different geometry, one should mention the work of Erdey-Gruz and Vollmer (1931). They suggest that often the rate determining step is the diffusion of an activated metal molecule along the surface from an active spot to the point where it enters into the crystal structure. Their electrical measurements were essentially D.C. measurements and our own results indicate that at the very low frequencies other reactions begin to take over the conduction process. There is a further difficulty in the theory as applied to the results given in this chapter, when one considers the magnitude of the impedance parameters. First of all, the limitation of the reaction to a few active spots greatly increases the Warburg term resulting from diffusion in the solution to these spots, unless the spacing of the active spots is small compared to the diffusion lengths. Hillson (1954) in his experiments with Cu: $CuSO_4$ electrodes assumed that the copper ions were involved in the reaction and used the magnitude of Warburg term to find the total area of these active spots.

His Warburg values, however, were no different from those obtained in very dilute solutions by other experimentors, and one would almost expect that, if he had used very dilute solutions, he would have been forced to abandon his argument for active spots, or at least admit their effective area was large.

The diffusion along the surface also presents a problem insofar as the magnitudes of the Warburg impedances are concerned. The geometry of the problem is more difficult, and the results will depend on factors such as the size of the active zones which is not known, and the surface diffusivity. The thickness of a monolayer of Cu atoms is only about 2×10^{-8} cm., but this geometric factor can be offset if there exists a large number of hot spots. The diffusion along the surface of the reaction product is an impedance which acts in series with the ordinary Warburg term. This theory does not seem to offer us an explanation of the impedance values measured, since the metal ions in solution should contribute a Warburg term that is too large. The main problem still appears to be an identification of the reacting ions.

The other weakness is, of course, the reaction rate theory itself. Before undertaking to change the theory, however, it would seem worthwhile to make a somewhat more extensive and better controlled experimental study.

For instance, most experimentors did not control the amount of
dissolved gases in their solutions, although they represent
very likely contributors to any electrode reaction. (In our
own measurements, when high temperature runs were made, the
volume of the system was kept constant, so that little change
in the dissolved gases was probably realized. The changes in
PH were made in such a short time that little gaseous exchange
could take place.) The circuit fitting procedure should prove
useful in any extended study, and it is hoped that other
laboratories will be able to make use of it, or similar programs.

Chapter III

ELECTRIC CONDUCTION AND POLARIZATION IN ROCKS
Theoretical Considerations

Simple Model Predictions

We know from studies previously referred to (Marshall and Madden, 1959) that only electrode and membrane polarization can lead to the observed polarization effects in rocks. The studies just reported in the first two chapters and those reported in Dr. Marshall's thesis (Marshall, 1959) should give one a fairly complete picture of the detailed nature of the polarizing mechanisms, but one must also consider the electrical environment within the rocks before attempting to predict or interpret their polarization properties. The simplest model of the electrical environment within a rock could be represented by an ordinary fluid zone, representing the pore passageways, in series with electrode or membrane zones, representing the blocking effect of the metallic minerals or clay and other membrane materials. It is further assumed that the conduction within the pore fluid is ionic conduction, taking place uniformly throughout the pore channels, and that the electrode and membrane zones completely blocked certain of these passages. The electrical impedance of such a system is given by two elements in series. One element will be a simple resistance representing the

resistance of the fluid conduction paths of the pore
passages and the other element will be the polariza-
tion impedance of the electrode or membrane zones.
The pore fluid resistance will depend on the ion concen-
tration and the temperature of the fluid, and in Table
3.1 are given some typical values.

Table 3.1

Resistivity of Common Electrolytes at $25^\circ C$(in ohm cm.)

electrolyte conc	.001	.01	.05	.1	N
KCL	6800	700	150	80	
NaCL	8000	840	180	95	
HCL	2300	230	50	25	

The electrode polarization impedance might be expected
to vary considerably, but the studies reported in Chapter
II show that this was not the case. Throughout much of
the frequency range of interest the electrode impedance
was primarily represented by a Warburg impedance. This
impedance is due to a diffusion flow phenomena, and its
magnitude was found to be relatively independent of the
type of electrode or of the salt concentration of the
fluids. At higher frequencies the electrode impedance
is eventually determined by the electrode capacity, and
at the lower frequencies the electrode impedance was
determined by a reaction resistance. These two para-
meters were much more variable for the different electrode

for the different electrode types. The frequencies at
which these various parameters control the electrode
impedance are shown in Table 3.2.

Table 3.2

Parameters Controlling Electrode Impedance

electrode	frequency below which electrode predominantly resistive	Warburg behavior	frequency above which electrode predominantly capacitive
st. steel	.01		150
Ni	.005		4
Cu	.2		1000
Graphite	.01	$Z \approx 2000\ f^{-\frac{1}{2}}\ \Omega \cdot cm^2$	.6
Pyrite	.04		150
Galena	.04		700
Magnetite	.01		25

Because of the predominant role played by the Warburg impedance
and because of the rather consistent nature of the Warburg
impedance, we can use our simple model to predict the impedance
of a mineralized rock. The parameters for such a model would
be the average separation between the metallic minerals block-
ing a given pore passageway, and the salt concentration in the
fluid of the pores. The effect of parallel unblocked paths
can be eliminated by considering the metal factor rather
than the impedance of the rock. The results of such calcula-
tions are given in Figure 3.1, where we have assumed a
resistivity for the pore fluids of 5,000 ohm-cm. In Figure 3.2

FREQUENCY DEPENDANCE OF SIMPLE MODEL OF MINERALIZED ROCK

L = AV. PORE LENGTH BETWEEN BLOCKING INTERFACES

P OF PORE SOLUTION = 5000 Ω cm.

L = .01 cm

L = 0.1 cm

L = 1 cm

L = 10 cm

METAL FACTOR (RELATIVE VALUES)

FREQUENCY IN CPS

Fig. 3.1

FREQUENCY DEPENDANCE OF MINERALIZED ROCKS

$(F)^{1/2}$

THEORETICAL
MODEL
L = .01cm

$(F)^{1/4}$

L =.01cm

AVE. OF
4 SAMPLES

L = .1cm

THEORETICAL MODEL L= 0.1cm

METAL FACTOR (RELATIVE VALUES)

1   10   100   1000   10,000

FREQUECY IN CPS
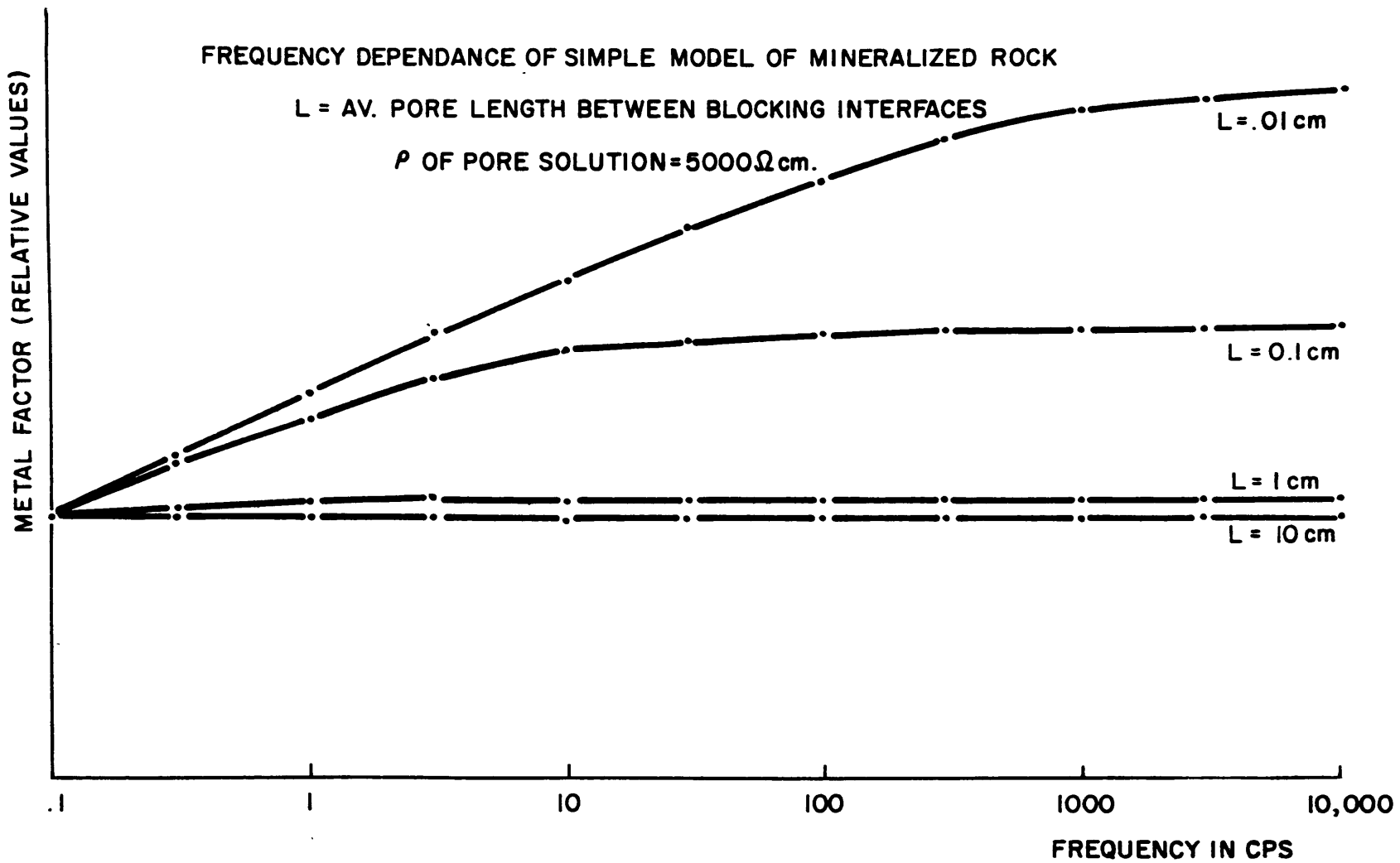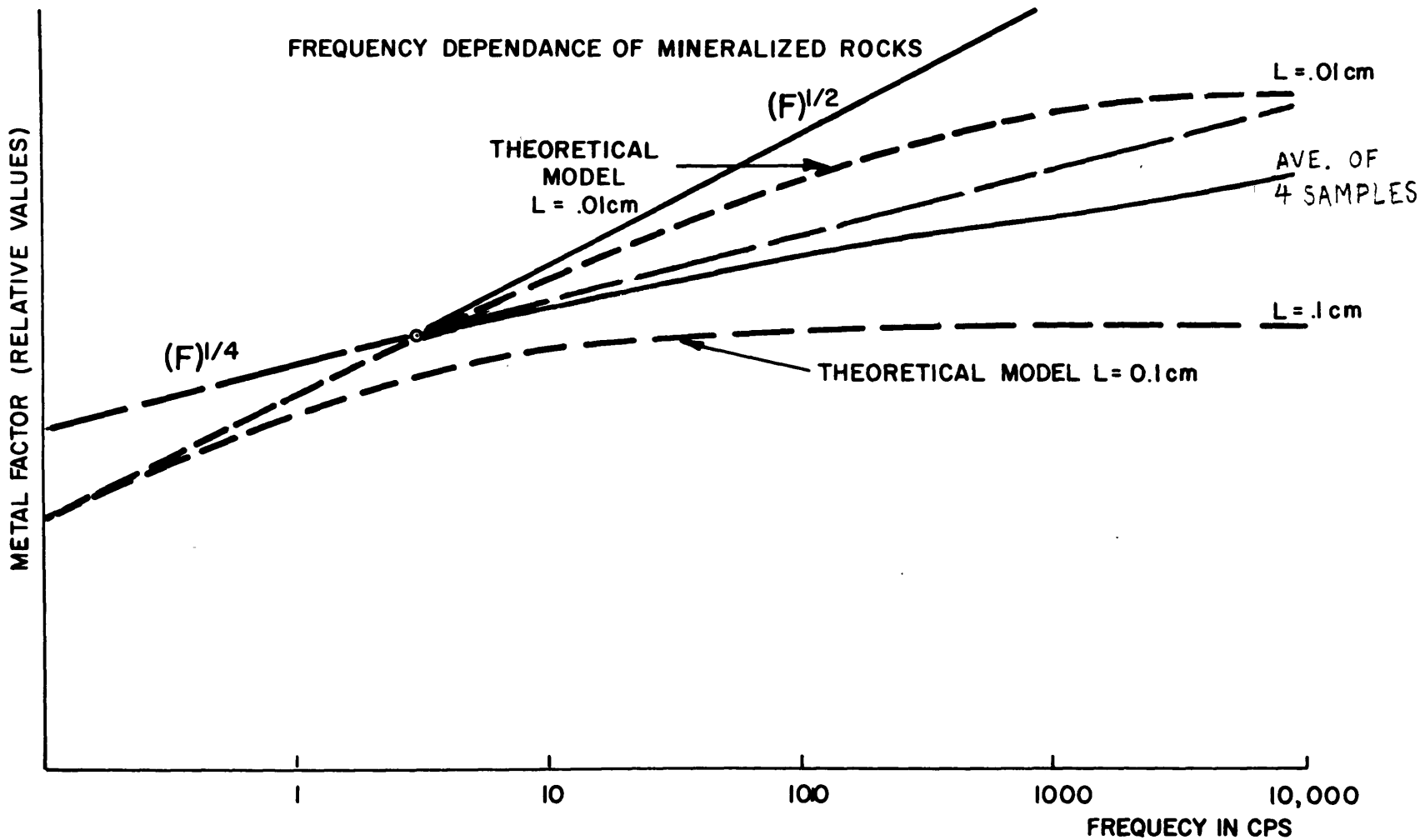
Fig. 3.2

are shown some typical results on actual mineralized rock samples. The rocks were kept immersed in water with a resistivity of 5000 ohm-cm.

The model results shown in Figure 3.1 would imply that the frequency effects for the polarization of a metallic-mineral-bearing rock should take place only at very low frequencies. To cause frequency effects in the audio range it was necessary to assume an average pore length of only .01 centimeters. The actual rock samples, some of whose results are given in Figure 3.2 show no appreciable tendency for their frequency effects to die off at the higher audio frequencies. It is extremely unlikely in any of these samples, however, that the spacing between the metallic minerals amounts to anything as small as .01 centimeters. It should also be noticed that the metal factor increases with frequency not as (frequency)1/2, but more like (frequency)1/4. It is quite apparent from these results that a better understanding of the electrical properties of these rocks is necessary before one can expect to understand fully their polarization properties.

Porosity, Tortuosity and Effective Pore Conductivity

It has been shown that too simple a model for the electrical environment within a rock can lead to a very poor prediction for the polarization properties of the rock. In order to better aquaint ourselves with the electrical environment a short series of experiments were undertaken to check

various aspects of this environment. Studies of the temperature dependance of the conductivity were made to try and gain a better insight into the medium through which the current carriers move. Other studies were made measuring the rate of diffusion into the rocks to gain an insight into the geometry of the pore passages along which the current flowed. Measurements were also made with changes in the salinity of the interstitial water, to study the effective conductivity of the pore fluids. These studies are an off-shoot of our main investigation into induced polarization, and therefore we will not develop them in great detail.

The theory of rate processes shows that the temperature dependance of the rate process gives information concerning the molecular energy barriers that must be overcome to carry out the process (Glasstone, Laidler and Eyring, 1941).

If the electric current is carried by ions moving through interstitial water, we would expect the temperature dependance of the resistivity to be the same as that of the viscosity of water. In Figure 3.3 we have shown the results of these temperature measurements. There is a good deal of scatter in the points shown in Figure 3.3, but there is no real indication that the mechanism of conduction is other than we have assumed. It is so well established that the conductivity of a rock at ordinary temperatures is due to its fluid content, that these temperature measurements would hardly seem worthwhile. The measurements do however, indicate that the physical properties of water within the rock are
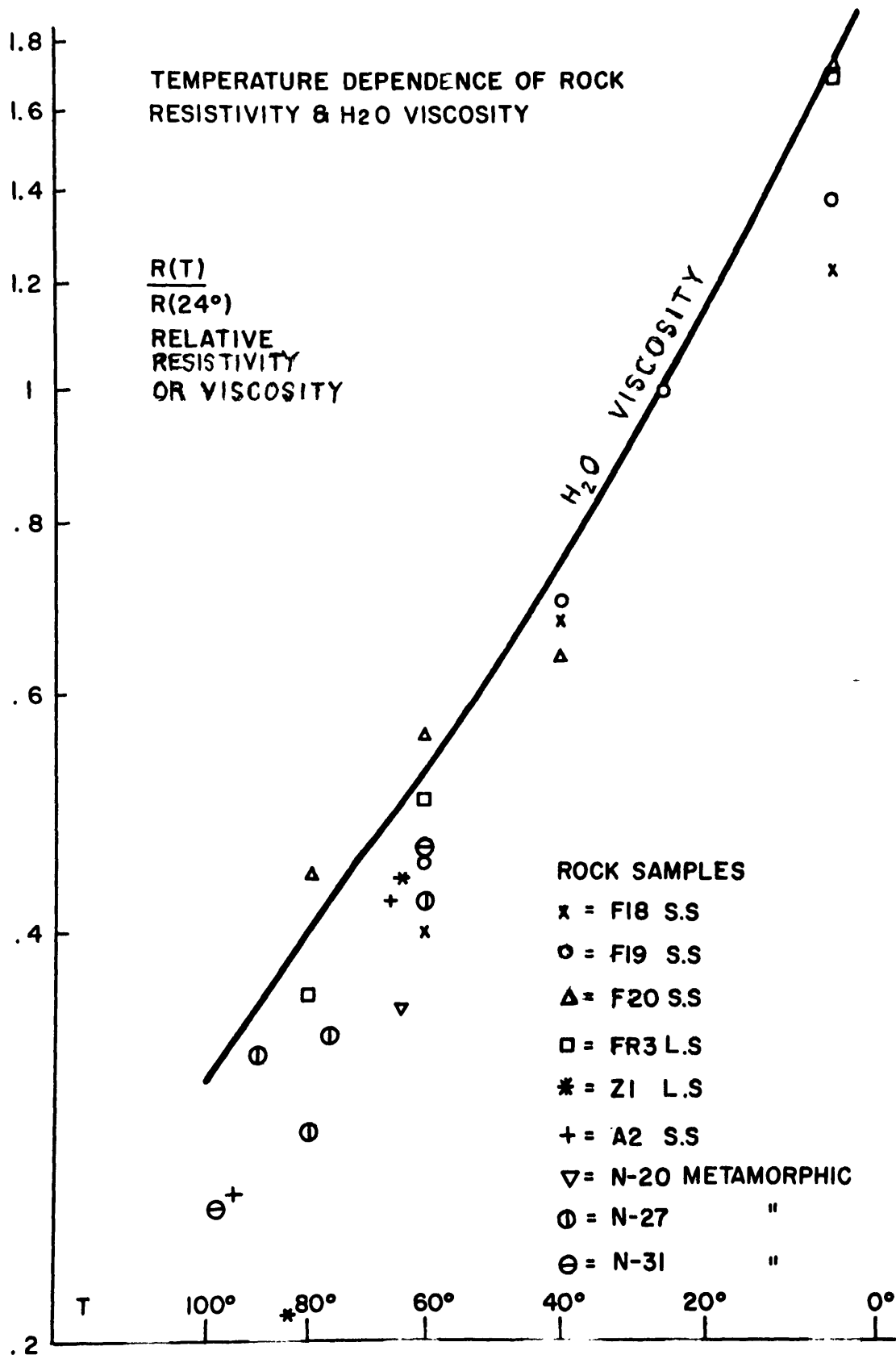
Fig. 3.3

probably not very different from those of ordinary water.
We should therefore expect for instance, that the ion
diffusivity within the rock pores should be the same as
in ordinary water.

One sample, marked "Z1" did show a rather anomalous high
temperature conductivity which could be duplicated on
repeated measurements. This sample is a limestone sample
with no apparent metallic minerals, exhibiting polarization
properties, and also posessing rather pronounced membrane
properties, (Madden et al, 1957). It is believed that
an explanation of its high temperature conductivity might
come from assuming that the sample lost its ability to
discriminate against the passage of negative ions at higher
temperatures. The evidence that the sample lost its
membrane properties at higher temperatures comes from the
observation that the polarization effects were also lost.
The remaining samples however, appear entirely normal.
Their polarization effects were independent of temperature,
but this is to be expected as long as the polarization is
due to diffusion effects and is controlled by the viscosity
of the pore fluids.

There is some indeterminancy in evaluating these temperature
results, as the surface ion concentrations can also vary
as a function of temperature. When the temperature runs
are made rapidly however, the ions do not have time to
diffuse in or out of the sample, and the measured effect can

be considered due to the viscosity changes.

Once we have established the diffusivity of the ions within
the pore fluids, we can use diffusion studies to tell us
something about the geometry of the pore passageways. Dif-
fusion measurements were made by coating cylindrical rock
samples so that only the end surfaces were exposed, and
immersing these samples into a fluid of high salinity. The
rate of diffusion of salt into the rock was then measured
by measuring the resistivity of the rock as a function of
time. The analysis of this problem is identical to the
heat flow problem, and is treated in standard texts such
as Carslaw and Jaeger, (1948). Their analysis shows that the
conductivity after a brief rapid initial change, approaches
the final conductivity exponentially, the exponent being
proportional to the diffusivity of the medium, and inversely
proportional to the square of the dimensions.

$$\sigma = \sigma_{Sat.} - A \sum \frac{1}{n} e^{-Dn^2 4\pi^2 T/l^2} \qquad 3.1$$

$$\sigma \cong \sigma_{Sat} - A e^{-D4\pi^2 T/l^2} \qquad ; \quad T > \frac{l^2}{16 D\pi^2} \qquad 3.2$$

An exactly similar analysis can be made to study the de-
salting of these specimens. In this case the conductivity
would be given by:

$$\sigma \cong \sigma_o + B e^{-D4\pi^2 T/l^2} \qquad 3.3$$

If several different independent pore systems existed
within the rock, each with a characteristic geometry,
this expression would appear as:

$$\sigma \cong \sigma_0 + \sum B_i e^{-D4\pi^2\tau/L_i^2} \qquad 3.4$$

In these equations L_i represents the effective length
of the pore passageways. L_i is invariably greater than
L, the sample length, and it is usual to attribute this
difference to the tortuosity of the pore passageways.

$$L_i = \tau_i L \qquad 3.5$$

A typical result is shown in Fig. 3.4, the solid curve
here represents a fitting using two independent pore
passageways whose geometry was determined by a gra-
phical fit to the data. In Table 3.3 is listed a
summary of these measurements giving the pore geome-
tries calculated by means of these diffusion studies.
It is seen from this table that a good deal of the
conductivity of these rocks is associated with pore
passageways showing an extremely large effective
length. A different explanation for these very slow
diffusion times might be that there exists a good many
dead-ended passageways which do not contribute to the
flow of the ions but do contribute to the total volume
of the pore fluids. In Fig. 3.5 are shown the two
extreme interpretations for tortuosity.

One might expect that the two geometries can be

CONDUCTIVITY IN ARBITRARY UNITS

CONDUCTIVITY DECREASE
DUE TO DIFFUSION OF NaCl
OUT OF ROCK SAMPLES

SAMPLE LENGTH = 4 CM.

TIME IN DAYS
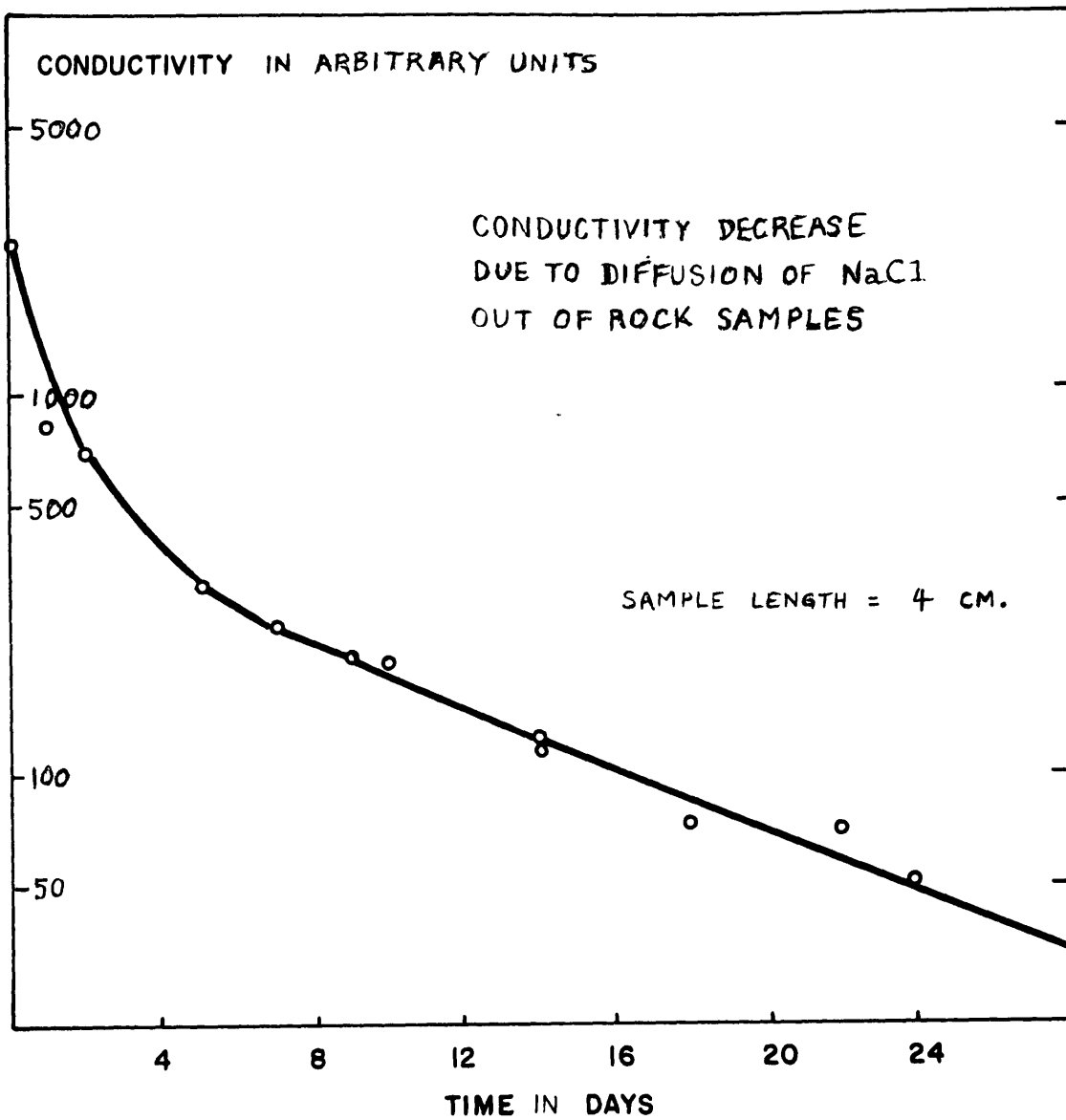
Fig. 3.4

Rock no. + type	τ_1	τ_2	A_1	A_2	$\dfrac{\rho\text{ rock saturated}}{\rho\text{ NaCl}}$	computed porosity %	measured porosity %
19 met.	1.1	3.1	.45	.55	1900	.31	.53
32 ign.	3.4	11.2	.94	.06	1800	1.02	.26
30 ign.	3.6	9.2	.96	.04	4450	.35	.26
S-2 met.	.94	8.9	.50	.50	7100	.57	.57
M-3 met.	3.1	5.8	.50	.50	6050	.36	.48
M-33 met.	1.6	3.4	.67	.33	2100	.25	.21
M-21 met.	2.6	8.2	.98	.02	1490	.53	.43
M-5 met.	3.0	10.6	.95	.05	1380	1.03	.59
S-51 met.	2.8	7.0	.64	.36	4200	.54	1.98
M-27 met.	2.1	5.5	.58	.42	5500	.28	.50
S-6 met.	1.4	5.0	.93	.07	9900	.04	.27
21A ign.	2.6	8.1	.98	.02	1600	.51	.52
21B ign.	2.6	8.3	.98	.02	1550	.52	.43
16 met.	3.0	–	1.00	–	1670	.54	.64
F19 sed.	4.0	–	1.00	–	680	2.4	3.2

Table 3.3

Tortuosity and Porosity Data on Typical Tight Rocks

$$\frac{\partial C}{\partial t} = \frac{\partial^2 C}{\partial s^2}$$

$$N\frac{\partial C}{\partial t} = \frac{\partial^2 C}{\partial x^2}$$

$\mathcal{T} = \frac{s}{x}$ = EXCESS LENGTH FACTOR

$\mathcal{T}^2 = N$ = EXCESS VOLUME FACTOR
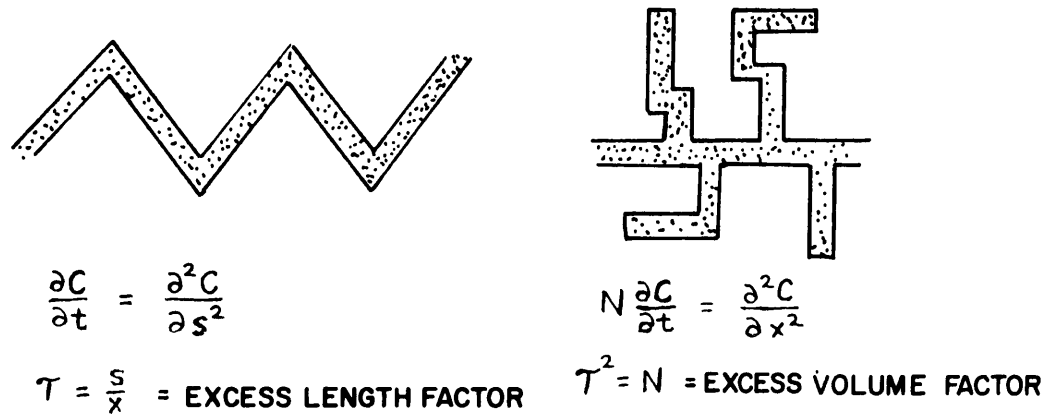
Fig. 3.5 Interpretations of Tortuosity.

NO. OF
SAMPLES

$\begin{bmatrix} \text{MEDIAN POROSITY} \\ \text{OF SAMPLES} = 0.5\% \end{bmatrix}$

5   10   20   50   100   200   500   1000
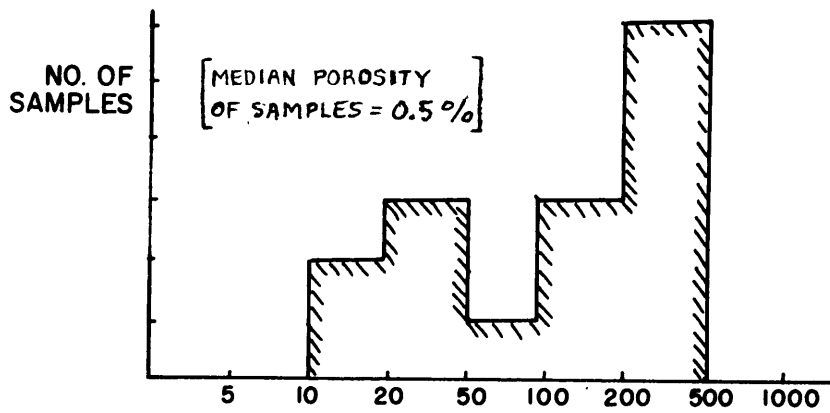
Fig. 3.6 Increase of Rock Conductivity for 1000x Increase of Fluid Conductivity.

Z_1 Z_1 Z_1 Z_1 $Z_1^{-1} = \sigma$ SURFACE

Z_2 Z_2 Z_2 Z_2 = ELECTRODE IMPEDANCE
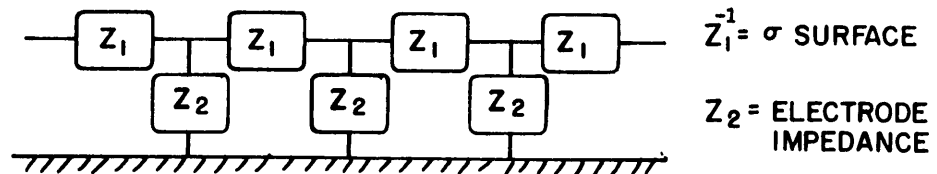
Fig. 3.7 Equivalent Circuit for Conduction Along Interface

differentiated by making resistivity and porosity
measurements on the samples, but the relationship
between the diffusion time and the resistivity-porosity
ratio are not independent. The porosity is given as:

$$p = \sum_i A_i F \tau_i^2$$

A_i = fraction of conduction associated with
tortuosity τ_i

F = resistivity factor = $\dfrac{\rho_{rock}}{\rho_{solution}}$

whether τ_i is considered as the excess length of the
pore passages or τ_i^2 is considered as the excess volume
of the pores.

If a more detailed investigation is made of the transient
flow through such porous media, it can be shown that the
two models behave differently during the early stages of
the transient, (Fatt 1959,1960). Unfortunately, the data
collected does not allow us to attempt such an analysis,
and we can only deduce the same generalized tortuosity
that appears in Fig. 3.6

A comparison of this computed porosity with a measured
porosity is helpful, however, in checking the reasonableness
of the assumptions made in computing the tortuosity. The
porosity measurements were made by weighing the samples
when saturated with fluid and then heating them for a
period of several hours at a temperature of about 120° C.
allowing them to cool in a desicator and then weighing the

samples dry. Estimates of the porosity can also be made from resistivity measurements with the saturated solution by using equation 3.6, and the diffusion-determined tortuosities. The aggreement is reasonably good, and indicates that in many samples a large fraction of the total fluid volume is associated with high tortuosity pore passages. The most likely interpretation of these high tortuosity values is that there exists a good deal of interconnectivity between the pore passageways, and that these interconnecting ways represent excess volume. This of course is quite reasonable when we consider the pore passageways to consist of the interstices between the rock-forming minerals. This picture also presents more possibilities for any metallic minerals present in the rock to be blocking passageways capable of passing current. The comparison between the measured and computed porosities is, of course, further evidence that the diffusivity of the ions is associated with the properties of ordinary water.

A great many studies have been made of the porosity-conductivity ratios of porous sedimentary rocks, and the picture is somewhat simpler. The tortuosity values obtained are much smaller and do not vary very much. They appear reasonable for the geometry of a loosely packed sand.

These measurements also showed up another very important

aspect of the rock conductivities. As the salt diffused into the rock, the rock conductivity increased, but the increase never amounted to the expected increase when comparing the salinity of the interstitial fluids before and after the salt diffused. In Fig. 3.6 is shown a histogram summarizing the measured increase of the rock conductivity for a thousand-fold increase of the pore fluid conductivity. We are assuming here that the pore fluid is identical with the fluids in which the rock specimens are immersed. The results shown in Fig. 3.6 are a clear indication that something is wrong with our assumptions, and that the effective conductivity of the pore fluids in a tight rock is considerably greater than $2 \times 10^{-2} \ \Omega^{-1} M^{-1}$ even when immersed in water of that conductivity.

Surface Conduction in Rocks

The results shown in Fig. 3.6 seem to indicate that the conductivity of the pore paths within the rock are higher than can be expected when only considering the specific conductivity of the fluids within the pores. This is in sharp contradiction to the assumption often used in analyzing the resistivity of the sedimentary rocks, and from this deducing the salinity of the pore fluids. One should notice however, that the samples used in obtaining the data of Fig. 3.6 are of very low porosity, so that the pore passages, which probably represent the intergranular spaces, are extremely narrow. When such is the case we could expect

the interface zone between the rock minerals and the
pore solution to become an important part of the pore
passages. We have been concerned previously with the
electrical properties of such interfaces when treating
the problem of electrode polarization. An excellent
review of thes properties has been given by Graham (1947).
An important property of these interfaces is the fact that
the minerals usually retain a net charge in equilibrating
themselves with the solution, and this charge in turn
attracts a diffuse layer of oppositely charged ions in
the solution which is immediately adjacent to the minerals.
The space-charge zone in the solution is known as the
"diffuse layer", and the concentration of the ions within
the diffuse layer is assumed to follow a Boltzman distri-
bution, wherein the energy levels are governed solely
by the electrostatic energy of the charged ions. There-
fore we have:

$$P = P_0\, e^{-F\psi/RT}$$
$$n = n_0\, e^{F\psi/RT}$$

3.7

p = positive ion conc.
n = negative ion conc.
F = Faraday constant = 96,500 coulombs/equivalent
T = absolute temp. in degrees Centigrade
R = gas constant = 8.314 absolute joule/mole degree
ψ = electrical potential in volts

If the potential existing at the point of nearest approach
to the mineral surface where the ions still retain their
lateral mobility, is designated as the Zeta potential, we can
compute the total excess charge concentration in terms of the Zeta potential.

This excess charge represents an addition to the current-carrying capacity of the pore passage, and is known as a surface conductivity. In Table 3.4 are shown some specific surface conductivities for different Zeta potentials and different concentrations of the pore fluids.

Table 3.4

Specific Surface Conductivity in mhos

conc. Zeta potentials	50 mv.	100 mv.	250 mv.
.1 N	2×10^{-9}	10^{-8}	2×10^{-7}
.001 N	2×10^{-10}	10^{-9}	2×10^{-8}
.00001 N	2×10^{-11}	10^{-10}	2×10^{-9}

The pore sizes at which surface conductivity becomes as important as the fluid conductivity can also be computed. These values are shown in Table 3.5 where it is assumed that the pore passageways are planer, and that the mobility of the ions in the diffuse layer is the same as those within the bulk of the solution. This assumption seems justified by the temperature dependance of the rock conductivity, which was mentioned previously.

Table 3.5

Critical Pore Width in cm.

conc. Zeta potential	50 mv.	100 mv.	250 mv.
10^{-1} N	4×10^{-7}	2×10^{-6}	4×10^{-5}
10^{-3} N	4×10^{-6}	2×10^{-5}	4×10^{-4}
10^{-5} N	4×10^{-5}	2×10^{-4}	4×10^{-3}

Values such as these could easily be obtained for the pore thicknesses in a tight rock, so that we have a fairly rational explanation for the observed electrical properties of the igneous rocks shown in Fig. 3.6. It is well known that the high electric conductivity of clay is essentially a surface phenomena, but it is not so well known that this is also true for a great many ordinary rocks.

Polarization Impedances

The realization that the effective conductivity of the pores is increased by the surface conduction helps in part to explain the results of Fig. 3.2 which showed the polarization effects in metallic bearing igneous rocks extending to much higher frequencies than expected. When the surface conductivity predominates however, one must re-examine the whole idea of the blocking of pore passages by metallic minerals, since some surface conductivity undoubtedly takes place around the metallic mineral grains.

If we examine the problem of passing current along an interface between a solution and a metallic surface we see it is quite similar to the transmission line problem. An equivalent circuit for the conduction along the interface is shown in Fig. 3.7. Z_1 represents the resistance to the ions moving along the interface, $Z_1 = \dfrac{1}{\sigma \text{ surface}}$, and Z_2 represents the interface or electrode impedance. The equations for such a system can be given as

$$\frac{\partial I}{\partial x} = \frac{V}{Z_2} \qquad\qquad 3.8$$

$$I z_1 = - \frac{\partial V}{\partial x} \qquad 3.9$$

leading to

$$\frac{\partial^2 V}{\partial x^2} = \frac{z_1}{z_2} V \qquad 3.10$$

If we choose the center of the zone as our origin, the solution exhibiting the proper symmetry is given as

$$V = A \sinh\left(\sqrt{z_1/z_2}\; x\right) \qquad 3.11$$

From this we have

$$I = \frac{A}{\sqrt{z_1 z_2}} \cosh\left(\sqrt{z_1/z_2}\; x\right) \qquad 3.12$$

$$Z = 2\sqrt{z_1 z_2}\; \tanh\left(\frac{L}{2}\sqrt{z_1/z_2}\right) \qquad 3.13$$

L = total length of surface along metallic mineral.

At low frequencies if $\quad z_2 \gg 4 z_1 / L^2$

$$Z \cong z_1 L \qquad 3.14$$

and is purely resistive

At higher frequencies if $\quad z_2 \ll 4 z_1 / L^2$

$$Z \cong 2\sqrt{z_1 z_2} \qquad 3.15$$

and is independent of the surface length.

Typical values of Z_1 would run around $5 \cdot 10^7 - 5 \cdot 10^8\, \Omega/cm$ for a cm. wide strip.

In the frequency ranges normally used, $Z_2 \cong 2 \cdot 10^3 f^{-1/2}\, \Omega cm$ for a cm. wide strip.

$$\sqrt{z_1/z_2} \cong \left(1.5\; 10^3 - 5\; 10^2\right) f^{1/4}\, cm^{-1} \qquad 3.16$$

This value would indicate that for all but the smallest mineral grains we would consider

$$Z \cong 2 \sqrt{Z_1 Z_2} \cong (2-6)10^6 \, f^{-\frac{1}{4}} \, \Omega \qquad 3.17$$

It should be noticed that this impedance is inversely proportional to the $1/4$th power of the frequency as opposed to the $1/2$ power of a Warburg impedance. It must also be pointed out that this impedance is less than the blocking impedance of the front of the metallic mineral for a pore passageway 10^{-4} cm. thick, even at 10,000 cps. if we use:

$$Z_{blocking} = 2 \times 10^3/f^{\frac{1}{2}} \, \Omega \, cm \qquad \text{for cm. wide strip.}$$

Thus it would appear that in tight rocks we could expect the blocking impedance to behave as the $1/4$th power of frequency instead of as a Warburg impedance.

In Fig. 3.2 it is seen that some typical metal factor values do indeed increase more as $f^{1/4}$.

A more extensive investigation of this point was made by computing the power law that the metal factor values listed in RME-3156(Madden and Marshall, 1958) followed in the frequency range of 0.1 to 10 cps. The results of this compilation are given in Fig. 3.8, and again we see the predominance of an $f^{1/4}$ behavior.

108

DISTRIBUTION OF FREQUENCY POWER LAWS n FOR ROCK SAMPLE METAL FACTOR

$$\frac{m.f. (10)}{m.f. (0.1)} = (100)^n$$
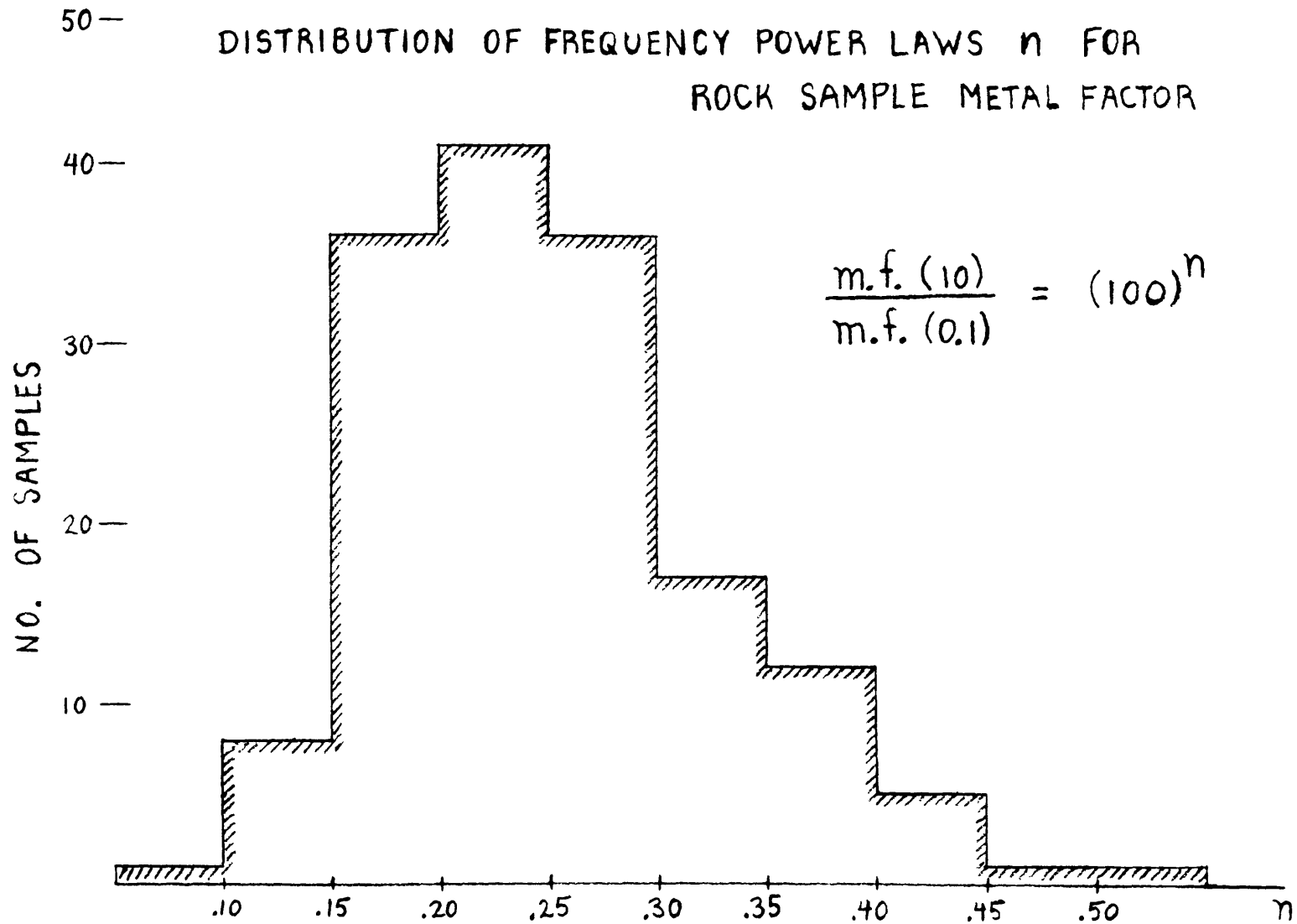
FIG 3.8

The simplest equivalent circuit that we could use to represent the electrical impedance of a mineralized rock should, according to these ideas, be represented by the circuit of Fig. 3.9. In this circuit R_0 and R_1 are simple resistances representing the resistances of the unblocked sections of the pores, while Z_M is the impedance associated with flow along the metallic mineral interface. The frequency dependance of Z_M in the range of .01-300 cps. is expected to follow a (frequency)$^{-1/4}$ law. The frequency dependance of the rock, $Z_R = \dfrac{R_0 (R_1 + Z_M)}{R_0 + R_1 + Z_M}$, will depend on the relative magnitudes of the parameters in the circuit. If we use R_1 / R_0 , and $Z_M (f_0)/R_0$ as parameters, where f_0 is a fixed frequency in the range of interest, and if we further assume $R_1 + Z_M (DC) \gg R_0$, the frequency behavior can be expressed as

$$\frac{Z_R (DC)}{Z_R (f)} = \frac{1 + \dfrac{R_1}{R_0} + \dfrac{Z_M (f_0)}{R_0} \left(\dfrac{f}{f_0}\right)^{-1/4}}{\dfrac{R_1}{R_0} + \dfrac{Z_M (f_0)}{R_0} \left(\dfrac{f}{f_0}\right)^{-1/4}} \qquad 3.18$$

The parameters $\dfrac{R_1}{R_0}$ and $\dfrac{Z_M (f_0)}{R_0}$ can be determined from the frequency effects at two frequencies. If the model has any validity in representing actual rock impedances, these values can then be used to predict the frequency
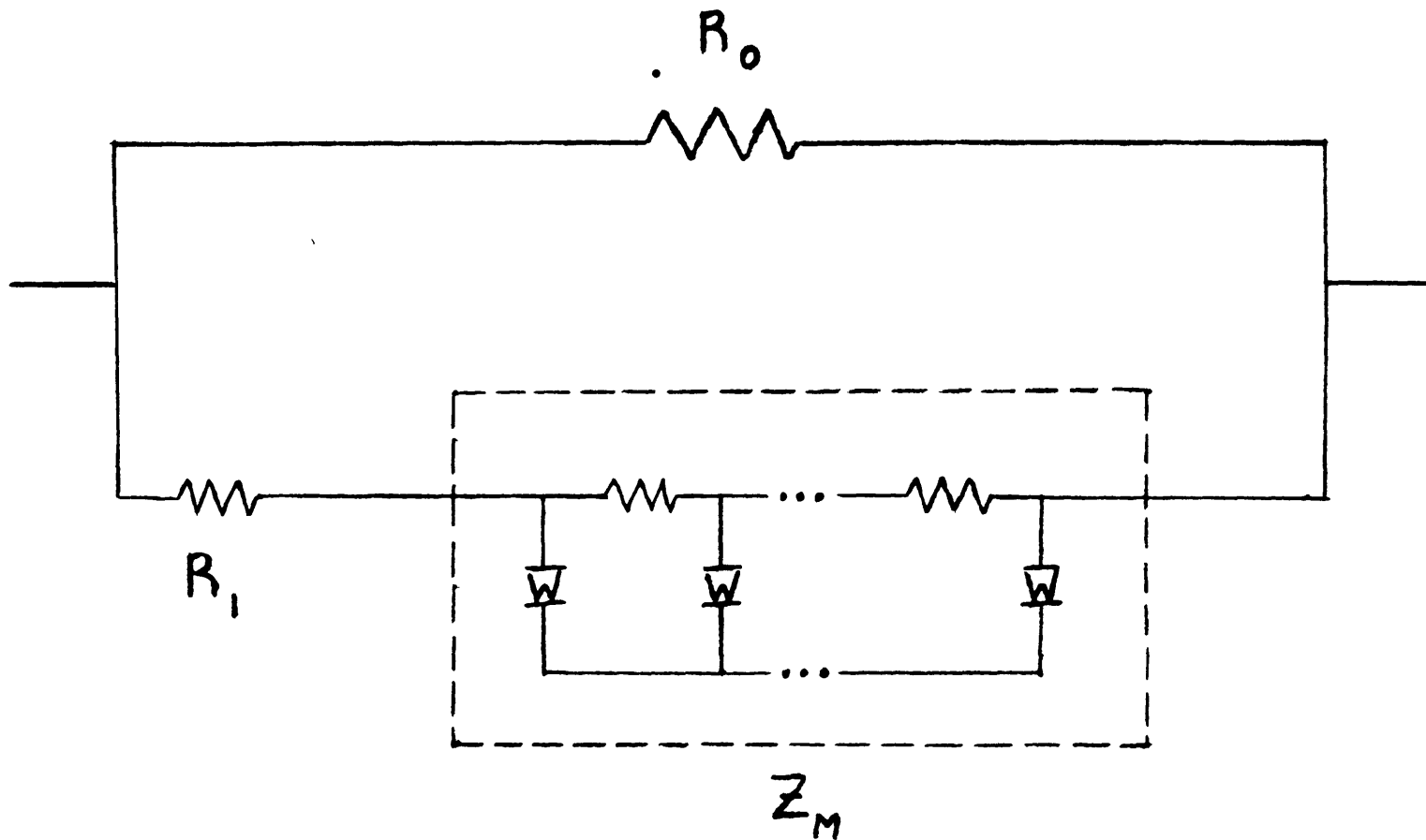
FIG 3.9   EQUIVALENT CIRCUIT FOR ELECTRICAL IMPEDANCE OF MINERALIZED ROCK

effects at other frequencies. Examples of such extra-
polations are given in Table 3.6. The extrapolations
in this table are based on data taken at 3 and 30 cps.,
which are only a decade apart and are used to predict
results of up to three decades beyond. In view of the
simplicity of the model, the results are remarkably
good. The only systematic errors of any significance
occurred at the high frequency end for the more resis-
tive samples where the model is expected to break down.
Further discrepancies can be expected from the effect
of errors in the data.

<div align="center">Table 3.6</div>

<div align="center">Impedance Parameters and Extrapolated Frequency Effects
in Rock Samples</div>

Sample no.	3		13		16		S25	
Rock type	gabbro		dolerite		quartzite (graphitic)		greenstone (pyritic)	
$Z_M^{(3)}/R_o$	5.50		2.18		4.03		2.83	
R_1/R_o	.40		1.15		.42		.40	
Freq. effects	meas.	pred.	meas.	pred.	meas.	pred.	meas.	pred.
3 cps.	1.17	–	1.30	–	1.23	–	1.31	–
10	1.23	1.22	1.34	1.36	1.29	1.29	1.40	1.40
30	1.29	–	1.42	–	1.37	–	1.50	–
100	1.35	1.37	1.48	1.48	1.47	1.48	1.65	1.64
300	1.42	1.47	1.56	1.55	1.56	1.59	1.77	1.78
1000	1.52	1.59	1.70	1.60	1.71	1.74	1.94	1.95
3000	1.71	1.73	1.92	1.65	1.88	1.88	2.12	2.11
10,000	2.04	1.89	2.42	1.69	2.05	2.05	2.36	2.30
ρ in Ω-M	7000		9000		1700		5500	

The effects of temperature and salinity changes on the
polarization properties of these rocks can also be studied
by means of the equivalent circuit parameters. In Table
3.7 are shown some results of the effects of temperature
on the electrical properties.

Table 3.7

Temp. Effect on Polarization Parameters

Temp.	$80^\circ C$	$60^\circ C$	$40^\circ C$	$24^\circ C$	$0^\circ C$
Sample no. 13					
$Z_M^{(3)}/R_o$	3.0	1.9	1.70	1.80	2.32
R_1/R_o	2.0	1.43	1.42	1.42	1.25
ρ in Ω-M	2600	3400	4600	7000	17,000
Sample no. S25					
$Z_M^{(3)}/R_o$	3.84	3.36	4.12	2.80	2.09
R_1/R_o	.33	.48	.23	.42	.41
ρ in Ω-M	2200	4600	4700	5500	10,000

There is some scatter in the parameter values, but compared
to the changes in the resistivity they are relatively
small changes, and are probably within the limits of the
accuracy of the data. This result is in keeping with the
model, as every impedance element is expected to follow
a temperature dependance equivalent to the H_2O viscosity
temperature dependance. Other measurements of the

113

temperature dependance of rock sample electrical properties
reported in RME-3150 showed this same behavior, with the
exception of one tremolite limestone sample. This sample
which has been referred to previously as Z-1, lost its
polarization properties at the higher temperatures and showed
a proportionally higher conductivity. It is believed, how-
ever, that this sample did not posess any metallic minerals
and that what was observed was a reversible deterioration
of its membrane properties at the higher temperatures. The
results of measurements on the effects of changes in pore
fluid salinity are given in Table 3.8. It is more difficult
to predict the results of such measurements because of the
unknown balance between the pore conductivity and the surface
conductivity in the various conduction paths. One would
expect the Z_M/R_0 ratio to increase as well as Z_M/R_1.
This latter expectation was not born out by the measurements.
Since the conductivity balance among the various possible
paths could not be expected to remain constant, one would
interpret these result as showing that the pore passages
with wider-spaced mineral grains were favored when saline
solutions were used. Considering the very large changes
in resistivity that occurred, the changes in the polari-
zation properties were minor.

Table 3.8

Salinity Effects on Polarization Parameters

Sample	normal salinity	high salinity
no. 13		
$Z_M^{(3)}/R_o$	2.18	4.00
R_1/R_o	1.15	2.25
ρ in Ω-M	9000	720
no. 16		
$Z_M^{(3)}/R_o$	4.03	2.76
R_1/R_o	.42	2.8
ρ in Ω-M	1700	330
S25		
$Z_M^{(3)}/R_o$	2.80	4.95
R_1/R_o	.42	2.20
ρ in Ω-M	5500	490

The consistant behavior of this equivalent circuit encourages one to accept it as a realistic model of the conduction effects within the rock. The parameters of this model, however are rather surprising in view of the large ratio predicted between Z_M and R_1. From 3.15 and 3.17 we would expect

$$\frac{Z_1^{(3)}}{R_1} = \frac{(1.5-4.5) \times 10^6}{(5-50) \quad \times 10^8 \quad L} \qquad 3.19$$

where L is the average pore length between the blocking mineral grains. Since our model parameters gave values

of $Z_M^{(3)}/R_1$ ranging from 2-14 we would predict values
of L ranging from 3 x 10^{-5} - 5 x 10^{-3} cm.

It was partly our disbelief in such short distances
between the metallic minerals that led us to undertake
this analysis, and yet we are again forced to this con-
clusion. There is some leeway when one considers the
limitations of a simple model and the extrapolations
from laboratory studies, but one cannot really escape
the conclusion that the polarization properties are
strongly influenced by minute mineral grains emplaced
within the pore structure of the rocks. This conclusion
is essentially based on the study of the frequency
structure of the induced polarization effects, but it
also helps explain the magnitudes. For instance tight
basic rocks are often found to have their resistivities
change by over a factor of 2:1 with different frequencies,
when their magnetite content is only a small percentage.
The presence of a few magnetite minerals among the other
minerals of the sample would never explain the electrical
effects. But if associated with these larger minerals
there is a fine-grained magnetite dissemination within
the pore structure, very large electrical effects are
possible. When the mineralization of the rock takes the
form of veinlets, there is little difficulty in explaining
the large frequency effects that are observed.

The realization that small amounts of metallic minerals strategically located within the pore structure can monopolize the polarization effects of a rock, poses difficulties with the interpretation of induced polarization measurements. It helps to justify the weighting of the frequency effects by the conductivity, as is often done in evaluating field measurements. It points out however, the necessity of collecting empirical evidence concerning the polarization properties of natural rocks, since the factors controlling the electrical properties are so difficult to observe by other measurements. The same conclusion could be made concerning the polarization effects resulting from other causes than metallic or semiconducting minerals. In his studies, Don Marshall showed that only membrane polarization effects are important, but that the membrane effects are maximized when the selective zones are separated by non-selective zones. Thus, a sparse distribution of clay minerals within the pores of a rock could produce the largest membrane polarization effect possible, but the total amount of clay involved would be so small as to be difficult to detect. For these reasons a study of the electrical properties of a large number of natural rock samples was undertaken, using both laboratory measurements and field measurements, and a summary of these results is given in the following chapter.

CHAPTER IV

MEASURED POLARIZATION PROPERTIES AND ANOMALOUS BACK-GROUND EFFECTS IN GEOLOGIC MATERIALS

Summary of Measured Polarization Properties

The ideas discussed in the last chapter show the impor-
tance of collecting empirical data on the electrical proper-
ties of natural samples. Although the electrical properties
are complex, simple models can predict quite well the
polarization effects to be expected from mineralized rocks.
The parameters of such models are difficult to predict
however, as minor constituents may play a prominant role.
The model consisted of a simple resistance R_0, in parallel
with a series combination of another resistance R_1 and an
impedance Z_M. The resistances represent the pore conduc-
tion paths, while Z_M represents the conduction paths along
a metallic mineral interface, and varies as (frequency)$^{-1/4}$.
The frequency dependance of the model impedance can be
described in terms of two parameters. In the previous
chapter the parameters $Z_M(freq)/R_0$ and R_1/R_0, were com-
puted for a few samples. The high ratio of Z_M/R_1 seemed
to indicate that a fine dissemination of metallic minerals
was present in the pore structure of the rocks, and this
dissemination was necessary to produce significant polari-
zation effects at audio frequencies. Since it is difficult
to observe these disseminations directly, the existence of
induced polarization effects in mineralized rocks needs
experimental verification.

Under the sponsorship of the AEC, laboratory measurements

of the polarization properties of a large number of rock samples were undertaken, and the data was listed in AEC report RME-3156. Other measurements have been made in the field, and a continuing program of laboratory measurements is still providing data. The results show that measurable polarization effects are always found in samples containing metallic minerals. To indicate the character of these polarization effects, some of this data has been systematized in Figure 4.1, using the model parameters as variables. In this figure the average properties and the standard deviation of groups of samples are plotted. The parameters plotted were computed at 1 cps., but by moving along the R_1/R_0 contours the parameters to be expected at other frequencies can be predicted. The frequency scale can be determined by noting that each Z_M/R_0 contour interval represents a frequency change of about a factor of 100:1. The vertical scale was actually determined by the measured ratio

$$\left(\frac{Z_R(DC)}{Z_R(10)} - 1\right) \bigg/ \left(\frac{Z_R(DC)}{Z_R(1)} - 1\right) \qquad 4.1$$

and the Z_M/R_1 scale adjusted to fit. According to the model there is an upper limit to the value of the ratio given in Fig. 4.1. This value was exceeded by some samples, but the deviations do not appear to be statistically significant in view of the errors of the frequency analysis. No standard deviation was given for the Ontario samples, as these samples did not represent any single rock group. Most of these samples represent typical disseminated mineralizations. The White

Legend:

- ● SED. COPPER , WHITE PINES
- △ GABBRO, DULUTH
- ○ QTZ. PORPHYRY, NEW MEX.
- X VOLC'S, CONG'S, KEWEENAW
- ⊛ ANDESITE, SAFFORD
- ◎ "DAKOTA" SANDSTONE, COLO.
- ✱ TUFF, SAFFORD
- ☐ METAMORPHICS, ONTARIO

$$\frac{Z_M(f)}{R_1}$$

$$\frac{\frac{Z_R(DC)}{Z_R(10f)} - 1}{\frac{Z_R(DC)}{Z_R(f)} - 1}$$

$R_1/R_0 = 0.3$

$\frac{Z_M(f)}{R_0} = 300$

$Z_R(DC)/Z_R(f)$
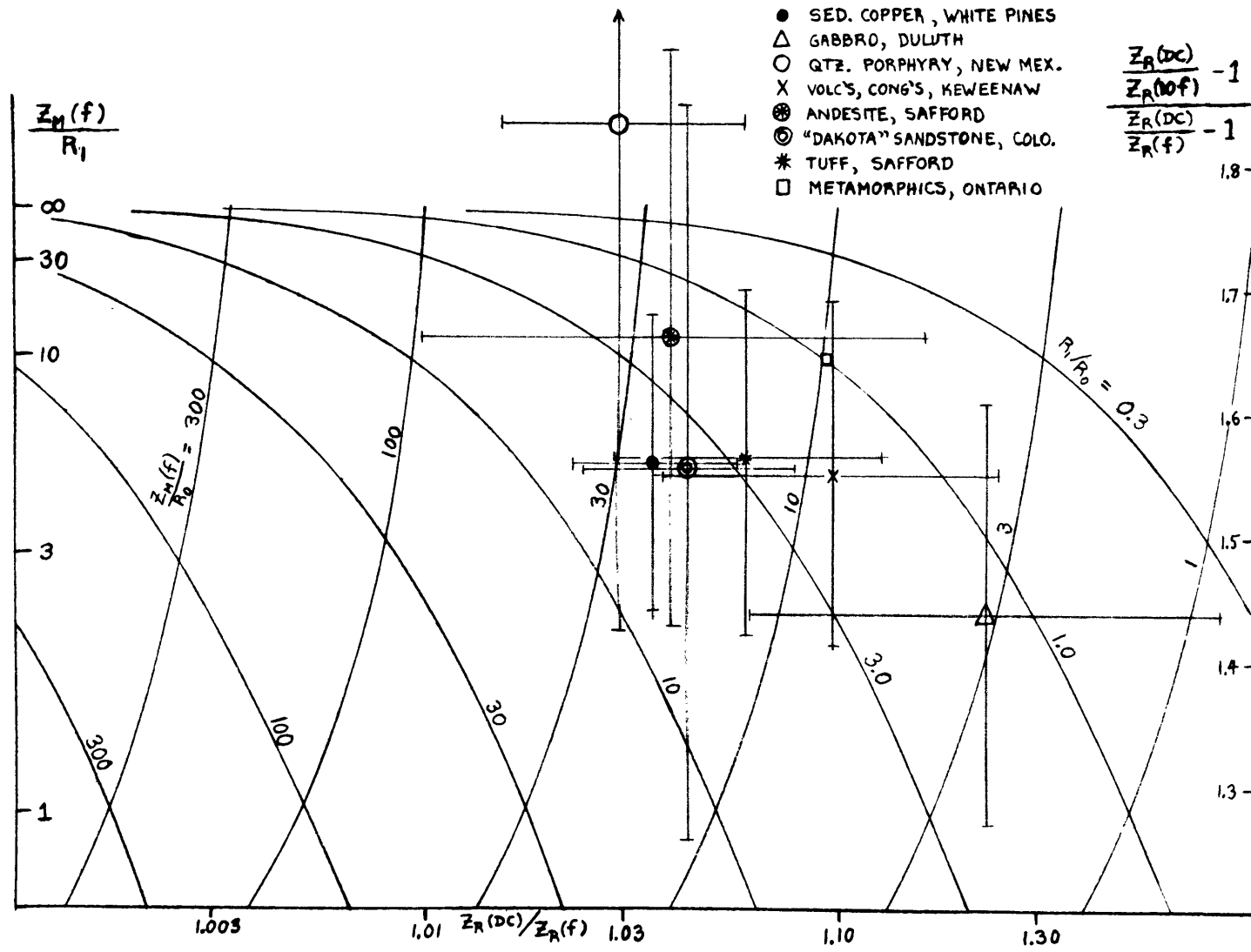
FIG. 4.1   POLARIZATION PARAMETERS OF NATURAL ROCK SAMPLES AT f = 1 CPS

Pines and Keweenaw samples contained copper mineralization; the quartz latite porphyry, the Dakota sandstones, and the metamorphics from Ontario were pyrite-bearing, while the Duluth gabbro was highly magnetic. The andesites and tuffs were not obviously mineralized, and their electrical properties are somewhat anomalous.

Intensely mineralized samples have been excluded from these summaries, as the core sample boundaries influence the measurements in an exaggerated fashion.

The points plotted in Fig. 4.1 show the same general pattern found in Chapter III when we first examined the model parameters, and the Z_M/R_1 ratios are all high. These results lead to two conclusions that are of some importance to the problems of using induced polarization measurements in exploration work. One of these conclusions is, that although some information is to be found in the details of the frequency structure of the polarization effects, this information will be limited, as the model parameters computed showed little spread, and as the success of the model extrapolations indicate few frequencies are needed. The other conclusion is that since very minor constituents appear to be controlling the polarization effects, care must be taken in interpreting the electrical measurements. The use of the parameter which we call the "metal factor" and which is a measure of the actual conductivity increase with frequency, rather than the percentage increase, would appear helpful in this respect.

In Fig. 4.2 metal factor values measured in the laboratory and in the field by our own and other groups are summarized. It is seen from this figure that in a general way induced polarization measurements do pick out mineralized rocks. There is little difficulty in identifying heavily mineralized rocks, and metal factor values of well over 1,000,000 have been measured in the field. As the sulphide mineralization becomes less massive the metal factor values decrease sharply, until the values merge into those values associated with the slightly mineralized host-rocks. The geometry of the metallic minerals, and the way they are placed within the rock and the rock pore system, plays a very important role in establishing the induced polarization properties. The high conductivity of sedimentary rocks makes the metal factor parameter somewhat less diagnostic with these rocks than with the igneous and metamorphic rocks.

On an empirical basis we can state a general rule of thumb: significant mineralizations of over 1 or 2% sulphides are associated with frequency effects of more than 5% and metal factor values of over 50 at 10 cps. We shall consider as anomalous all those mineralized rocks whose polarization properties exceed these values, or mineralized rocks whose polarization properties are smaller than these values. Since we are aware that polarization effects can arise from membrane effects without metallic minerals being present (Marshall,1959) the greatest interpretation problems arise from anoma-

Ranges of Metal Factor Values

$$MF = 2\pi \left(COND(10\ CPS) - COND(dc)\right) \times 10^5$$

```
|      |      |      |      |      |
|      10     10²    10³    10⁴    10⁵   MF IN MHOS/FOOT
|      |      |      |      |      |
```

SEDIMENTARY AREAS

DIRTY SS & LS

GRAPHITIC SS & LS

SS + SULPHIDES < 2%

CLAYS

SHALE + SULPHIDES

IGNEOUS AND METAMORPHIC AREAS

GRANITE

BASALT

TUFF

SLIGHT SULPHIDES

PORPHYRY COPPERS

HIGH MAGNETITE

HEAVY SULPHIDES
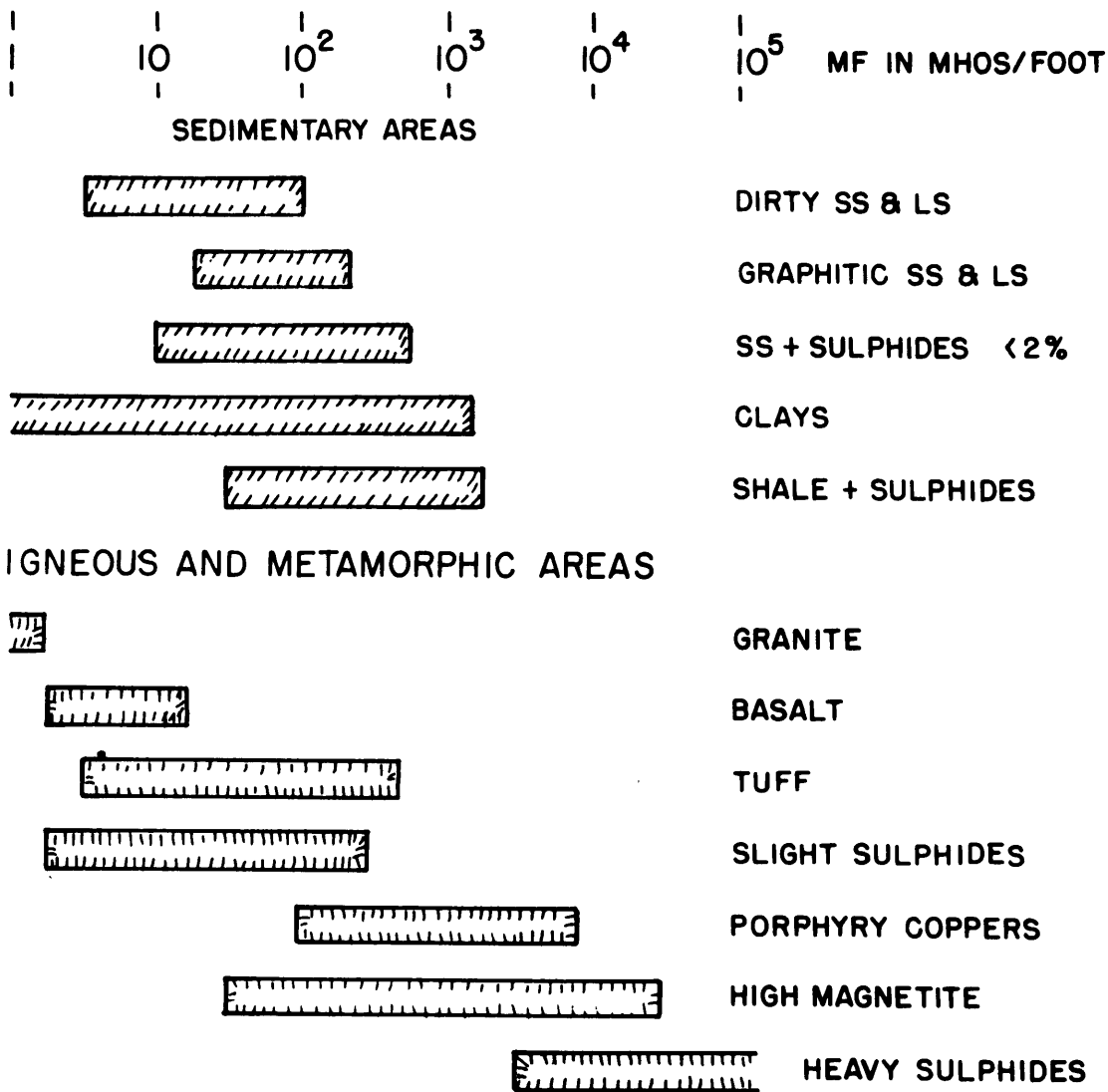
Fig. 4.2

lously high polarization effects. There are occasional mineralized samples which show abnormally low polarization properties. Such rocks are usually very tight rocks whose mineralization appears as disseminated. In view of the results discussed in the previous chapter, their low polarization properties are not too surprising. Some examples of such cases, listed in RME-3156, were the mineralized quartzite from Rhodesia, and the copper ores from the White Plains area in Michigan.

In order to acquaint ourselves with the difficulties in interpreting induced polarization results, we assembled all the rock sample data that appeared to have anomalously high polarization effects. This data included measurements on flow rocks from Michigan, andesite flows and tuffs from Arizona, and a large number of conductive sedimentary rocks from Colorado. Because of the high conductivity of some of these samples, delicate polarization measurements were necessary as some of the frequency effects were very small. An analysis of the measuring system showed that small polarization effects could be introduced by the measuring electrodes, unless proper switching and locating of the electrodes were used. A discussion of this problem is given in Appendix A. These changes were incorporated in the measuring system, and the samples were remeasured. Some of the anomalies disappeared when the measurement errors were corrected, but we should like to discuss these rocks in more detail, as they represent the most troublesome samples that we have come across. Some result of Dr.

Vacquier's studies on clays are also included in order to help evaluate the natural rock samples.

DIRTY SANDS

We know from our theoretical discussions and our experimental studies that polarization effects can be associated with membrane properties. Clay minerals have very pronounced membrane properties, and therefore it is to be expected that some polarization effects should be associated with the presence of clays within a rock. Clay minerals are often found in sedimentary rocks and in altered rocks, and careful attention should be given to the possibility of such rocks causing anomalous polarization effects. Geometric studies on membrane polarization would lead one to expect less polarization from a massive clay zone than one might perhaps obtain from a slight scattering of clay particles such as one would find in a sedimentary rock whose grains are coated with clay minerals(Marshall, 1959). For this reason, many people are suspicious of the polarization properties of dirty sands. In the work done at New Mexico Institute of Mining and Technology under Professor Vacquier, artificial dirty sands were formed by mixing sand and clay, or by flushing clay slurries through the sands. A large number of their results have been listed (Vacquier et al, 1957) but the form in which these results are presented is different from that which we have been using here. By comparing decay curves we can extrapolate their results into the form that we have been using here. It is found

125

that the 5 second millivolt / volt IP response which is

listed by Vacquier and his workers for a 20 second exita-

tion time, when divided by two gives approximately the

percentage frequency effect at 10 cycles / second. Unfor-

tunately they do not list the resistivity of their sand-

clay mixtures, but we can make estimates of this resistance

using the given resistivities of the solutions and

assuming the pore geometry for the unconsolidated sands.

These estimates will represent upper limits for the

resistivity since no allowance for any surface conduction

has been made. A summary of these results is shown in

Table 4.1.

Table 4.1

Polarization Properties of Artificial Dirty Sands
(extrapolated from Vacquier et al, 1957)

clay	electrolyte	frequency effect at 10 cps.	ρ/π(max) in Ω-ft	m.f.(min) at 10 cps.
2.5% montmorillonite natural state sample saturated with electrolyte solution	NaCL	1.7%	70	24
	CaCL$_2$	1.3%	65	20
	ALCL$_3$	1.3%	65	20
	Na$_2$SO$_4$	1.7%	70	24
	CaSO$_4$	1.5%	80	19
	AL$_2$(SO$_4$)$_3$	1.5%	100	15
	Na$_3$PO$_4$	3.9%	70	56
2.5% electrodialyzed montmorillonite saturated with electrolyte solution	NaCL	2%	70	30
	CaCL$_2$	1.5%	65	20
	ALCL$_3$	1%	65	15
	Na$_2$SO$_4$	2%	64	30
	CaSO$_4$	2%	75	25

Table 4.1 Cont.

Polarization properties of Artificial Dirty Sands
(extrapolated from Vacquier et al, 1957)

clay	electrolyte	frequency effect at 10 cps.	$\rho/2\pi_{(max)}$ in Ω-ft	m.f.(min) at 10 cps.
2.5% montmotillonite saturated with .1N solution, then washed with distilled water, and percolated with electrolyte solution	$CaCL_2$	9%	320	27
	$AlCL_3$	4%	320	12
	$CaSO_4$	10%	320	30
	$Al_2(SO_4)_3$	5%	320	15
	$CaSO_4$	16%	1300	13
	$CaSO_4$	11%	310	35
	$CaSO_4$	5%	80	60
	$CaSO_4$	2%	25	80
	K_2SO_4	2%	310	6
	K_2SO_4	2%	65	30
1% electrodialyzed montmorillonite saturated with electrolyte solution	$CaSO_4$	3%	1200	3
	$CaSO_4$	3%	280	11
	$CaSO_4$	2%	70	30
	$CaSO_4$	1%	23	40
	K_2SO_4	2%	60	33
	K_2SO_4	3%	260	12
5% kaolin,electro-dialyzed and percolated	$AlCl_3$	1%	280	4
	$CaCL_2$	1%	300	3
	NaCL	1%	325	3
5% kaolin, ion saturated and percolated	$AlCl_3$	0.6%	280	3
	$CaCL_2$	2%	300	6
	NaCL	0.8%	325	3

The results shown in Table 4.1 point out differences between
the different clay types in their polarizing properties, but
they also show the influence of the treatment which the clay
has undergone, and the type of solution percolating through

the sands. The montmorillonite clays gave significantly larger polarization effects than the kaolinite clays did. The results also showed that clays treated by presaturating them with strong salt solutions gave stronger polarization effects than clays used in their natural state. Frequency effects as high as 16% and metal factor values of 100 were achieved in some of their measurements. With natural rocks, however, the clays should be more in equilibrium with the pore solutions, and we should not expect such large frequency effects, although the metal factor values may be as high, since the surface conductivity could give us much lower resistivities. For this reason it seems important to seek out natural dirty sands and to measure their electrical properties. It turns out in practice however, that it is difficult to find such specimens which do not contain pyrite, graphite, or other electronic conducting minerals which are known to cause polarization effects in themselves. Thus it is usually necessary to back up the polarization measurements with studies on the mineralogy of the samples before attempting to classify their electrical properties as being anomalous or not. In Table 4.2 is shown one sequence of such rocks that were suspected of being anomalous from the results previously reported in RME-3156.

Table 4.2

Polarization Properties of Naturally-Occurring Dirty Sands

Dakota Sandstone Sequence - Lower Cretaceous Age

sample no.	freq.effect 10 cps.	$\mathcal{C}/2\pi$ Ω-ft	m.f. 10 cps.	carbon content	remarks
dirty sand					
7002	2.5%	26	95		
alternating sand and shale					
7003	0.9%	35	26		beds parallel to current flow
7011	1.7%	30	57		beds parallel to current flow
7007	2.5%	34	91	1.1%	beds perpendicular to current flow
7009	2.7%	264	10	0.5%	
dirty sand, carbonaceous material					
7010	3.3%	91	36	0.85%	

This group consists of well-core samples from the muddy sands, a part of the Dakota sandstone sequence. They are dirty sands and shales with some carbonaceous material. Several of these samples contained appreciable amounts of carbon, readily observed in the hand specimens. Its presence was confirmed by spectrographic analysis kindly carried out for us by Professor Dennen at the M.I.T. Cabot Spectrographic laboratory, and the results of this analysis in weight percent of carbon are listed in the above Table. No pyrite was visible in sample 7009, and 7010 under the binocular microscope. DTA analysis was made on 7009 and 7010 which indicated a slight amount of clay in 7009, but no measurable amount of clay in 7010.

The frequency effects listed in Table 4.2 are considerably reduced from those given in the earlier report, but the

high conductivities for these samples led to metal factor values that are still quite high. Some of these results may be due to the carbon content, for undoubtedly some of this carbon is of a conductive form. Nevertheless, in view of our studies and Vacquier's work, we cannot over-look the fact that one or two percent frequency effects can be associated with their clay content.

Another sandstone sequence was suspected of anomalous polarization properties and is shown in Table 4.3. This group of samples, supplied to us by the Atomic Energy Commission, consists of core samples from drill holes in Edgemont, South Dakota. When it was thought that the samples might be anomalous, DTA and heavy mineral analysis were carried out on them. Pyrite is easily identified in sample 9001, but other samples did not contain obvious pyrite, though slight rusting was observed on some of them after prolonged soaking. The DTZ analysis showed a strong exothermic reaction with sample 9001, which was undoubtedly due to its pyrite content, but little, beyond the quartz peak, appeared with other samples. The heavy mineral ana-lysis that was also carried out is capable of detecting smaller amounts of pyrite, although an appreciable amount of the sample is lost in the fines during separation. If the fractionation occurring in the fines is not too pro-nounced, the other samples can probably be stated to have less than .2% pyrite content. None of the samples show any indication of a large clay mineral content on the

Table 4.3

Polarization Properties of Naturally Occurring Sands

Sandstone from Uranium Prospect, Edgemont, South Dakota

sample no.	freq. effect	$\rho/2\pi$ Ω-ft	m.f 10 cps.	remarks
poorly consolidated sandstone				
9001	14.4%	52	275	2% pyrite
9002	2.0%	20	100	0.2% pyrite
9007	0.4%	8	52	0.1% pyrite
9007a	0.9%	14	66	
9007b	1.0%	15	68	
9009	0.1%	17	6	0.2% pyrite
mudstone				
9008	3.5%	120	30	
9003	0.9%	134	7	
very fine sandstone, calcareous streaks				
9005	0.8%	20	41	
impervious sandstone				
9006	5.4%	643	8	

thermogram, but this does not exclude the possibility of a very minor clay content. The electrical properties listed in Table 4.3 appear consistent with these results. The only large frequency effect is associated with sample 9001, and this sample contains obvious pyrite. There are some fairly high metal factor values in the other samples, but these are associated with their high conductivities and not with pronounced frequency effects.

Colorado Plateau - Uranium Bearing Sediments

Most uranium ores are not found in the form of metallic minerals, so that we would not expect them to present induced polarization targets. The ores, however, are often associated with sulphides, so that electrical measurements may prove useful as guides, in the prospecting for such ores. The environment of many of these deposits is such that we can expect clay mineralization to be present, and the usefulness of induced polarization measurements might be limited by the magnitude of the anomalous background effects. For this reason, several suites of rock from uranium prospecting areas were sent to us by the Raw Materials Division of the AEC. A summary of these results is given in Table 4.4. These results are quite similar to our previous ones. Most of the sulphide-bearing rocks are easily identified from their weak electrical properties, although occasional ones gave very weak polarization effects. Again, some of the sand-stones without sulphides gave quite high metal factor

values, but these samples had high conductivities and rather small frequency effects. These results show us, however, that it is always possible to obtain 2 or 3% frequency effects at 10 cps. from rock samples whether or not they contain electronic conducting minerals. Because of this it would seem necessary to compute metal factor values only in terms of frequency effects in excess of this 2 or 3% background value. This puts definite limitations on the resolving power of induced polarization measurements, but appears unavoidable in light of our knowledge of the electrical properties of rocks.

Table 4.4

Polarization Properties of Naturally Occurring Sandstones
Sandstones from Uranium Prospects, Colorado Plateau

sample no.	freq. effect 10 cps.	$\rho/2\pi$ Ω-ft	m.f. 10 cps.	remarks
Chinle				
	barren, no pyrite			
9010	3.6%	35	103	$.2\%$ pyrite
9036	3.4%	200	17	
	ore, no pyrite			
9015	5%	100	50	
9016	5.2%	61	85	
9034	2.1%	243	10	
	ore + pyrite			
9029	12.7%	71	178	
9031	219.5%	5	46,600	
9032	96.2%	15	6,230	
9033	131%	6	21,800	
9035	7.4%	455	16	

Table 4.4 cont.

Polarization Properties of Naturally Occurring Sandstones

Sandstones from Uranium Prospects, Colorado Plateau

sample no.	freq. effect 10 cps.	$\rho/2\pi$ Ω-ft	m.f. 10 cps.	remarks
Morrison				
barren, no pyrite				
9010	1.8%	525	3	
9020	1.3%	38	34	
9022	0.5%	184	3	
ore, no pyrite				
9018	4.4%	81	57	
barren + pyrite				
9023	3.9%	760	5	
9030	2.2%	230	10	
ore + pyrite				
9012	2.3%	16	140	
9014	21.4%	19	1,150	
Moenkope				
barren + pyrite				
9027	0.2%	33	6	no apparent pyrite
ore + pyrite				
9017	4.7%	35	134	
unidentified Colorado Plateau sediments				
sandstone, no pyrite				
9040	2.8%	32	90	
9041	3.9%	47	83	
9042	3.7%	45	83	
poorly consolidated sandstone, uranium bearing, no pyrite				
9046	1.7%	12	141	
9047	1.8%	21	84	
9048	1.5%	6	250	

Flow Rocks

In several localities flow-rocks, not directly associated with the ore minerals, gave suspiciously high polarization effects, and some of these were studied in the laboratory. Among these rocks were andesite flow-rocks from a porphry-copper area in Arizona that were previously reported in RME-3156. These rocks are altered and it was believed that perhaps their anomalous properties might be due to clay minerals. When they were measured again, however, with the improved equipment, they were found not to be anomalous, as is shown in Table 4.5. Sample 7103 and 7113 gave large frequency effects, but these were found to contain metallic minerals, and are not to be considered anomalous either.

Table 4.5

Polarization Properties of Andesite Flow-Rocks

sample no.	freq. effect 10 cps.	$\rho/2\pi$ Ω-ft.	m.f. 10 cps.
7104	0.7%	64	11
7107	1.4%	89	16
7114	3.2%	82	40
7123	1.4%	56	25

Quite high frequency effects were observed in ophytic trap samples from the Keweenaw flows as was shown by sample 1205 and 1206 (RME-3156). Somewhat similar values were obtained in the field when measurements were made in the same area. Professor Lloyal Bacon, of the Michigan College of Mining and Technology, has been making a study of the electrical properties of such rocks, and he kindly sent us some additional samples of anomalous electrical properties.

There was some suspicion that chlorite minerals might be
the cause of the induced polarization effects, although
laboratory analyses indicate that there was some magnetite
ilmenite and copper mineralization in a very finely divided
state (Bacon , 1959). In Table 4.6 is shown the results
of the measurements on these new samples.

Table 4.6

Polarization Properties of Ophytic Trap Rock from
Keweenaw Peninsula

sample	freq.effect 10 cps.	$\rho/2\pi$ Ω-ft.	m.f. 10 cps.	magnetite content	ilmenite content
A-3	48.4%	670	70	0%	2.5%
A-4	48.5%	510	95	0.5%	3.0%
A-8	35.6%	685	53	0.3%	1.0%
B-12	12.1%	140	87		
C-10	30.8%	210	148		
C-11	22.0%	260	85		

It is seen that the frequency effects are very large, and
when the measurements are carried out at even higher fre-
quencies it is possible to get effects of over 100%. Pro-
fessor Bacon's studies are not completed, but on the basis
of our measurements we believe the polarization properties
are due to metallic minerals and not to membrane effects.
The fact that the metallic minerals are in a very finely
divided state probably helps to contribute to the very high
frequency effects, as the current flow is forced to pass
through many interfaces. The electrical properties of these
samples are somewhat unusual, but they cannot be classified
as anomalous. Insofar as these samples turn out to be not
of ore grade, they will prove extremely bothersome when

attempts are made to use electrical measurements in the area.

Tuffs

S,ome of the most puzzling electrical properties which we have observed have been associated with a group of crystal lythic tuffs from Arizona. These rocks are made up of extremely fine grained minerals and are quite conductive, undoubtedly due to rather large surface conductivities. Some of these samples had fair frequency effects resulting in metal factor values of over 500. When these samples were remeasured with more accurate equipment the values were modified a bit, and are shown in Table 4.7, but the basic results are not changed significantly.

Table 4.7

Polarization Properties of Volcanic Tuff

sample no.	freq. effect 10 cps.	$\rho/2\pi$ Ω-ft.	m.f. 10 cps.	t^+	%Fe	%S
7111	11.6%	111	105		1.2	0.13
7117	2.2%	23	95	.51	1.3	0.06
7124	5.9%	50	116		1.6	0.14
7129	9.4%	18	530	.72	1.3	0.04
7131	3.4%	59	58		1.5	0.05
7133	1.0%	25	40		1.1	0.14
7134	1.6%	28	57		1.1	0.14
7136	6.4%	59	108		0.8	0.13
7139	5.3%	79	67		0.8	0.13

These rocks appear to be devoid of sulphide mineralization and this was verified by an iron and sulpher analysis. Some of these rocks are slightly magnetic, so that some of the

iron may be in the form of magnetite. The amount of
magnetite present, however, hardly seems capable of
explaining the metal factor values. DTAs were run on
several of these samples, but they gave no obvious clay
peaks. As we have mentioned before however, the sensi-
tivities of the DTA analysis is not high enough for a
negative result to be really significant. Transference
measurements were made on sample 7117 and sample 7129
to look for membrane properties. As is shown in Table
4.7 the transference properties of 7129 were quite pro-
nounced, but sample 7117 did not show a very stong mem-
brane effect. Two of the samples, 7124 and 7129, were
heated to $600^\circ C$. in an attempt to destroy the clay minerals
without destroying the magnetite minerals. In Table 4.8
is shown the electrical properties of these samples before
and after the heat treatment.

Table 4.8

Effect of Heating on Polarization Properties of Crystal
Lythic Tuffs

	sample	freq. effect 10 cps.	$\rho/2\pi$ Ω-ft.	m.f. 10 cps.
before	7124	5.9%	50	116
after 600° heating		5.1%	181	28
before	7129	9.4%	18	530
after 600° heating		3.9%	74	53

The heat treatment tended to destroy most of the metal
factor values for these samples, but this was accomplished

due more to a decrease in the conductivity of the samples and only slightly due to a decrease in the frequency effect. More work should be done on these rocks to clarify the exact causes of their measured properties, but it may turn out that the effect is a combination of electrode polarization and high surface conductivity. In any case some of these tuffs have to be classified as anomalous in their electrical properties.

These tuffs represent the most anomalous samples that have been covered in our measurements. One isolated sample that was reported in RME-3150, a limestone sample from Arizona labeled Z1, produced the largest frequency effect observed from samples without metallic minerals, but its conductivity was low and its metal factor value was only about 10. This sample is of interest because it reversibly lost its polarization properties at more elevated temperatures; we believe this to be due to a decrease in the efficiency of the membrane zones acting within the sample as the temperature is raised. Other limestone samples from the same area showed no particular polarization effects. The tuffs, on the other hand, have been reported by others to be troublesome in their electrical properties, so that the results reported here may not be isolated samples.

Frequency Spectrum of Polarization

In our evaluation of the polarization effects of the rock samples we have been using a very crude criteria which is simply a magnitude criteria. It was hoped when the investigations were begun that the study of the polarizing mechanisms might lead one to expect certain characteristic differences in the polarization effects of membrane zones as compared with the electrode polarization effects of metallic minerals. Unfortunately the theoretical investigation showed that the principal factor contributing to the electrode impedance is a diffusion phenomenon, and this is the same factor involved in membrane polarization. Furthermore, the geometric complications that arise in natural rock samples tend to smooth out the frequency spectra of the polarization effects so that the impedances show a wide and gentle frequency variation, making any discrimination on this basis very difficult. This result was born out in the measurements on rock and clay samples. The phase shifts of the metal factor, which should represent approximately the phase shift of the impedance of the blocked conduction paths, were computed from an analysis of transient measurements at .1, 1, and 10 cps. for hundreds of samples. Although the results were often quite characteristic of a given rock or clay type, there seemed to be no clear separation between those samples with electrode polarization and those with membrane polarization. Some typical values are shown in Table 4.9.

The highly magnetic altered ultra-basics listed in the
Table cannot be considered as representative samples,
as the magnetite zones were solid throughout the length
of the samples, and the impedance was all due to the
solution electrode interface at the end of the sample.
The phase shifts indicate that the impedance was almost a
pure Warburg impedance.

Table 4.9

Metal Factor Phase in Degrees

Sample type frequency cps.	10	1	0.1
Kaolinite clays	9	14	22
Mica clays	8	12	19
Ion exchange resins	13	29	51
Sediments from Colorado Plateau			
with sulphides	12	20	30
little or no sulphides	9	15	21
Sedimentary copper ores	12	18	19
Rhodesian copper ores	18	27	41
Field data porphyry copper body		18	31
Lithic tuffs little or no sulphides	12	22	34
Graphitic sandstones	13	16	22
Dirty Sands from Dakota	11	17	30
Manganese ores	9	14	22
Highly magnetic altered ultrabasics	42	41	47

These results represent only a somewhat limited frequency
range, and a wider frequency analysis might prove to be
more discriminating. There are severe practical difficulties in
attempting this analysis from field data however, and there-
for we have not tried to extend the analyses. With the
field measurements the higher frequencies become influenced
by electro-magnetic coupling; the lower frequencies, while
measurable in principle, become masked by the natural earth cur-
rent noise.

The success of the simple model shown in Fig. 3.9 in extra-
polating the frequency effects is further evidence that
very diminishing returns are to be expected from more de-
tailed frequency measurements. If any further information
is possible from I.P. measurements it is most likely to be
found in the low frequency end of the spectrum where the
model breaks down. Such measurements are very tedious to carry
out however, and under field conditions are difficult to
achieve because of the telluric noise.

SUMMARY AND CONCLUSIONS

This study was undertaken in order to better understand
the factors controlling the induced polarization proper-
ties of mineralized rocks, and thus to help in interpre-
ting geophysical induced polarization surveys. The know-
ledge developed about electrode polarization when combined
with considerations of the electrical environment in rocks,
led to a qualitative understanding of the observed polar-
ization effects. There were two factors however, which
create certain difficulties in a quantitative evaluation
of induced polarization measurements. One of these factors
is the dominant role of diffusion processes in the electrode
polarization impedances. Since diffusion processes also
cause polarization effects in membrane systems, it becomes
difficult sometimes to identify the cause of polarization
effects in natural samples. The other factor is the in-
ferred role of metallic disseminations within the pore
structure of some mineralized rocks. This concept implies
that in some cases, very minor constituents of a rock may
be responsible for the observed polarization effects.
Because of these factors it is very difficult to infer much
from observations of small polarization effects. Membrane
polarization effects are more limited in magnitude than
electrode polarization effects, and this seems to be the
easiest criterion for making a distinction. The empirical
evidence is that with most natural samples the frequency

effects due to membrane polarization are less than 3% at 10 cps. Many of these samples are quite conductive however, so that fairly large metal factor values may still result. It is therefore recommended that metal factor calculations should be based on frequency effects in excess of 2 or 3%. This will not materially affect the results for a large number of sulphide mineral zones, but does eliminate the possibility of detecting certain types of mineral occurrances. We can set up a rule of thumb for evaluating the polarization results which seems to hold in the great majority of cases. If a rock contains more than 1 or 2% sulphides or other semiconducting minerals, it should have a frequency effect at 10 cps. of greater than 5% and a metal factor of over 100. There are some types of mineralization that present very poor electrical targets and do not come up to this criterion. There seem to be very few unmineralized rocks however, which would ever exceed this criterion. Of all the rocks measured in our study, it would appear that only the tuffs represented such an anomaly.

The problems raised in the understanding and application of induced polarization measurements have not all been solved, as the previous reference to anomalous samples so aptly points out. Where the interest is in the exploration applications of these measurements, it is the author's opinion that the most useful advances can be made in the quantitative evaluation of the field measurements. When

making the field measurements the targets are usually separated from the measuring equipment, so that the observed polarization effects are only a fraction of the polarization properties of the mineralized targe zones. The dilution of the observed polarization effects by this geometric factor is very pronounced, and there is a great need for good quantitative methods of taking this into account.

More work can also be done on analysing the polarization properties of certain rock types, such as the tuffs, which we must still call anomalous, since their properties are not fully understood. And a detailed study of the correlation of the metallic minerals, their size distribution, their mode of emplacement, and their relationships to the pore structure of the rock, with the polarization properties of the rocks, should enhance our ability to interpret induced polarization measurements.

A large part of the effort here has been devoted to pointing out the problems entailed, but this should not detract from the fact that induced polarization measurements can be very useful, especially in mining exploration for metallic minerals; and these techniques should occupy a firm place in the battery of tools for exploration geophysics.

These studies on electrode polarization were done with a very practical and limited objective, but some very interesting possibilities arose to further our knowledge of electrode phenomena. The success of the electrode model in fitting

the observed electrode impedances would indicate that one
can establish quantitative measures from electrode impedance
measurements, that have direct physical significance. These
measures will be very helpful in systematic studies of elec-
trode phenomena. It is already apparent from our own mea-
surements that the electrode reactions at low current den-
sities are not the ones postulated from the usual high
current density electrode studies. In fact, it may well
be that in none of the electrode studies made at low
current densities reported in the literature, were the
postulated reactions actually taking place. If all the ele-
ments of the solution were varied, and the electrode impedance
parameters determined for each case, the variations of the
Warburg impedance should indicate which elements were in-
volved. Other studies of a similar nature seem possible
using these techniques, but since they deviate quite widely
from the author's field of geophysics, they were not pursued
further.

APPENDIX A

Laboratory Measurements of Small Polarization Effects

The measurement of induced polarization effects either in the laboratory or in the field is quite easy as long as the polarization effects are pronounced. It was mentioned in the introduction that the measurements could be made either in the time domain or in the frequency domain. The choice of methods is essentially an instrumental problem, and both methods are used in practice. Practical numerical techniques to derive frequency information from transient data, or vice versa, are discussed in AEC report RME-3156.

When the polarization properties to be studied are very small, much more care is needed in making measurements, and certain procedures must be avoided to prevent introducing extraneous results. A discussion of a simple but workable laboratory system is given below.

Although the frequency and time domain data are equivalent to each other in theory, in practice they involve quite different aspects. In general the techniques for eliminating extraneous noise are easier to achieve in the frequency domain, and equipment for field measurements is simpler if frequency techniques are used. There are two important exceptions however, where time domain measurements involve a greater simplicity. These exceptions are measurements at very low frequencies, and measurements of very small polarization effects. This last factor is the

one that concerns us here.

The difficulties with the frequency domain measurements
are the extreme accuracy required, and the errors intro-
duced by the polarization of the measurement electrodes.
If we wish to extend our analysis to rocks with polari-
zation effects as small as 0.1%, the relative accuracy
of the impedance measurements must approach 0.01%.
The same accuracy can be achieved in the time domain
with equipment accurate to only 10%. If we use a
current system that is on for a time interval, off for
a time interval etc., the voltages appearing across the
sample during the off cycles is a differential measure
proportional to the polarization effect. The only res-
trictive instrumental requirement is the sensitivity to
detect these polarization voltages. Since one can
usually develop more than 1 volt across the sample with-
out introducing non-linear effects, a sensitivity of
1 millivolt is adequate for observing 0.1% polarization
effects.

A greater difficulty with the frequency measurements is
the effect of the polarization of the measuring electrodes.
The impedance of the electrodes causes small errors in
the measured voltage, and these errors are frequency de-
pendant. This results in an apparent negative polari-
zation effect in the sample, or a lessening of the actual

polarization, unless the input impedance of the measuring
system is very high. In the time domain measurements that
were outlined above we can achieve an effective high input
impedance by merely open-circuiting the receiving electrodes
during the on-current cycles. Under these conditions the
input impedance of the measuring system has only modest
requirements. A switching circuit that accomplishes these
ends is shown in Fig. A.1. The time intervals used depend
on the frequency range of interest. In the measurements used
for this thesis, $t_{n+1}-t_n = 7.5$ seconds, which allowed the
computation of frequency effects down to 0.1 cps. The de-
lay, δt, should be as short as possible when turning S-3 on,
as this determines the high frequency limit of the polariza-
tion information. By using fast mechanical relays, such as
the Stevens-Arnold milisec relay, δt can be made less than
1 milisecond, and the polarization spectrum can be extended
as far up as 10 cps. Solid state relays are much faster,
but unfortunately to date none have been developed with
open circuit impedances high enough for our purposes. Such
devises can be used however, to replace S-1 and S-2 with
some simplification in circuitry, since present day silicon
switches have leakage currents 10^{-4} x their conduction
currents.

Since the conductivity of the rocks is predominantly due to
the ion current through the water-saturated pores of the rock,
it is necessary that an electrolytic contact be made with
the end surfaces of the samples being measured. This can be
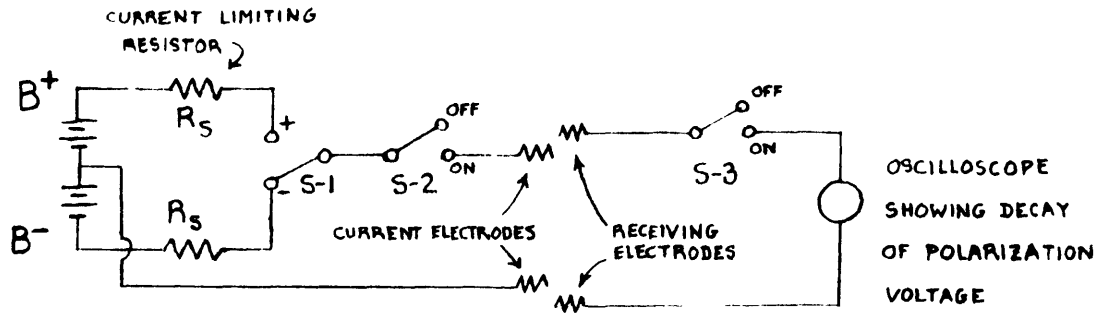
Switching Sequence

| S-1 | $+$ | $t_{4n} - \delta t$ |
| | $-$ | $t_{4n+2} - \delta t$ |

| S-2 | ON | t_{2n} |
| | OFF | t_{2n+1} |

Scope sweep trigger t_{2n+1}

| S-3 | ON | $t_{2n+1} + \delta t$ |
| | OFF | $t_{2n} - \delta t$ |

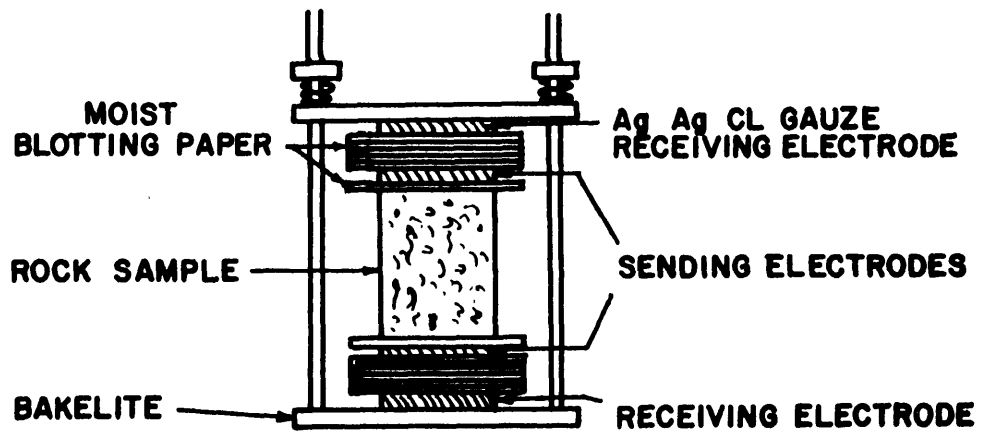Fig. A.1 Switching circuits for observing polarization effects.

Figure A.2 Sample holder for measurement of small polarization effects

achieved quite easily by using moist blotting paper or felt between the electrodes and the sample. The sample holder that was used is shown in Fig. A.2. This holder incorporates three features that are also important for achieving a high sensitivity in polarization measurements. First it should be noted that the receiving electrode is separated from the sending or current electrode. The discharge of current from the sending electrodes affects the chemical environment in the vicinity of the electrode, and these environmental changes would affect the receiving electrode potentials if they are located too close to the sending electrodes. It has also been noted that unpredictable polarization effects occur if the current passes through the receiving electrodes. To prevent these effects the receiving electrodes are placed outside the sending electrodes. Lastly, a small separation is used between the sending electrode and the sample, because the blotting paper itself has some polarization properties, and its impedance must be kept as small as possible.

The sample itself should be kept saturated as this is the usual condition for rocks in situ. Some rock samples are very poorly consolidated, and coating the outside of such samples with a thick plastic coating is helpful in preventing the sample disintegration.

The electrodes should have as small an impedance as possible, for this lessens all the difficulties of detecting small

polarization effects in the sample. Their potentials should also be stable, as drifts make the measurements very difficult. This means that reversible electrodes are needed. We have found that Ag-AgCl electrodes work very well in dilute solutions. When silver gauze is used as a base, these electrodes are ideally suited for the apparatus shown in Fig. A.2. The AgCl is formed on the electrode by electrolysis, the electrode being set up as an anode in a chloride solution. Only a thin layer of AgCl is desired, and the electrodes should be periodically recoated.

With this system polarization voltages of less than 1 mv. and frequency effects of 0.1% can be studied, although very few rocks are found with such small effects. A good check on the system is to have a sample exhibiting low resistivity and low polarization, and to use this sample occasionally as a standard to test the reliability of the system.

APPENDIX B

Equivalent Circuit Fitting for Electrode
Impedances - 704 Program

The evaluation of the measured electrode impedances is
difficult because so many factors are involved. For this
reason it was decided to analyze the impedances by adjusting
the parameters of the theory to give an optimum fit of the
model predictions to the measured values. Such an attack is
quite feasible with the availability of high speed computing
machines, and a program was written to carry these computa-
tions out on an I.B.M. 704.

The model that was used can be represented as an electrical
circuit, and is shown in Fig. 2.1. The parameter values are
all restricted to positive, but their magnitudes can vary over
wide ranges. The form of the equations relating the impedance
as a function of frequency to the parameter values is non-
linear, so that linear programming techniques cannot be
applied. The standard techniques of steepest descent appear
poorly suited to handle the wide variations in parameter va-
lues that are possible, as well as the restriction on the
sign of the parameter. These two difficulties can be coun-
tered however, if one works with the log. of the parameter
values instead of the parameter values themselves. The
algebraic complexities become quite involved with this
approach however, and the author decided to use a similar
but simpler concept.

In all least squares fitting problems, one can envision the

error measure mapped in the parameter space as a surface.
This surface is always above the error = 0 plain, and
for well-formulated problems one should have a clearly
defined low spot. The location of this spot is the fitting
problem. Difficulties arise in the solution of this problem
if metastable low spots occur, or if in the vicinity of
the true-minimum error point the surface slopes gently.
The standard numerical methods of solution find the direc-
tion of the surface, and estimate the distance down-slope
to the bottom. Because of the algebraic complexities
involved in our particular problem, it was decided to
hunt for the bottom point by a simple trial-and-error
technique. The parameters can be varied and the new error
terms computed to see if the change is up-slope or down-
slope. A crude analysis indicated it should be most effi-
cient if only a few error spots were computed for each
parameter variation, and the parameters were varied
cyclicly. The adopted scheme started with a preliminary
set of parameter values. One of these parameters was then
altered. If the parameter change reduced the error, the
change was adopted and the next parameter varied. If the
error was increased, a change in the opposite direction
was tried. If this change reduced the error it was adopted,
if not, the parameter was left unchanged. The next para-
meter was then varied. Because of the wide variation of
the measured impedance as a function of frequency, the sum
of the percentage errors squared, was used as the error measure.

In order to accomodate large changes in the parameter values, and in order to maintain the sign of the parameters, the parameter changes involved either a multiplication or a division of the parameter by a constant. This constant started as 10 for each parameter, but was systematically reduced for each parameter every time it was found that both parameter variations increased the error. The subsequent factors were 3, 1.5, 1.25, 1.10, 1.05, 1.025, 1.015, and 1.01. This last factor was the finest variation used.

If the solution progressed to the point where a 1% change in every parameter increased the error, the minimum error was assumed to have been reached, and the iterations were stopped. The iterations were also stopped after a fixed number of steps, even if the minimum had not been reached.

In Fig. B.1 the flow chart of the I.B.M. program that carried out these computations is shown. The data input could accept four types of data, which encompassed the usual methods of determining the electrode impedance. These were: amplitude and phase values of the impedance, Lissajon figure values, together with the value of the series resistance and scope impedance, and bridge measurements with parallel or series RC circuits. The data input also included the frequencies involved, the starting parameter values, and special instructions. These special instructions gave the program flexibility and helped speed up the computations. By freezing certain parameters, and assigning them open or short circuit
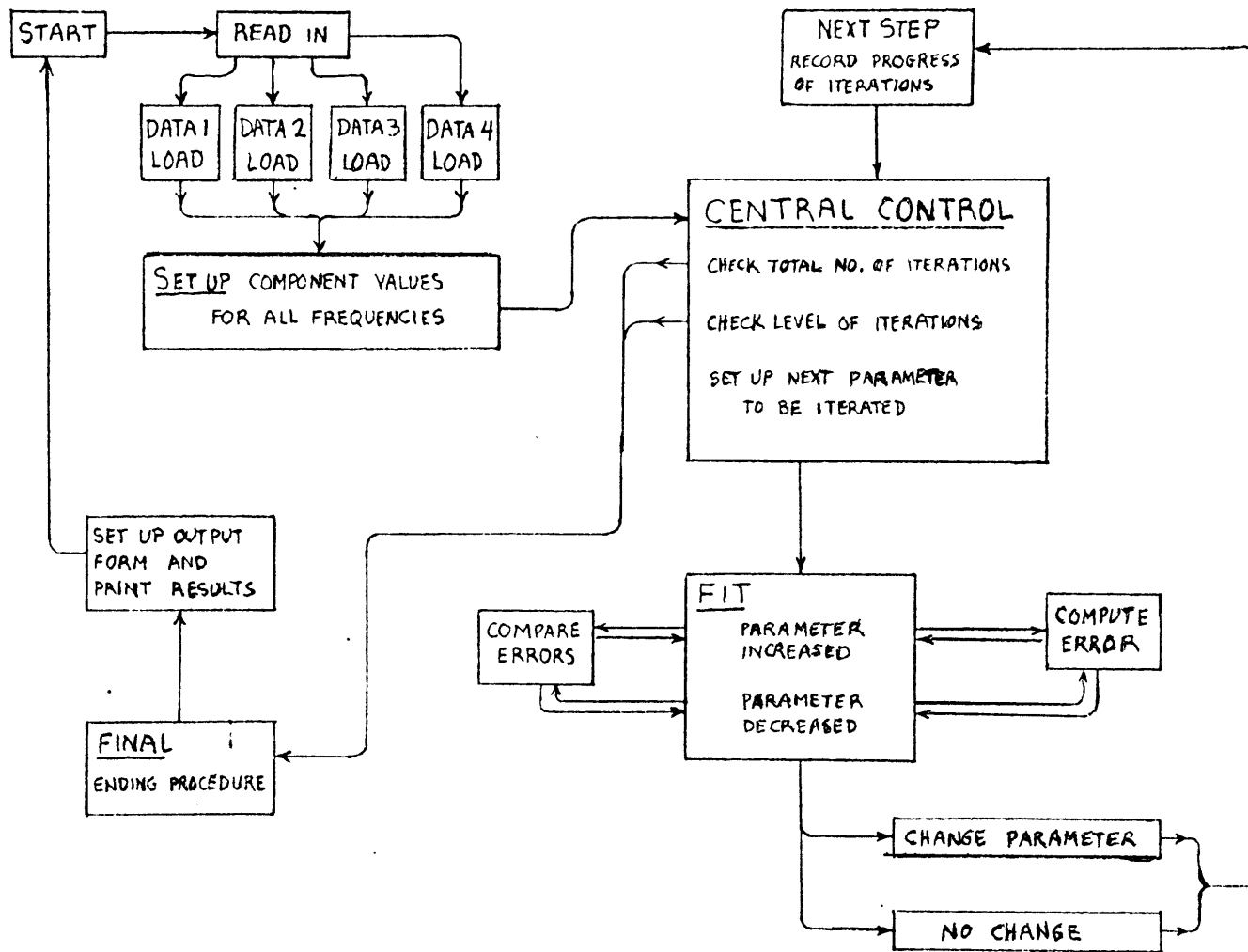
FIG. B.1   FLOW CHART OF ELECTRODE ANALYSIS COMPUTER PROGRAM.

156

values, the equivalent circuit could be simplified in any way desired. Instructions could also be given to test the variation of any parameter only over those frequencies where it was felt the parameter contributed significantly to the impedance . These steps lowered the usual computation time to about 30 seconds per case. The maximum number of iteration cycles was also an instruction, but the program could not handle more than 30 cycles. [This limitation could be easily changed were it deemed desirable.]

The output of the program not only gave the final parameter values and the error measure, but it also printed out the impedances of the electrode and of the equivalent circuit for direct comparison. The progress of the iterations were also listed, so that one could see which parameters the error was sensitive to, and how rapidly the corrections converged to a solution. This information was helpful in evaluating the general character of the solution and in determining if simplifications or complications in the circuit were desirable. If large errors were obtained, metastable solutions were suspected, and different starting parameters were tried. Only one clear cut case of a metastable solution was encountered however. This case was using the most complicated circuit, and the fit involved an oscillation of the circuit impedance about the measured impedance. Unfortunately there are few analytic guides to such problems,

and the investigator's feeling for the problem is called for. The consistency of the solution for different starting parameters is perhaps the best test of a solution. In the cases reported upon in Chapter II, the solutions were mostly well behaved, and the errors of fit were for half the cases about equal to the measurement errors.

A duplication of the 704 program and full instructions for the data format may be obtained from the author by referring to program M335-206-6, General Electrode Impedance.

BIBLIOGRAPHY

Bacon, L., Personal Communication.

Bockris, J. O'M., 1954, Modern aspects of electrochemistry,
    Ch. IV, London, Butterworth's Scientific Publications.

Brant, A.A., Personal Communication.

Carslaw, H.S. and Jaeger, J.C., 1950, Conduction of Heat
    in Solids, Oxford, Clarendon Press.

Denbigh, K.G., 1955, Principles of Chemical Equilibrium,
    Cambridge, University Press.

Fatt, I., 1959, Pore structure of sintered glass from
    diffusion and resistance measurements, J. of Phys.
    Chem., 63, 751.

Fatt, I. et al, 1960, Non steady-state fluid flow and diffusion
    in porous media containing dead end pore volume, J. of
    Phys. Chem., 64, 1162.

Glasstone, S., Laidler, K.J., and Eyring, H., 1941, The
    Theory of Rate Processes, New York, McGraw-Hill Book Co..

Grahame, D.C., 1946, The effect of frequency on the capacity
    and resistance of ideal polarized electrodes, J. of
    Am. Chem. Soc., 68, 301.

Grahame, D.C., 1947, The electrical double layer and the
    theory of electro-capillarity, Chem Rev., 41, 441.

Grahame, D.C., 1952, Mathematical theory of faradaic
    admittance, J. of Electrochem. Soc., 99, 370.

Guillemin, E.A., 1953, Computational Techniques which Simplify
    the Correlation between Steady-state and Transient
    Response of Filters and Other Networks, Tech. Rpt. no.268,
    Research Laboratory of Electronics.

Hillson, P.J., 1954, The mechanism of the reaction at a
    Cu/Cu^2 electrode, Trans. Faraday Soc., 50, 385.

Jaffe, G. and Rider, J., 1952, Polarization in electrolytic solutions, Part II, measurements, J. Chem. Phys., 20, 1077.

Jones and Christian, 1935, J. Am. Chem. Soc., 57, 272.

MacDonald, J.R., 1953, The theory of AC space-charge polarization effects in photoconductors, semiconductors and electrolytes, Phys. Rev., 92, 4.

Madden,TR., Marshall,D.J.,Fahlquist,D., and Neves,A., 1957, Background Effects in the Induced Polarization Method of Geophysical Exploration, U.S. AEC Rpt. RME-3150, Geology and Mineralogy.

Madden,T.R. and Marshall,D.J., 1958, A Laboratory Investigation of Induced Polarization, U.S. AEC Rpt. RME-3156, Geology and Mineralogy.

Madden,T.R. and Marshall, D.U., 1959, Electrode and Membrane Polarization, U.S. AEC Rpt. RME-3157, Geology and Mineralogy.

Madden,T.R. and Marshall,D.J., 1959, Induced Polarization: A Study of Its Causes and Magnitudes in Geologic Materials, U.S. AEC Rpt. RME-3160, Geology and Mineralogy.

Marshall,D.J. and Madden,T.R., 1959, Induced polarization: a study of its causes, Geophysics, 24, 790-816.

Randles, 1947, Kinetics of rapid electrode reactions, Disc. Faraday Soc., no.1, 11.

Vacquier,V., Holmes,C.R., Kintzinger,P.R. and Lavergne,M., 1957, Prospecting for ground water by induced electrical polarization, Geophysics, 22, 660-687.

BIOGRAPHY OF THE AUTHOR

Theodore R. Madden was born in Boston, Massa-
chusetts in 1925. He entered M.I.T. in 1942,
but left to join the U.S. Marine Corps. He
served as a radar technician assigned to the
4th Marine Air Wing. In 1949 he graduated from
M.I.T. with a B.S. in physics, and entered the
graduate school at M.I.T. in the Department of
Geology and Geophysics. He was appointed Assis-
tant Professor in Geophysics in July 1958. He
has spent most of his summers doing mining geo-
physical work, except for four summers spent
on oceanographic and geophysical cruises of the
Lamont Geophysical Laboratory.